12-2020

Electrospun Polyvinyl Alcohol/Cellulose Nanocrystals Composite Nanofibrous Filter: Investigation of Fabrication and Application

Qijun Zhang
University of Tennessee, qzhang37@vols.utk.edu

To the Graduate Council:

I am submitting herewith a dissertation written by Qijun Zhang entitled "Electrospun Polyvinyl Alcohol/Cellulose Nanocrystals Composite Nanofibrous Filter: Investigation of Fabrication and Application." I have examined the final electronic copy of this dissertation for form and content and recommend that it be accepted in partial fulfillment of the requirements for the degree of Doctor of Philosophy, with a major in Natural Resources.

Siqun Wang, Major Professor

We have read this dissertation and recommend its acceptance:

Timothy M. Young, David P. Harper, Terry Liles

Accepted for the Council:

Dixie L. Thompson

Vice Provost and Dean of the Graduate School

(Original signatures are on file with official student records.)

ELECTROSPUN POLY(VINYL ALCOHOL)/CELLULOSE NANOCRYSTALS COMPOSITE NANOFIBROUS FILTER: INVESTIGATION OF FABRICATION AND APPLICATION

A Dissertation Presented for the

Doctor of Philosophy

Degree

The University of Tennessee, Knoxville

Qijun Zhang

August 2020

DEDICATION

To My Family

Xiaoqing Gao and Xizhi Zhang

ACKNOWLEDGEMENTS

I would love to express my most sincere gratitude to my co-advisor Dr. Siqun Wang for guiding and supporting me in many ways, and my co-advisor Dr. Timothy M. Young for his encouragement, support and inspiration. I would also love to thank Dr. David P. Harper and Dr. Terry Liles for serving as my doctoral committees and giving me valuable advices.

I want to thank Dr. Qian Li, Dr. Qiang Wu and all other co-authors for their suggestions and help. I appreciate Dr. John Dunlap's generous help for the use of electron microscopy facilities. Thanks to all my colleagues in Center for Renewable Carbon. It is wonderful and joyful to work with them.

Special thanks to Dr. John Stier, Dr. Jie Zhuang and their colleagues for establishing the partnership program between Nanjing University and the University of Tennessee, which provided me the opportunity to study here.

I am grateful to my families, especially my wife Xiaoqing Gao, for their constant support and belief in me. Their understanding and love have given me the faith to move forward and the courage to overcome challenges.

This research was financially supported by the University of Tennessee's Department of Forestry, Wildlife and Fisheries, the China Scholarship Council, USDA National Institute of Food and Agriculture (Hatch project 1012359), SDSU Sungrant Regional Program (A18-0659), and project of National Natural Science Foundation of China (51603189).

ABSTRACT

Particulate matter (PM) pollution has become a global environmental issue because it poses threat to public health. To protect individuals from PM exposure, one common method is using air filters for indoor air purification. However, conventional air filters have various drawbacks, such as high air resistance, the filters are not fabricated with environmentally friendly technology, and they cannot be easily regenerated. In this dissertation, a new electrospun poly(vinyl alcohol) (PVA)/cellulose nanocrystals (CNCs) composite nanofibrous filter was successfully developed. This PVA/CNCs composite material was demonstrated as air filter for the first time. The CNCs improved the filtration performance by increasing the surface charge density of the electrospinning suspension and thereby reducing diameter of fibers. High $PM_{2.5}$ removal efficiency was achieved (99.1%) with low pressure drop (91 Pa) at a relatively high airflow velocity (0.2 m s^{-1}), under extremely polluted condition ($PM_{2.5}$ mass concentration >500 μg m^{-3}). The integral effect of various electrospinning suspension properties on filtration performance was also investigated using response surface methodology. With a face-centered central composite design, the operating parameters for fabricating PVA/CNCs air filters were optimized, and the optimum conditions were a suspension concentration of 7.34% and a CNCs percentage of 20%. Additionally, the water-soluble PVA/CNCs composite was converted to be completely water-resistant when the electrospun material was heated at 140 ^{o}C for only 5 min. The mechanism of the change of water solubility of the fibers was investigated systematically. Our results revealed that increased crystallinity is the key factor for improving the aqueous stability, and CNCs provided additional nucleation sites for PVA crystallization during both electrospinning and heating process. The heated filters were effectively regenerated by water washing and the filtration performance was satisfactorily maintained. Because both PVA and CNCs are nontoxic and biodegradable, no organic solvents or crosslinking agents were used in the whole fabrication process, and the heating process is facile, the method proposed in this dissertation for fabricating electrospun PVA/CNCs nanofibrous filters is environmentally friendly and cost-effectively. This new cellulose-based air filter, which possesses high removal efficiency for PM, low pressure drop, and long lifetime, is very promising.

TABLE OF CONTENTS

LIST OF TABLES

LIST OF FIGURES

INTRODUCTION

This dissertation consists of three journal articles: (1) "A novel method for fabricating an electrospun poly(vinyl alcohol)/cellulose nanocrystals composite nanofibrous filter with low air resistance for high-efficiency filtration of particulate matter"; (2) "Optimization of electrospun poly(vinyl alcohol)/cellulose nanocrystals composite nanofibrous filter fabrication using response surface methodology"; (3) "Preparation of electrospun nanofibrous poly(vinyl alcohol)/cellulose nanocrystals air filter for efficient particulate matter removal with repetitive usage capability via facile heat treatment". The first article was published on *ACS Sustainable Chemistry & Engineering* in 2019 (Zhang et al., 2019); the second article was submitted to *Carbohydrate Polymers* on July 10th, 2020; and the third article was published on *Chemical Engineering Journal* in 2020 (Zhang et al., 2020). Each article is presented as an individual chapter in this dissertation.

With rapid development of industry, expanded population in urban areas and increased motor vehicle use, air pollution has become a serious global environmental issue (Landrigan et al., 2018). According to World Health Organization's report, more than 90% of the world population was affected by poor air quality in 2016 (World Health Organization, 2016). Particulate matter (PM) is one major air pollutant, which consists of extremely small solid particles and liquid droplets (Harrison et al., 2016). It is usually categorized as PM_{10} and $PM_{2.5}$ based on its size, which represent the diameters of the particles less than or equal to 10 and 2.5 μm, respectively. Because of its small size, PM can penetrate into lungs and bronchi when inhaled, causing respiratory and cardiovascular diseases (Brook et al., 2010, Pope III et al., 2002, Raaschou-Nielsen et al., 2013). About 4.2 million premature deaths around the world could be attributed to $PM_{2.5}$ pollution in 2015 (Cohen et al., 2017). Therefore, it is pressing to control and reduce PM pollution.

Studies have shown that people spend most of their time indoors. Hence, improving indoor air quality can greatly reduce the risk posed by PM pollution (Liu, 2007, Xu et al., 2014). Air filters equipped in air circulation system are feasible to remove PM by capturing the particles. However, the filter medium of conventional high efficiency particulate air filters is thick, which result in high energy consumption and frequent clogging (Hutten, 2007, Yun et al., 2007). To reduce the air resistance while keeping relatively high PM

removal efficiency, numerous studies have been focused on developing new materials and fabricating methods for air filtration (Dai et al., 2018, Gopal et al., 2007, Khalid et al., 2017, Kim et al., 2018, Liu et al., 2015b, Vanangamudi et al., 2015, Xu et al., 2016, Zhang et al., 2016a, Zhang et al., 2016b, Zhang et al., 2016c). Among various technologies for preparing air filters, electrospinning is an effective technique to produce ultrafine nanofibrous filter (Doshi and Reneker, 1995, Huang et al., 2006). Smaller fiber diameter could provide large surface area to capture PM (Kenawy et al., 2002, Podgórski et al., 2006), and also allows air molecules pass through due to slip-effect (Brown, 1993, Hung and Leung, 2011, Zhao et al., 2016). But the process of electrospinning often involves organic solvents due to the need to dissolve the polymers used. The use of large amounts of organic solvents, which can be both flammable and toxic, may cause health and environmental problems (Jiang et al., 2016, Zhu et al., 2018). To avoid this kind of issues, water-soluble, biodegradable and environmentally friendly polymer should be used for the electrospinning. Poly(vinyl alcohol) (PVA) is a polymer that meet these requirements and commonly used in electrospinning for numerous applications (Finch, 1973). However, the fibers made from PVA are not mechanically strong. Cellulose nanocrystals (CNCs) are ideal additives to enhance the mechanical strength of PVA fibers because of their outstanding mechanical properties (Habibi et al., 2010, Moon et al., 2011). Previous studies have demonstrated that adding CNCs into PVA polymer matrix could significantly increase the tensile strength and storage modulus (Miri et al., 2015, Peresin et al., 2010). Since CNCs are primarily isolated from cellulose fibers by acid hydrolysis, and cellulose is the most abundant natural polymer on the earth, this nanosized material has attracted great interest. The unique mechanical properties and biosafety of CNCs make this renewable nanomaterial very promising.

The filtration performance of air filters fabricated via electrospinning is affected by many process parameters. Status between the repulsive and constrictive forces along the initial jets at the Taylor cone determines the morphology of generated fibers and the structure of the nanofiber network (Garg and Bowlin, 2011, Huang et al., 2006, Reneker and Yarin, 2008, Thompson et al., 2007). Previous studies have investigated the effect of electrospinning parameters, like voltage, working distance, solution feed rate etc., through one-factor-at-a time method (Ding et al., 2002, Garg and Bowlin, 2011, Supaphol and

Chuangchote, 2008, Thompson et al., 2007). But this type of method is time consuming and unable to examine the interaction effects. In addition, the properties of electrospinning solution, such as viscosity, conductivity and surface tension, are normally varied simultaneously as the concentration or the composition of the solution changes. Therefore, it is no longer applicable to use one-factor-at-a-time method to study the effects of these factors. To evaluate the filtration performance of the filters with considering the integral effect of different electrospinning solution properties, and optimize the fabricating conditions effectively, utilizing design of experiments is necessary. Response surface methodology (RSM) is an effective statistical modeling tool, which can be used for extended reasoning, interaction study and parameter optimization (Montgomery, 2017). It is a technique that maximizes the inference of results while minimizing the number of experimental runs and costs of experimentation (Bösiger et al., 2018, Fu et al., 2016, Meng et al., 2015, Sarlak et al., 2012).

Although using water-soluble polymers in electrospinning can avoid large amounts of organic solvent, the air filters made from water-soluble polymers is not stable in high-humidity environment and cannot be regenerated by water-washing after use. Non-reusable filters have higher costs given one-use which requires more cumulative raw materials and the related energy consumption during the manufacturing process. Additionally, inappropriate disposal of waste filters may cause environmental issues as well (Fan et al., 2018a, Fan et al., 2018b). To improve the aqueous stability of the filters, crosslinking the polymers is one commonly used strategy (Peresin et al., 2014, Qin and Wang, 2008, Shalom et al., 2019, Song et al., 2016). But the added crosslinking agents are often toxic and may create new environmental concerns (Liu et al., 2017, Zhu et al., 2018). Several studies have shown that water stable PVA materials could be prepared via heat treatment. The increased crystallinity is the reason caused the change in water solubility (Hong, 2007, Wong et al., 2010). Because CNCs may act as nucleating agent and promote crystallization of PVA (Popescu, 2017, Rescignano et al., 2014, Uddin et al., 2011), it is expected that a waterproof PVA/CNCs composite material could be obtained under an even milder heating condition.

In general, conventional air filters are not ideal for the removal of fine particles, such as PM_{10} and $PM_{2.5}$. The removal efficiency for PM and the air resistance of the filter cannot

be well compromised, which makes the air permeability of the filter has to be sacrificed to ensure a high PM removal efficiency. In another word, more filtering materials are required to be stacked, which greatly increased the energy consumption. To overcome these problems, one feasible strategy is to reduce the fiber diameter of the fibrous air filter to nanoscale, so that the specific surface area to volume ratio and the porosity of the filter medium can be improved. The air resistance of air filter could be reduced due to the nanometer-level fibers while keeping a high removal efficiency for PM. However, many of the polymers used for fabricating nanofibers are not environmentally friendly, and a large amount of organic solvents may be used during the manufacturing process. The toxic materials and solvents may cause new environmental concerns, thereby lowering the significance of air filters for the protection of individuals and the improvement of environment. In addition, the most air filters on the market at this time are not reusable, which will inevitably lead to higher energy consumption for production, increased demand for raw materials, and increased working load to treat and recycle the waste after use. All these drawbacks force the existing air filter fabrication technology to be improved, and it is urgent to develop a green and environmentally friendly filter preparation method.

The research objective of this dissertation was to develop a novel method, which utilized cellulose-based materials, to fabricate environmentally friendly reusable air filter with high PM removal efficiency and low pressure drop. The problem of the compromising between the removal efficiency and the air resistance of air filter was solved with this new air filter fabrication technique. The use of harmful materials during the manufacturing process was avoided. Therefore, neither the preparation procedure nor the final product would generate pollutants to the environment. The reusability of the filter also reduced the cost for cumulative use of raw materials. Additionally, the use of renewable materials demonstrated in this dissertation may promote the production and use of green air filters. This would not only reduce energy consumption, but also decrease potential carbon and microplastic emissions. Since cellulose is the most abundant natural polymer on the earth, the efficient utilization of it may expand the application prospect and market of renewable resources, thus further increasing the economic value of agricultural and forestry products.

In this dissertation, a new electrospun nanofibrous PVA/CNCs composite air filter was successfully fabricated in Chapter I. The filtration performance for PM was evaluated, and

the influence of CNCs on PVA fiber formation and filtering performance was investigated. Results indicated that adding CNCs can significantly improve the PM removal efficiency and decrease the pressure drop. The overall filtration performance of the fabricated PVA/CNCs air filter is superior. To further investigate the optimum filtration performance, the conditions of electrospinning suspensions were optimized using RSM in Chapter II. A face centered central composite design (CCF) was applied for the RSM. 'Suspension concentration' and 'CNCs percentage' were selected as independent variables, and 'removal efficiency' and 'pressure drop' were the responses. The constructed prediction quadratic models were proved to be reliable, and the operating conditions were optimized effectively. In Chapter III, the water-soluble electrospun PVA/CNCs filter was completely converted into water-resistant via a facile heat treatment without adding any crosslinkers. The mechanism was systematically investigated, and the heated PVA/CNCs filter was able to be regenerated effectively. In general, the novel method proposed in this dissertation is believed to be environmentally friendly and cost-effectively. This dissertation demonstrated the promise of electrospun PVA/CNCs air filter for air purification. It also provided guidance on the cleaning and recycling strategies of CNCs-based electrospun filter for long-term usage.

CHAPTER I

A NOVEL METHOD FOR FABRICATING AN ELECTROSPUN POLY(VINYL ALCOHOL)/CELLULOSE NANOCRYSTALS COMPOSITE NANOFIBROUS FILTER WITH LOW AIR RESISTANCE FOR HIGH-EFFICIENCY FILTRATION OF PARTICULATE MATTER

A version of this chapter was originally published on *ACS Sustainable Chemistry & Engineering* by Qijun Zhang, Qian Li, Timothy M. Young, David P. Harper and Siqun Wang. Reproduced with permission from ref. Zhang et al. 2019. Copyright 2019 American Chemical Society.

Zhang, Q.; Li, Q.; Young, T. M.; Harper, D. P.; Wang, S. A novel method for fabricating an electrospun poly(vinyl alcohol)/cellulose nanocrystals composite nanofibrous filter with low air resistance for high-efficiency filtration of particulate matter. *ACS Sustain. Chem. Eng.* **2019,** *7*, 8706-8714.

Authors:

Qijun Zhang, Qian Li, Timothy M. Young, David P. Harper, Siqun Wang
Center for Renewable Carbon, University of Tennessee, Knoxville, TN, United States

Qian Li
School of Engineering, Zhejiang A&F University, Hangzhou, China

Q. Zhang's primary contribution to this paper includes identifying the research objective, design and conduct of the experiments, process and interpretation of the data, drafting the paper.

Co-researchers' contributions are listed as follows:
Q. Li provided research guideline, worked with Qijun to fabricate the nanofibrous air filters and analyze the data of rheological measurements.
T.M. Young revised and language polished the paper.
D.P. Harper worked with Qijun to performed rheological measurements and FTIR tests.
S. Wang identified the research objective, provided research guideline and revised the paper.

Abstract

Particulate matter (PM) air pollution poses a risk to public health, especially in rapidly industrializing countries. One major way to protect individuals from PM exposure is to use fiber-based filters for indoor air purification. In this study, a new low pressure drop poly(vinyl alcohol) (PVA)/cellulose nanocrystals (CNCs) composite nanofibrous filter was fabricated using electrospinning. This electrospun PVA/CNCs filter was demonstrated as an air filter for the first time. The CNCs not only contributed to the PVA/CNCs system as mechanical reinforcement agents but also increased the surface charge density of the electrospinning solution, thereby reducing fiber diameter. The thinner fibers reduced pressure drop significantly and increased the efficiency of the PM removal. Our results indicate that high $PM_{2.5}$ removal efficiency was achieved (99.1%) under extremely polluted conditions ($PM_{2.5}$ mass concentration >500 μg m^{-3}) with low pressure drop (91 Pa) at an airflow velocity of 0.2 m s^{-1}. Considering that PVA and CNCs are both nontoxic and biodegradable, this high-efficiency composite filter with low air resistance is environmentally friendly and shows promise in indoor air purification applications.

1. Introduction

Particulate matter (PM) is a combination of extremely small solid particles and liquid droplets in air; it is composed of organic compounds, black carbon, sulfate, nitrate, ammonia, and trace metals (Harrison et al., 2016). In recent years, due to rapid industrial and economic development, PM pollution has occurred more frequently, especially in developing countries such as China and India. The living quality of people is tremendously influenced from PM pollution which effects atmospheric visibility (Watson, 2002), climate (Booth and Bellouin, 2015) and poses potentially serious threats to public health (Koplitz et al., 2017). On the basis of particle sizes, PM can be categorized by its aerodynamic diameter as PM_{10} and $PM_{2.5,}$ which represent particle diameters less than or equal to 10 and 2.5 μm, respectively (Harrison et al., 2016). Studies have shown that PM_{10} is small enough to be able to be inhaled, enter people's lungs, and pose potential health risks, while $PM_{2.5}$ is even more harmful since it may penetrate bronchi and enter extrapulmonary organs and possibly the central nervous system itself, through the bloodstream (Brook et al., 2010, Pope III et al., 2002, Raaschou-Nielsen et al., 2013).

To protect individuals and reduce the risks of long-term exposure to PM, masks are a preventive measure used outdoors. Studies show that people spend 85% of their time indoors, where $PM_{2.5}$ concentrations have been found to exceed daily average limits by approximately 6 times during hazy days (Liu, 2007, Xu et al., 2014). Air filters are a feasible way to remove indoor PM by filtering, whether that occurs through the use of ventilation, air conditioning, or air purifiers. Various strategies have been developed to fabricate air filters, such as spun-bonded (Zhang et al., 1997), needle-punched (Anandjiwala and Boguslavsky, 2008), and melt-blown (Lee and Wadsworth, 1990). However, conventional fiber-based filters prepared by these methods are usually not very efficient in the filtration of fine particles because of the large pore sizes of micrometer-level fibers (Barhate and Ramakrishna, 2007, Thomas et al., 2001). To improve the efficiency of conventional air filters, a thicker filter medium is necessary. High efficiency particulate air (HEPA) filters and ultralow particulate air (ULPA) filters can achieve 99.97% and 99.999% filtration efficiencies when capturing PM, respectively (Hutten, 2007). However, the high pressure drops in HEPA filters result in high energy consumption

and frequent clogging (Yun et al., 2007). To achieve the best compromise between air flow and filtration efficiency, new air-filter materials must be developed.

Electrospinning has emerged as an effective technique to obtain uniform nanofibers with diameters from 1 to 1000 nm (Doshi and Reneker, 1995, Huang et al., 2006). Smaller fiber diameters increase the specific surface area to volume ratio as well as the porosity of the filter medium (Kenawy et al., 2002, Podgórski et al., 2006) allowing air molecules to pass through the filter effectively. This is especially true when the diameters of nanofibers range from 200 to 60 nm, where the slip-effect promotes aerodynamic slip and decreases the collision of the air molecules with the nanofibers (Brown, 1993, Hung and Leung, 2011, Zhao et al., 2016). Thus, many polymers, such as polyacrylonitrile (PAN) (Bian et al., 2018b, Yun et al., 2007), polystyrene (PS) (Liu et al., 2015b), polyamide (PA) (Ahn et al., 2006), polyimide (PI) (Zhang et al., 2016), polyurethane (PU) (Scholten et al., 2011), and polysulfone (PSU) (Gopal et al., 2007), have been successfully electrospun to produce high-performance air filters, demonstrating that electrospinning is ideal for producing filters with high filtration efficiency and low air resistance. In addition, the interconnected geometries and morphologies of electrospun nanofibers are tunable (Ding et al., 2002, Doshi and Reneker, 1995, Supaphol and Chuangchote, 2008), which makes the filtering performance controllable.

The process of using electrospinning to fabricate nanofibrous filter material often involves dissolving polymers, such as those above, in organic solvents. Generally, the electrospinning solution is prepared at a concentration of less than 30%; thus, the fabrication process involves large amount of organic solvents, which can be both flammable and toxic. Exposure to such solvents at high concentration during the manufacturing process or even long-term exposure at low concentration from the end-use products may result in health and environmental problems (Jiang et al., 2016, Zhu et al., 2018). Further, disposal of the used air filters may also cause environmental pollution (Liu et al., 2017). Air filters prepared with protein-based materials, including zein (Fan et al., 2018b, Tian et al., 2018), silk fibroin (Bian et al., 2018a, Lang et al., 2013) and whey (Fan et al., 2018a), are considered environmentally sustainable and have shown excellent PM removal efficiency. Another approach in the avoidance of new environmental concerns is the use of biodegradable, water-soluble, environmentally friendly polymers for the

electrospinning. Poly(vinyl alcohol) (PVA) is a water-soluble, nontoxic, fully biodegradable, and biocompatible polymer, which is commonly used in electrospinning for numerous applications (Finch, 1973). However, PVA fibers are not mechanically strong. Several strategies to strengthen them have been studied, such as post treatment (Jeun et al., 2009), cross-linking (Peresin et al., 2014), blending (Ding et al., 2004) and the use of nanofillers (Wong et al., 2009). But cross-linkers and additives may create other environmental concerns (Liu et al., 2017, Zhu et al., 2018). Cellulose nanocrystals (CNCs) obtained from renewable resources have attracted great interest because of their minute size, biodegradability, and outstanding mechanical properties. In fact, used as reinforcement agents, CNCs have been demonstrated to significantly improve the mechanical properties of composite materials (Feng et al., 2017, Huang et al., 2017, Huang et al., 2018, Ma et al., 2017). Previous studies have shown that by the addition of CNCs into a PVA polymer matrix, the tensile strength was increased by 80% and the storage modulus was strengthened 3-fold (Miri et al., 2015, Peresin et al., 2010). Other studies also demonstrated that cellulose-based materials can be successfully utilized for air filtration (Long et al., 2018, Lu et al., 2018, Su et al., 2018).

Despite numerous studies investigating electrospun materials, no studies in the public domain have been reported on the development of PVA/CNCs composite fibers as air filter for fine particle filtration. This study introduces a novel, environmentally friendly, PVA/CNCs nanofibrous air filter with high PM removal efficiency and low air resistance. In this research, PVA aqueous solutions were mixed with CNCs by means of ultrasonication and then fabricated into nanofibers via electrospinning. A commercial window screen was applied as a collector for the electrospun fibers across the mesh holes, forming a network for filtration. The fabricated PVA/CNCs filters were characterized, and the PM filtering performance was evaluated. The PM used in this study was generated by burning incense. Previous research has demonstrated that the PM from incense smoke is more difficult to remove than rigid inorganic PM due to its large carbon and water content (Liu et al. 2015b). The aim of this study was to not only add CNCs as PVA reinforcements but also investigate the influence of CNCs on PVA fiber formation and filter performance. Considering that CNCs are negatively charged and could increase the surface charge density of electrospinning solutions, it is expected that fabricated fiber diameters could be

tuned by varying the amounts of CNCs added into the PVA (Stranger et al., 2009). In addition, the effect of filter basis weight (mass of electrospun filter media per unit area) on both PM capture and pressure drop was also studied.

2. Experimental section

2.1. Materials

PVA (99+% hydrolyzed, M_w 85000-124000) was purchased from Sigma-Aldrich (St. Louis, MO). CNCs (~12 wt%, 5-20 nm in width, 150-200 nm in length) were purchased from the University of Maine (Orono, ME), which were prepared by sulfuric acid hydrolysis. PVA and CNCs were used as received. Commercial window screens with 0.25 mm wire diameter and 1.2 mm × 1.2 mm mesh size were purchased from Saint-Gobain ADFORS (Clear Advantage, Grand Island, NY).

2.2. Preparation of PVA and PVA/CNCs suspensions

PVA was dispersed in deionized water and stirred at 85 ^{o}C until it was fully dissolved. After the PVA solution had cooled to room temperature, specified amounts of CNCs were added to obtain the following CNC percentages of PVA content: 5%, 10%, 15%, and 20% (w/w) while total concentrations were kept at 7 wt%. The dry weight of CNCs was determined every time before use. For comparison purposes, neat PVA solution was also prepared at 7 wt%. All PVA and PVA/CNCs suspensions were sonicated using an ultrasonic processor (Sonics VCF-1500, Newton, CT) in an ice bath for 2 min under 600 W of power. As previous studies have indicated, the short time and low power ultrasonication conducted in an ice bath did not change the viscosity and surface charge density of PVA and CNCs (Dong et al., 1998, Mohod and Gogate, 2011, Shafiei-Sabet et al., 2012).

Prepared suspensions were denoted to indicate their CNC content; for example, PVA/CNC-5 represented a PVA/CNCs suspension with 5% CNCs.

2.3. Electrospinning of PVA and PVA/CNCs nanofibrous filters

A 5 mL plastic syringe with a 22-gauge needle was used to load the prepared suspension. The needle was connected to the positive end of a voltage generator (PS/EK40P15011, Glassman High Voltage, High Bridge, NJ). The window screen was

directly placed on a 7.6 cm diameter metal circular cylinder as a collector. The cylinder was grounded and placed at a working distance of 10 cm from the needle tip. The operating voltage was set at 22 kV. Solution was pumped out at a constant 0.5 mL h^{-1} flow rate during electrospinning by a syringe pump (NE-1800, New Era Pump System, Farmingdale, NY). Electrospinning was performed at room temperature and 50 ± 5% relative humidity. Electrospinning times of 2, 4, 6, and 8 min were applied to control the basis weight (mg m^{-2}) of the electrospun fibers.

The resulting electrospun air filters were labeled to denote their CNC content and electrospinning time. For instance, PVA/CNC-10-4 represented a filter fabricated with PVA/CNCs suspension with 10% CNCs and an electrospinning time of 4 min, and PVA-2 represented neat PVA with 2 min of electrospinning.

2.4. Morphology characterizations

The morphology of the electrospun nanofibrous filters was studied by means of a scanning electron microscope (SEM, Zeiss Auriga SEM/FIB crossbeam workstation, Germany) with an acceleration voltage of 5 kV. All samples were sputter-coated with gold before observation. Diameters were evaluated by SEM images and 50 fibers were measured for each filter.

2.5. Zeta potential measurements

Zeta potentials of the PVA and PVA/CNCs suspensions were determined by a Zetasizer Nano ZS (Malvern, Westborough, MA). The suspensions were diluted to 0.7 wt% for the zeta potential measurement. The pH values of all PVA and PVA/CNCs suspensions were found to be within the range of 6.51 ± 0.04, so the pH effect on zeta potential measurements was considered negligible and no further pH adjustment was applied. All measurements were conducted at 25^{o}C, and the collected data were averaged over 5 measurements.

2.6. Rheological measurements

Suspension viscosities were measured by a stress-controlled rheometer (AR-G2, TA Instruments, New Castle, DE) equipped with a cone-plate geometry (cone with 2^{o} angle, 40 mm diameter and 56 μm truncation) at 25 ^{o}C. Viscosity tests were performed within a

shear rate range of 0.01-1000 s^{-1}. A solvent trap was used to prevent water evaporation during the measuring procedure.

2.7. Fourier transfer infrared spectroscopy (FTIR) analysis

The basic chemical characteristics of electrospun filters were analyzed by a FTIR spectrometer (Spectrum Two, Perkin Elmer, Llantrisant, UK) over a wavenumber range of 4000-500 cm^{-1}. All spectra were collected with a resolution of 4 cm^{-1} after 16 scans.

2.8. Filtration performance of electrospun PVA and PVA/CNCs filters for PM

Figure I-1 shows the experimental system for PM filtration. Two glass bottles customized by Adams & Chittenden were used as the filtration unit. Each bottle possessed one flange and two ports. The fabricated filter was clamped between the two flanges of the bottles with a sealing ring. The ports of the bottles were used to connect to the air flow and the pressure gauge. PM particles were generated in a smoke-generating bottle by burning incense, which produces more than 45 mg g^{-1} PM when burned; gases such as CO, CO_2, SO_2, NO_2, as well as volatile organic compounds, including toluene, benzene, aldehydes, xylenes, and polycyclic aromatic hydrocarbons, were also generated (Lin et al., 2008, Mannix et al., 1996). This complex smoke is a model system to simulate hazy days because it contains many components that can be found in polluted air. The particle size of the PM that was generated varied from <0.3 to >10 μm. The concentration of the PM in the smoke-generating bottle was controlled at >500 μg m^{-3}, and the PM concentration was measured by a particle counter (CEM DT-9851M, China). Removal efficiencies were calculated by comparing the PM concentrations in the filtered air with and without filters. The air flow rate was controlled at 0.2 m s^{-1}. Pressure drops across the filters were measured by a differential pressure gauge (Testo 510, Germany). All experiments were conducted in triplicate. To evaluate the overall performances of the electrospun filters in terms of both efficiency and pressure drop, a quality factor, Q_f, was used as an indicator. Q_f is defined as:

$$Q_f = -\ln(1-E)/\Delta P \quad (1)$$

where E is PM removal efficiency and ΔP is pressure drop across the filter.

2.9. Statistical analysis

The significance tests for the effect of CNC content on fiber diameter and filter pressure drop were evaluated by *t*-test using JMP software (version 14, SAS Institute, Cary, NC). The differences between group means with *p*-values equal or less than 0.05 were considered statistically significant.

3. Results and Discussion

3.1. Characterizations of PVA and PVA/CNCs suspensions and electrospun fibers

The morphologies of the electrospun PVA and PVA/CNCs fibers are shown in Figure I-2. The electrospun fibers formed smoothly without beads, indicating that adding CNCs did not induce capillary instability of the Taylor cone during electrospinning (Reneker and Yarin, 2008). As shown in Figure I-2f, the diameter of the electrospun fiber was strongly dependent on how much CNCs were added. Statistical analysis results of diameter distribution of each air filter are shown in Table I-1. From the *t*-tests, the means of each group are significantly different (Table I-2). The average diameter of the neat PVA fibers was 209.4 nm. With the addition of CNCs ranging from 5% to 20%, the fiber diameters decreased gradually and achieved the lowest value of 127.6 nm for PVA/CNC-20-6. With the addition of 20% CNCs in terms of PVA content, which is only 1.4% of the total amount of the PVA/CNCs suspension, the fiber diameter decreased 39.1% compared with that generated using the neat PVA fiber. Such a significant effect might be attributed to the negative charge of the CNCs. It is known that charge density is one important parameter affecting electrospun fiber diameter. An increase in charge density may cause stronger electrostatic forces and lead to the formation of a Taylor cone with a steeper angle. Thus, the initial jet could emerge with a smaller diameter (Stranger et al., 2009). CNCs possess a negative electrical charge due to the sulfate groups ($-O-SO_3^-$) that were introduced onto its surface during sulfuric acid hydrolysis. Zeta potential measurement studies showed that the zeta potential values of PVA and PVA/CNCs suspensions decreased with increasing CNC content (Figure I-3). The negative zeta potential value of PVA, -0.6 ± 0.2, is probably due to the existence of acetate groups on its surface. When CNCs were added as 5%, 10%, 15% and 20% levels, the zeta potential values decreased to -6.9 ± 0.4, -11.8 ± 0.6, -12.4 ± 1.3 and -15.7 ± 0.8, respectively. A 25-fold increase in zeta potential value was induced by

the addition of 20% CNCs. Considering that the volumes of the PVA and PVA/CNCs suspensions were constant, we can infer that the surface charge densities of the suspensions increased considerably as the CNC amounts were increased. The results of the zeta potential measurements are consistent with the variation tendencies of the electrospun fiber diameters reported above, implying that the increased suspension surface charge density plausibly reduced the electrospun fiber diameter.

To further support the hypothesis mentioned above, the viscosities of all PVA and PVA/CNCs suspensions were measured. The viscosity of the suspension plays an important role during electrospinning and may strongly affect the diameter and structure of the electrospun fiber (Garg and Bowlin, 2011). Steady-state viscosity as a function of the shear rate of each of the PVA and PVA/CNCs suspensions are shown in Figure I-4. It was observed that the suspension viscosity was independent of the CNC content. This can be attributed to the small amount of CNCs added. Since the added amount of CNCs came up to 20% of the PVA content and the suspension concentration was 7%, the total amount of CNCs added into the suspension only amounted to 1.4%. Thus, the decrease in the electrospun fiber diameter was not driven by the viscosity of the suspension. Furthermore, the viscosities of both the PVA and PVA/CNCs suspensions decreased with increases in the shear rate, indicating shear-thinning behavior. It is evident that CNCs did not cause any phase transition because the five shear-thinning curves almost overlap each other. Hence, the small amount of CNCs did not affect the rheological property of the PVA solution. Therefore, it was further confirmed that the negatively charged CNCs favored the formation of smaller-diameter electrospun fibers.

The SEM images of the fiber surface morphologies of PVA-2, PVA/CNC-10-2 and PVA/CNC-20-2 filters are presented in Figure I-5. As CNC content was increased to 10% and 20%, there was no CNCs agglomerate or other protrusion formed on the fiber surface (Figure I-5b and I-5c), which indicated that CNCs were embedded inside the PVA/CNCs fibers. On the basis of previous studies, the electrospinning process facilitated the orientation of CNCs along the axis of electrospun fibers, while some nonoriented CNCs can occur at the same time along the direction of fiber cross-section (Bian et al., 2018c, Wanasekara et al., 2015). Since the lengths of the CNCs range from 150 to 200 nm, which are greater than the average diameters of PVA/CNC-10-2 and PVA/CNC-20-2 (155.8 ±

24.6 nm and 127.6 ± 16.9 nm, respectively), the CNCs were unlikely to be oriented perpendicular to the direction of fiber axis. Therefore, the CNCs were possibly oriented along the PVA/CNCs fiber axis uniformly.

The FTIR spectra collected for electrospun filters with different CNC content are shown in Figure I-6. For pure PVA filter, the strong absorption peak at 1087 cm^{-1} is due to C-O stretching and O-H bending (Peresin et al., 2014). The peaks at 2942 and 2908 cm^{-1} are the typical O-H and C-H stretching peaks. The broad band from 3200 to 3550 cm^{-1} corresponded to the stretching of O-H bond from intermolecular and intramolecular hydrogen bonds. For PVA/CNCs composite filters, the peak observed at 1058 cm^{-1} was assigned to the C-OH stretching of cellulose. It was noticed that the presence of CNCs and the increase in CNC amount caused the change in shape of the main band between 3200 and 3550 cm^{-1}, which can be attributed to the formation of hydrogen bond network between PVA and CNC molecules (Peresin et al., 2010).

3.2. Filtration performance of electrospun PVA and PVA/CNCs filters for PM

The quantified $PM_{2.5}$ and PM_{10} removal efficiencies by all the electrospun nanofibrous filters are shown in Figure I-7. It clearly indicates that the addition of CNCs effectively improved the removal efficiencies for both $PM_{2.5}$ and PM_{10}. These improved efficiencies are attributed to the decrease in fiber diameter, as can be seen in the electrospun fiber diameter distribution reported above. Interestingly, as CNC content was increased from 0% to 20%, the PM removal efficiency improved significantly at first and then only slightly. For example, the removal efficiency of PVA-2 filter (average diameter 209.4 nm) for $PM_{2.5}$ was 56.0 ± 3.3% (Figure I-7a). With increases in CNC content to 5% and 10%, the average fiber diameter decreased and the removal efficiency increased dramatically to 70.1 ± 6.4% (PVA/CNC-5-2 filter, 181.8 nm) and 82.3 ± 7.8% (PVA/CNC-10-2 filter, 155.8 nm), respectively. However, continued increases in CNC content to 15% and 20%, resulted in improvements in the removal efficiencies of 82.9 ± 5.0% (PVA/CNC-15-2 filter, 140.7 nm) and 84.9 ± 7.4% (PVA/CNC-20-2 filter, 127.6 nm), respectively. Similar results have also been observed for PM_{10} removal efficiency by all electrospun filters (Figure I-7b). These results imply that when the fiber diameter of the electrospun filter is lower than ~150 nm, fiber dimension is no longer the dominant factor affecting the ability to capture smoke PM. When electrospinning time was 2, 4, 6 and 8 min, the basis weights of fabricated filters

were 20, 40, 60 and 80 mg m^{-2}, respectively (Figure I-8). As the thickness of the electrospun filters was increased, removal efficiencies for both $PM_{2.5}$ and PM_{10} increased (Figure I-7); >95% removal of $PM_{2.5}$ was achieved after the electrospinning time was increased to 6 min, and >99% removal was achieved when the time was increased to 8 min. A comparison of the efficiencies of the filters fabricated with 2 min electrospinning and window screen (0 min electrospinning time) shows that with a low basis weight (20 mg m^{-2}), the efficiencies of the PVA-2 filter are ~47% and 59% higher than window screen for $PM_{2.5}$ and PM_{10}, respectively. Furthermore, CNCs as additives showed superior effectiveness in air filters for PM removal; that is, the substitution of 2 mg of PVA with CNCs to fabricate one square meter PVA/CNC-10-2 composite air filter resulted in the removal efficiencies of $PM_{2.5}$ and PM_{10} being improved to approximately 82% and 83% from approximately 56% and 61%, respectively.

To characterize the interaction between electrospun filter fibers and captured PM, the filters, before and after filtration test, were studied by SEM; the resulting images of the PVA/CNC-20-2 filter are shown in Figure I-9. Smoke PM generated by burning incense is considered to be soft PM, due to its larger contents of carbon and water than those of rigid inorganic PM. Instead of simply attaching to the surface of the nanofiber as inorganic PM, soft PM has been demonstrated, in a previous study, first to deform after contacting and then to wrap around the nanofiber (Liu et al., 2015b). As shown in Figure I-9b, smoke PM wrapped around nanofibers as a coating and formed bead-shaped particles on the fibers. In addition, PM particles were also able to attach directly to the PM already captured on the fiber and became aggregated. As the PM merged together, bigger size particles were formed and filled the pores, especially at the junctions of the nanofiber network. The wrapping of the PM around the fiber indicates that the fiber surface of the electrospun filter possesses an affinity for the smoke-generated particles, which leads to the enlargement of the contact area. Since soft PM is generally considered more difficult to be captured than rigid inorganic PM, our electrospun nanofibrous filters appear to be promising for both soft and rigid PM filtration applications.

Besides removal efficiency, another important factor in air filters, pressure drop, was also evaluated (Figure I-10). An increase in electrospinning time results in an increase of the thickness of the fabricated air filter, making the filter more air resistant. As shown in

Figure I-10, pressure drop clearly increased as electrospinning time was increased from 2 to 8 min. The pressure drop results also indicate that the addition of CNCs improves the air permeability of fabricated filters. For these filters with four different thicknesses, the increase of CNC content from 0 to 20% resulted in pressure drop reductions from ~178 to 91 Pa, 102 to 56 Pa, 72 to 38 Pa and 37 to 15 Pa, respectively. The effect of CNC content on pressure drop is statistically significant (Table I-3 to I-10). This pressure drop reduction could be attributed to the decrease in fiber diameter; smaller fibers tend to form a nanofibrous network with higher porosity at the same basis weight, allowing the air molecules to pass through more easily. Furthermore, previous studies have indicated that nanofiber diameters ranging from 60 to 200 nm promote aerodynamic slip and decreased collision of air molecules with nanofibers by means of the slip-effect (Brown, 1993, Hung and Leung, 2011, Zhao et al., 2016). As mentioned above, the improvement in PM removal efficiency is relatively limited with a CNC content higher than 10%. Nevertheless, a continuous increase in CNC content, along with the reduction in pressure drop, contributes significantly to that improvement.

The quality factor (Q_f) was employed to evaluate the overall performance of the fabricated filters. The Q_f values for all PVA and PVA/CNCs filters were calculated based on their $PM_{2.5}$ removal efficiency. Among the air filters with >95% removal efficiency, the PVA/CNC-15-6 and the PVA/CNC-20-6 had the highest Q_f (0.054 Pa^{-1}), followed by the PVA/CNC-20-8 filter (0.052 Pa^{-1}) (Table I-11). The Q_f of the other fabricated filters ranged from 0.019 to 0.029 Pa^{-1}. Air filters with outstanding performance that have been used in other studies are also summarized in Table I-11 for comparison.

In addition, face velocity was considered when the Q_f values of different filters were evaluated; the penetration of particles and pressure drop would be both increased at higher face velocity (Ahn et al., 2006, Bian et al. 2018c). As listed in Table I-11, only the PVAc filter (Matulevicius et al., 2016) had a slightly higher Q_f value (0.055 Pa^{-1}) and it was obtained at a much lower face velocity (0.058 m s^{-1}). Therefore, the fabricated PVA/CNC-15-6, PVA/CNC-20-6 and PVA/CNC-20-8 filters showed superior overall filtration performances.

4. Conclusions

In this study, a PVA/CNCs composite filter with low air resistance and high PM removal efficiency was fabricated via electrospinning for the first time. The addition of a small amount of CNCs (2 to 16 mg m^{-2}) resulted in a dramatic improvement in the overall filtration performance (Q_f value went as high as 0.054 Pa^{-1}). These results indicate that CNCs effectively reduced the electrospun fiber diameter because of their negative charge. In addition, the entire manufacturing process of the electrospun filters was environmentally friendly. No organic or toxic solvents were involved, and both PVA and CNCs are environmentally benign materials. Furthermore, the basis weight of the filter was very low, which made the filters potentially cost-effective. This electrospun PVA/CNCs filters are highly promising for indoor air purification applications.

Appendix I

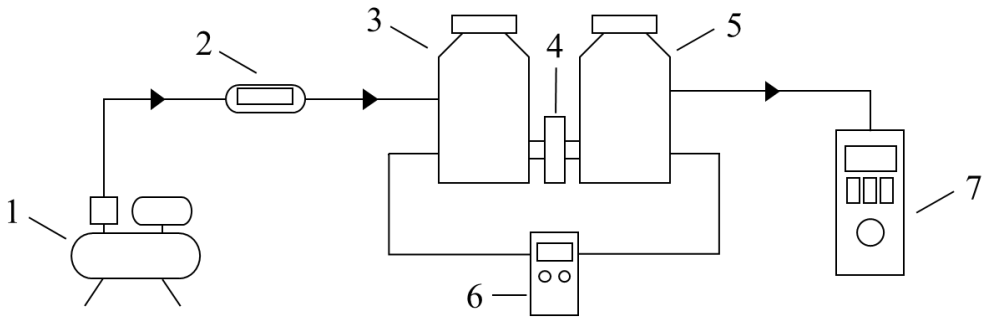

Figure I-1 Scheme of PM filtration set. 1. Air compressor; 2. Flow meter; 3. Smoke-generating bottle; 4. Air filter; 5. Air filtered bottle; 6. Differential pressure gauge; 7. Particle counter.

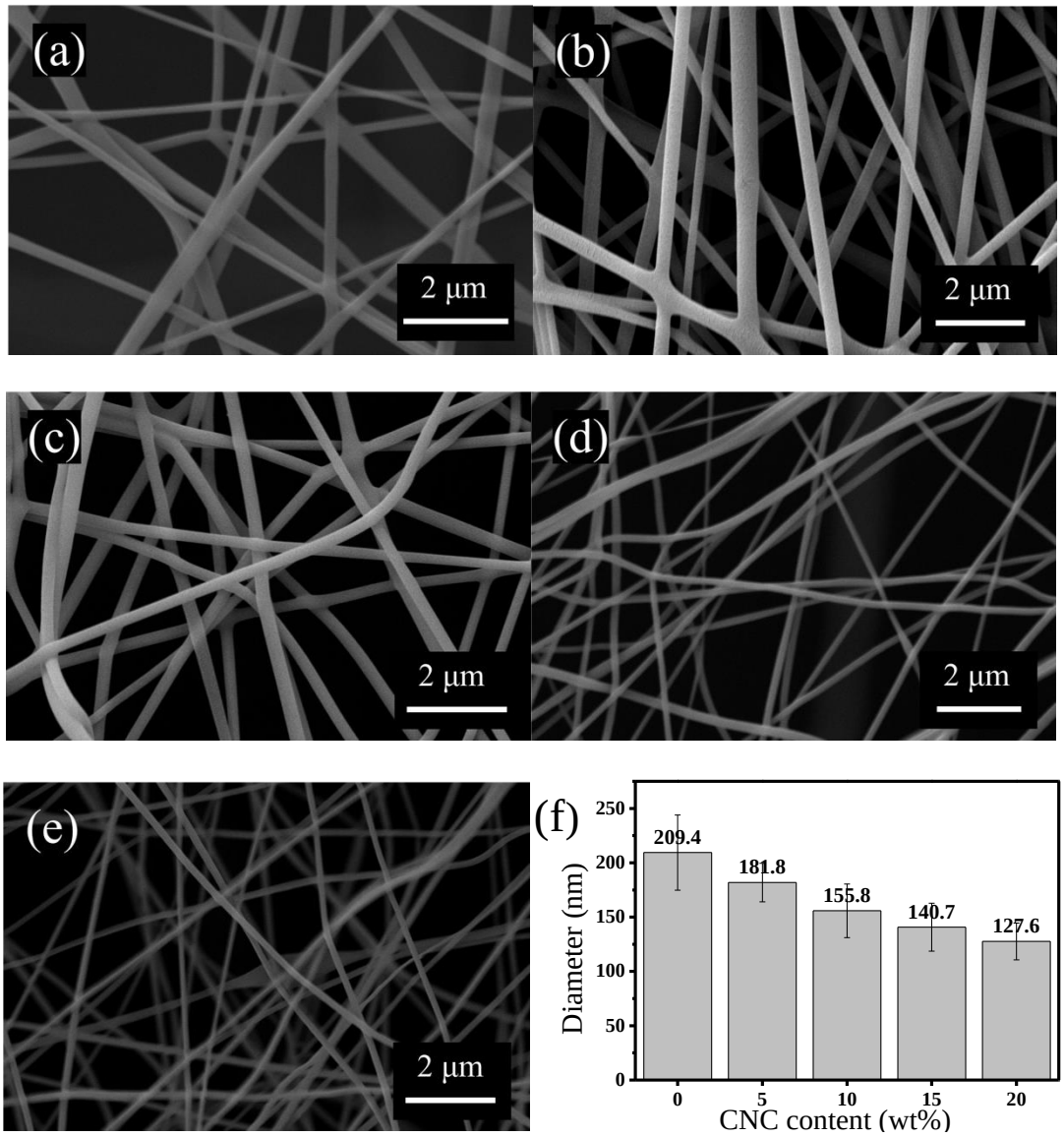

Figure I-2 SEM images of electrospun PVA and PVA/CNCs nanofibrous filters fabricated with various CNC content (0~20%): (a) PVA-6, (b) PVA/CNC-5-6, (c) PVA/CNC-10-6, (d) PVA/CNC-15-6 and (e) PVA/CNC-20-6. (f) Effect of CNC content on fiber diameter distribution of electrospun PVA and PVA/CNCs nanofibrous filters.

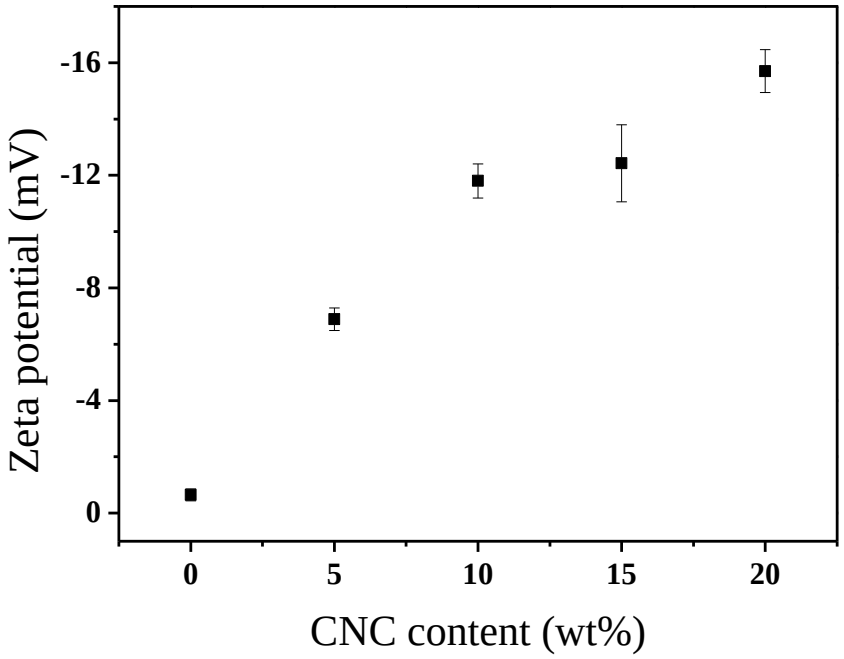

Figure I-3 Zeta potentials of prepared PVA and PVA/CNCs suspensions.

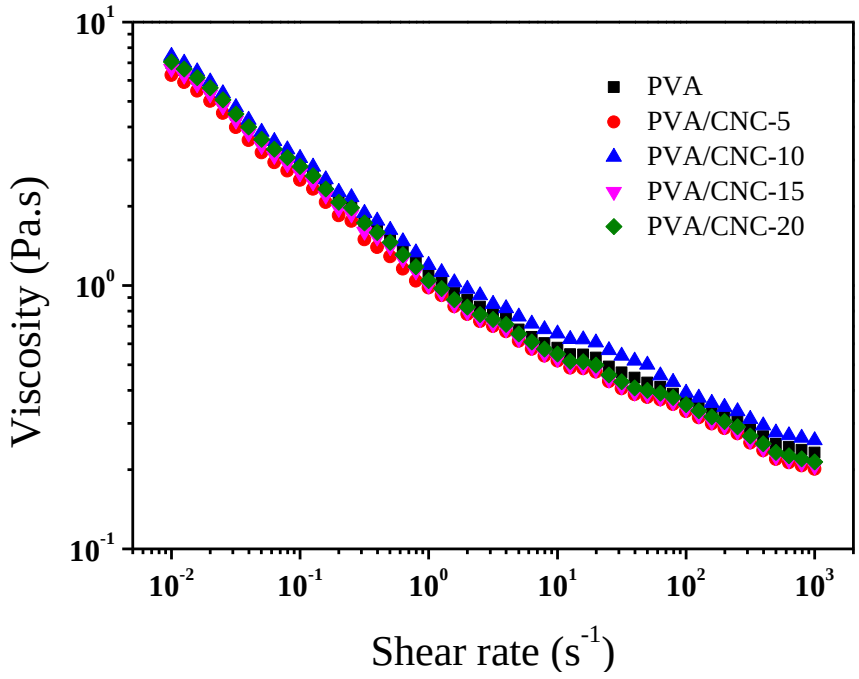

Figure I-4 Viscosities of prepared PVA and PVA/CNCs suspensions.

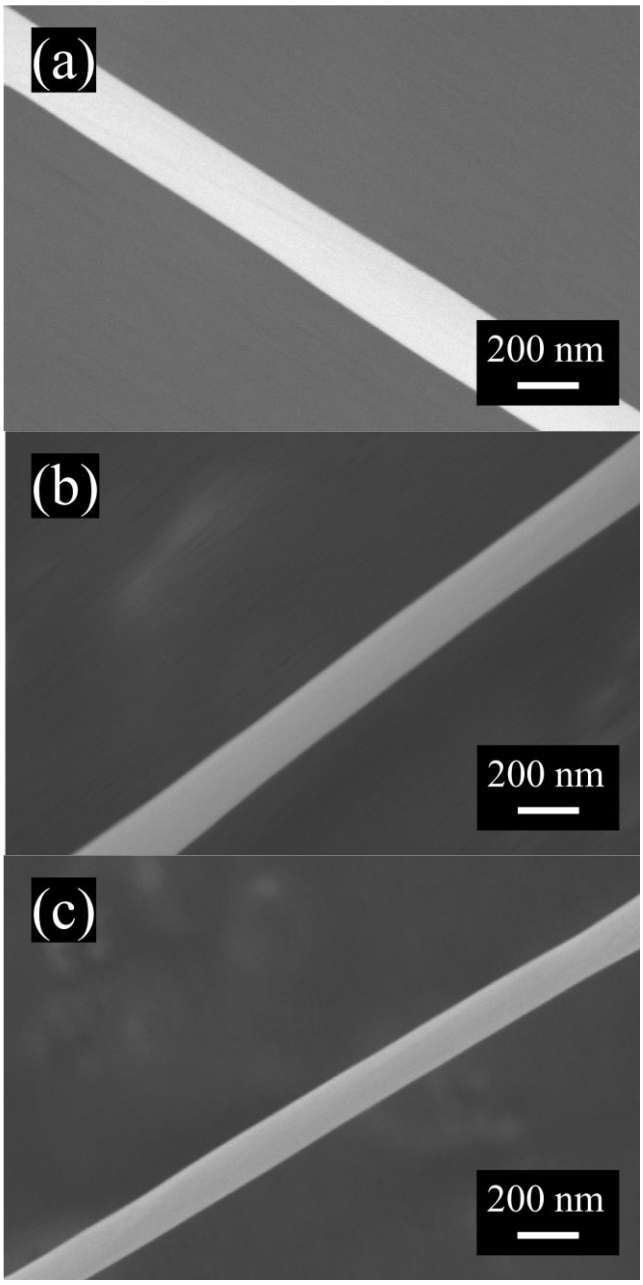

Figure I-5 SEM images of fiber surface (a) PVA-2, (b) PVA/CNC-10-2 and (c) PVA/CNC-20-2.

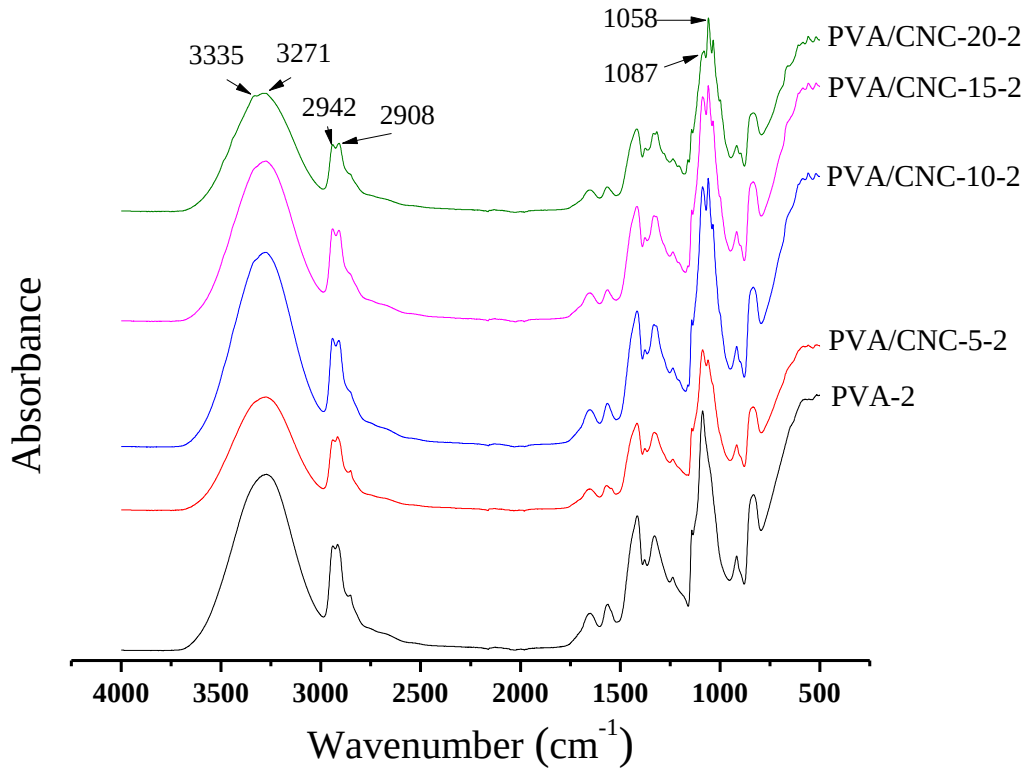

Figure I-6 FTIR spectra of PVA-2, PVA/CNC-5-2, PVA/CNC-10-2, PVA/CNC-15-2 and PVA/CNC-20-2 electrospun air filters.

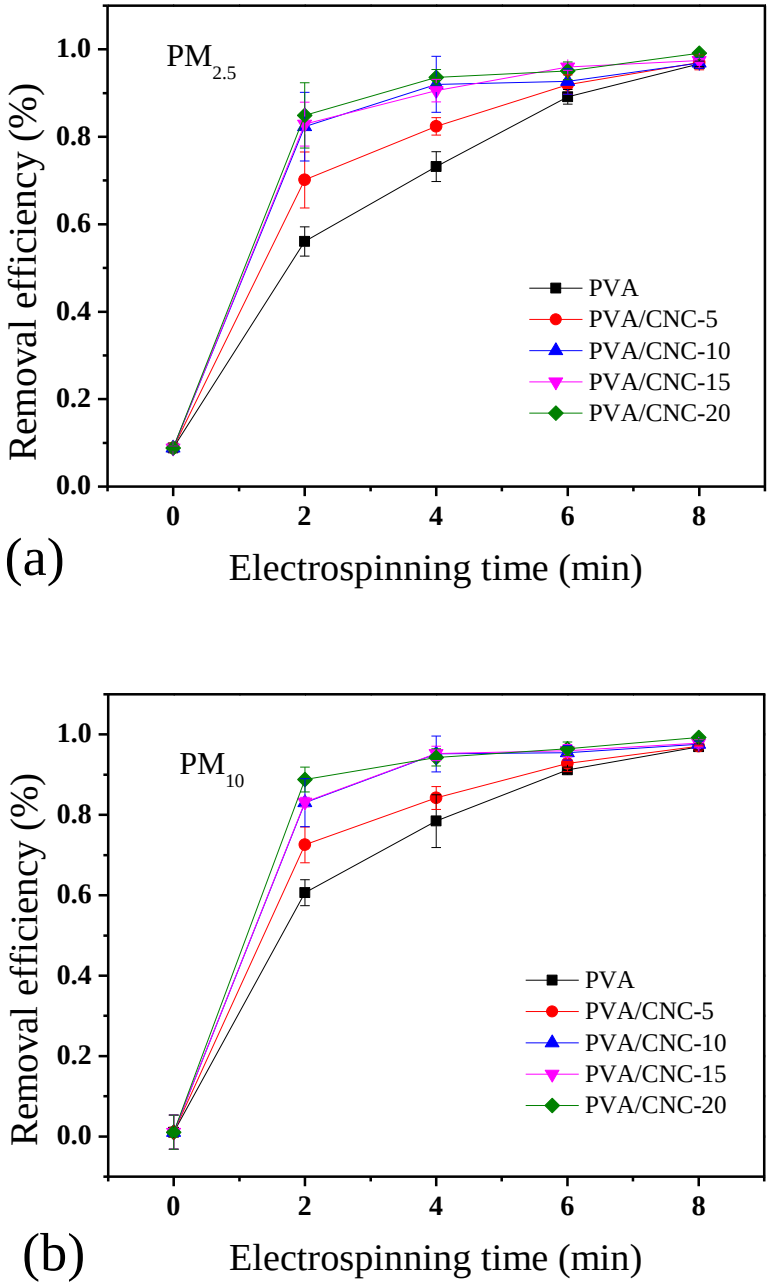

Figure I-7 (a) $PM_{2.5}$ and (b) PM_{10} removal efficiencies of PVA and PVA/CNCs filters versus electrospinning time.

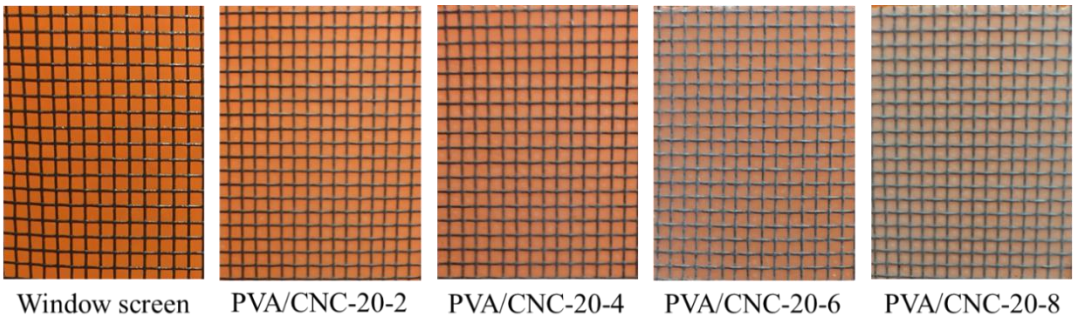

Figure I-8 Photographs of window screen and fabricated PVA/CNCs filters with different basis weights.

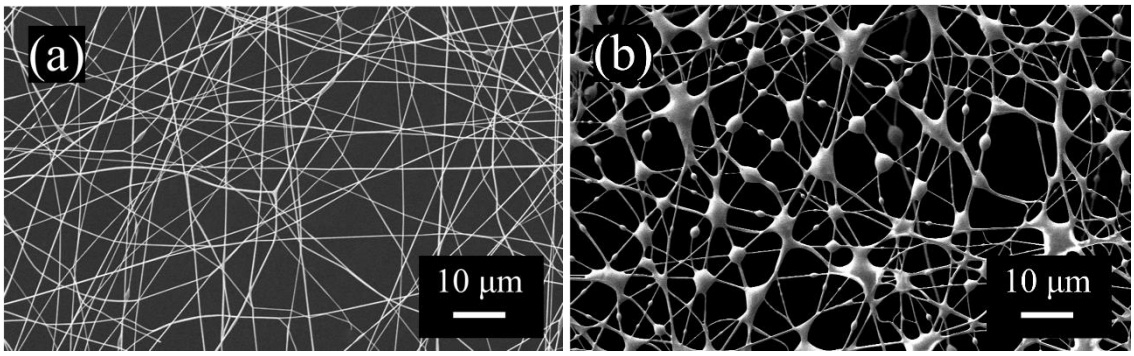

Figure I-9 SEM images of PVA/CNC-20-2 filter a) before and b) after particle capturing. PVA/CNC-20-2 represents filter fabricated by PVA/CNCs suspension with 20% CNCs and the electrospinning time was 2 min.

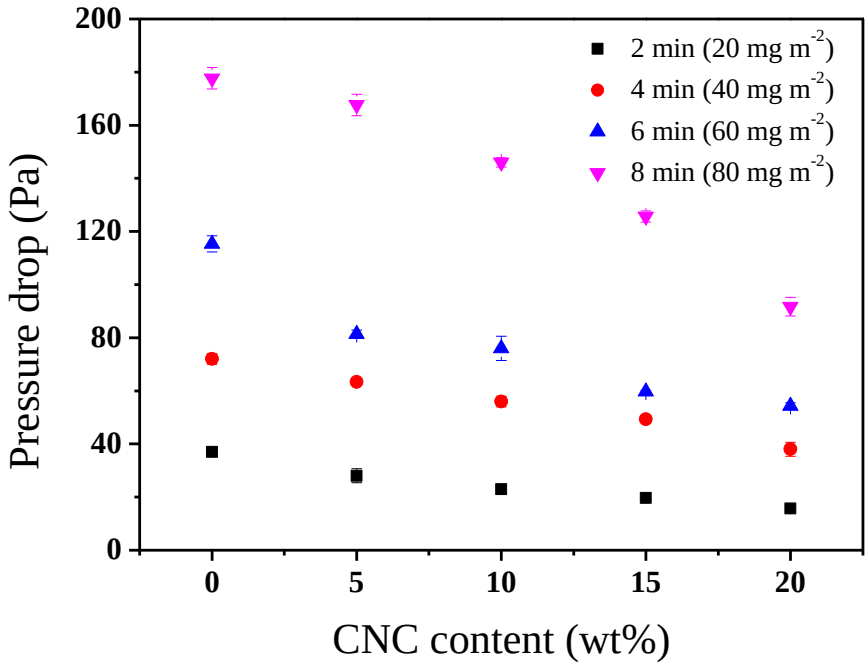

Figure I-10 Pressure drops of PVA and PVA/CNCs filters fabricated with different electrospinning time (different basis weight) versus CNC content.

Table I-1 Diameters of electrospun air filters with different CNCs content.

Level	Mean (nm)	Standard deviation	Coefficient of variance
0% CNC	209.4	34.6	16.52%
5% CNC	181.8	17.8	9.79%
10% CNC	155.8	24.6	15.79%
15% CNC	140.7	22.0	15.64%
20% CNC	127.6	16.9	13.24%

Table I-2 *t*-test of filter diameters between groups with different CNC content.

Level	- Level	Difference	Standard error of deviation	*p*-value
0% CNC	5% CNC	27.6	5.4	<0.0001*
5% CNC	10% CNC	26.0	5.4	<0.0001*
10% CNC	15% CNC	15.1	5.1	0.0034*
15% CNC	20% CNC	13.1	5.1	0.0106*
0% CNC	20% CNC	81.8	5.4	<0.0001*
0% CNC	15% CNC	68.7	5.1	<0.0001*
5% CNC	20% CNC	54.2	5.4	<0.0001*
0% CNC	10% CNC	53.5	5.4	<0.0001*
5% CNC	15% CNC	41.1	5.2	<0.0001*
10% CNC	20% CNC	28.3	5.4	<0.0001*

Table I-3 Pressure drops of air filters fabricated with electrospinning time of 2 min.

Level	Mean (Pa)	Standard deviation	Coefficient of variance
PVA-2	37.0	1.7	4.68%
PVA/CNC-5-2	28.0	2.6	9.45%
PVA/CNC-10-2	23.0	1.0	4.35%
PVA/CNC-15-2	19.7	0.6	2.94%
PVA/CNC-20-2	15.7	1.5	9.75%

Table I-4 *t*-test of pressure drops between groups with different CNC content. Electrospinning time is 2 min.

Level	- Level	Difference	Standard error of deviation	*p*-value
PVA-2	PVA/CNC-5-2	9.0	1.3	<0.0001*
PVA/CNC-5-2	PVA/CNC-10-2	5.0	1.3	0.0041*
PVA/CNC-10-2	PVA/CNC-15-2	3.3	1.3	0.0331*
PVA/CNC-15-2	PVA/CNC-20-2	4.0	1.3	0.0142*
PVA-2	PVA/CNC-15-2	17.3	1.3	<0.0001*
PVA-2	PVA/CNC-10-2	14.0	1.3	<0.0001*
PVA-2	PVA/CNC-20-2	21.3	1.3	<0.0001*
PVA/CNC-5-2	PVA/CNC-20-2	12.3	1.3	<0.0001*
PVA/CNC-5-2	PVA/CNC-15-2	8.3	1.3	0.0001*
PVA/CNC-10-2	PVA/CNC-20-2	7.3	1.3	0.0003*

Table I-5 Pressure drops of air filters fabricated with electrospinning time of 4 min.

Level	Mean (Pa)	Standard deviation	Coefficient of variance
PVA-4	72.0	2.0	2.78%
PVA/CNC-5-4	63.3	1.2	1.82%
PVA/CNC-10-4	56.0	2.0	3.57%
PVA/CNC-15-4	49.3	1.2	2.34%
PVA/CNC-20-4	38.0	2.6	6.96%

Table I-6 *t*-test of pressure drops between groups with different CNC content. Electrospinning time is 4 min.

Level	- Level	Difference	Standard error of deviation	*p*-value
PVA-4	PVA/CNC-5-4	8.7	1.5	0.0002*
PVA/CNC-5-4	PVA/CNC-10-4	7.3	1.5	0.0007*
PVA/CNC-10-4	PVA/CNC-15-4	6.7	1.5	0.0015*
PVA/CNC-15-4	PVA/CNC-20-4	11.3	1.5	<0.0001*
PVA-4	PVA/CNC-10-4	16.0	1.5	<0.0001*
PVA-4	PVA/CNC-15-4	22.7	1.5	<0.0001*
PVA-4	PVA/CNC-20-4	34.0	1.5	<0.0001*
PVA/CNC-5-4	PVA/CNC-15-4	14.0	1.5	<0.0001*
PVA/CNC-5-4	PVA/CNC-20-4	25.3	1.5	<0.0001*
PVA/CNC-10-4	PVA/CNC-20-4	18.0	1.5	<0.0001*

Table I-7 Pressure drops of air filters fabricated with electrospinning time of 6 min.

Level	Mean (Pa)	Standard deviation	Coefficient of variance
PVA-6	115.3	3.1	2.65%
PVA/CNC-5-6	81.3	1.5	1.88%
PVA/CNC-10-6	76.0	4.6	6.03%
PVA/CNC-15-6	59.7	0.6	0.97%
PVA/CNC-20-6	54.3	1.2	2.13%

Table I-8 *t*-test of pressure drops between groups with different CNC content. Electrospinning time is 6 min.

Level	- Level	Difference	Standard error of deviation	*p*-value
PVA-6	PVA/CNC-5-6	34.0	2.1	<0.0001*
PVA/CNC-5-6	PVA/CNC-10-6	5.3	2.1	0.0318*
PVA/CNC-10-6	PVA/CNC-15-6	16.3	2.1	<0.0001*
PVA/CNC-15-6	PVA/CNC-20-6	5.3	2.1	0.0318*
PVA-6	PVA/CNC-10-6	39.3	2.1	<0.0001*
PVA-6	PVA/CNC-15-6	55.7	2.1	<0.0001*
PVA-6	PVA/CNC-20-6	61.0	2.1	<0.0001*
PVA/CNC-5-6	PVA/CNC-15-6	21.7	2.1	<0.0001*
PVA/CNC-5-6	PVA/CNC-20-6	27.0	2.1	<0.0001*
PVA/CNC-10-6	PVA/CNC-20-6	21.7	2.1	<0.0001*

Table I-9 Pressure drops of air filters fabricated with electrospinning time of 8 min.

Level	Mean (Pa)	Standard deviation	Coefficient of variance
PVA-8	177.7	4.0	2.27%
PVA/CNC-5-8	167.7	4.0	2.41%
PVA/CNC-10-8	146.0	1.7	1.19%
PVA/CNC-15-8	125.7	2.1	1.66%
PVA/CNC-20-8	91.7	3.5	3.83%

Table I-10 *t*-test of pressure drops between groups with different CNC content. Electrospinning time is 8 min.

Level	- Level	Difference	Standard error of deviation	*p*-value
PVA-8	PVA/CNC-5-8	10.0	2.6	0.0036*
PVA/CNC-5-8	PVA/CNC-10-8	21.7	2.6	<0.0001*
PVA/CNC-10-8	PVA/CNC-15-8	20.3	2.6	<0.0001*
PVA/CNC-15-8	PVA/CNC-20-8	34.0	2.6	<0.0001*
PVA-8	PVA/CNC-10-8	31.7	2.6	<0.0001*
PVA-8	PVA/CNC-15-8	52.0	2.6	<0.0001*
PVA-8	PVA/CNC-20-8	86.0	2.6	<0.0001*
PVA/CNC-5-8	PVA/CNC-15-8	42.0	2.6	<0.0001*
PVA/CNC-5-8	PVA/CNC-20-8	76.0	2.6	<0.0001*
PVA/CNC-10-8	PVA/CNC-20-8	54.3	2.6	<0.0001*

Table I-11 Performance summary of air filters for $PM_{2.5}$.

Polymers/filters	E (%)	ΔP (Pa)	V (m s^{-1})	Q_f (Pa^{-1})	Reference
PVA-8	96.7	178	0.20	0.019	
PVA/CNC-5-8	97.0	168	0.20	0.021	
PVA/CNC-10-8	96.9	146	0.20	0.024	
PVA/CNC-15-6	96.0	60	0.20	0.054	
PVA/CNC-15-8	97.4	126	0.20	0.029	
PVA/CNC-20-6	95.1	56	0.20	0.054	
PVA/CNC-20-8	99.1	91	0.20	0.052	
PAN	96.1	133	0.21	0.024	Liu et al., 2015b
Nylon	99.0	250	0.50	0.018	Liu et al., 2018
PLA	99.9	165	0.14	0.023	Wang et al., 2015
PVAc	98.8	80	0.053	0.055	Matulevicius et al., 2016

E, PM removal efficiency; ΔP, pressure drop; Q_f, quality factor, $Q_f = -\ln(1-E)/\Delta P$; V, face velocity.

CHAPTER II

OPTIMIZATION OF ELECTROSPUN POLY(VINYL ALCOHOL)/CELLULOSE NANOCRYSTALS COMPOSITE NANOFIBROUS FILTER FABRICATION USING RESPONSE SURFACE METHODOLOGY

A version of this chapter was submitted to *Carbohydrate polymers* on July 10th, 2020.

Authors:

Qijun Zhang, Timothy M. Young, David P. Harper, Terry Liles, Siqun Wang
Center for Renewable Carbon, University of Tennessee, Knoxville, TN, United States

Terry Liles
Huber Engineered Woods, Commerce, GA, United States

Q. Zhang's primary contribution to this paper includes identifying the research objective, design and conduct of the experiments, process and interpretation of the data, drafting the paper.

Co-researchers' contributions are listed as follows:
T.M. Young identified the research method, provided research guideline, worked with Qijun to analyze the data and revised the paper.
D.P. Harper worked with Qijun to fabricate the nanofibrous air filters.
T. Liles revised the paper.
S. Wang provided research guideline, worked with Qijun to investigate the experimental parameters and revised the paper.

Abstract

A Poly(vinyl alcohol) (PVA)/cellulose nanocrystals (CNCs) composite nanofibrous air filter was fabricated via electrospinning. CNCs were added to improve the overall filtration performance for particulate matter (PM) removal. The integral effect of different properties of electrospinning suspension on the $PM_{2.5}$ removal efficiency and pressure drops were studied. To optimize the fabrication parameters, variables such as suspension concertation and CNCs percentage at different levels were systematically investigated using response surface methodology. The feasible operating space, where the suspension concentration and CNCs percentage were varied from 6% to 8% and 5% to 20%, respectively, was evaluated with reduced experimental runs using a face-centered central composite design. Our results indicate the quadratic models developed for predicting responses were adequate. The optimum filtration performance for $PM_{2.5}$ was achieved with 7.34% of suspension concentration and 20% of CNCs percentage, where the removal efficiency was 94% and the pressure drop was only 34.9 Pa.

1. Introduction

In the recent decades, particulate matter (PM) pollution has become a global concern due to its influence on public health (Heal et al., 2012, Lepeuleet al., 2012, Pope III et al., 2002). To reduce the exposure to PM, especially $PM_{2.5}$, which can deeply penetrate into lungs and bronchi due to their smaller size, numerous strategies have been proposed to develop air filters (Fan et al., 2018b, Gopal et al., 2007, Jeong et al., 2017, Li et al., 2017, Liu et al., 2015b, Zhang et al., 2016c). Among those approaches, electrospinning is one commonly used technique because it is able to produce ultrafine fibers effectively (Doshi and Reneker, 1995, Huang et al., 2006). The reduced fiber diameter could increase the specific surface area and the porosity of the filter medium. Therefore, the filter can capture more PM while allowing air molecules to pass through (Kenawy et al., 2002, Podgórski et al., 2006). This is particularly true when the diameter is less than 200 nm, where the slip-effect applies, and air molecules bypass the nanofibers without colliding with them (Brown, 1993, Hung and Leung, 2011, Zhao et al., 2016). The decreased pressure drop could effectively reduce the energy consumption during the filtration process (Yun et al., 2007).

In our previous study, an electrospun poly(vinyl alcohol) (PVA)/cellulose nanocrystals (CNCs) air filter with superior $PM_{2.5}$ filtration efficiency and low air resistance was successfully developed via an environmentally friendly method (Zhang et al., 2019, Zhang et al., 2020). The PVA and CNCs polymer hybrid was utilized for fabricating nanofibrous filters because it is nontoxic, biodegradable and water-soluble. The use of water-soluble polymer avoided large amount of organic solvents during electrospinning. More importantly, CNCs improved both the mechanical property and the overall filtration performance of the electrospun filter (Feng et al., 2017, Huang et al., 2017, Zhang et al., 2019). The negative charge of CNCs was revealed as a key factor affect the filtration performance as it promoted the formation of finer fibers. Since cellulose is one of the most abundant natural polymers on the earth, CNCs are very promising to be used as additives in electrospinning polymer matrix for fabricating air filters.

However, the process of electrospinning is also affected by many other parameters. Only a balanced status between the repulsive and constrictive forces along the jets at the Taylor cone would generate fibers with desired uniform morphology (Huang et al., 2006, Reneker and Yarin, 2008). The properties of the electrospinning solution, such as viscosity,

conductivity and surface tension, have an integral effect on the stability of the Taylor cone. These properties affect not only the diameter of the electrospun fibers, but also the shape of the fibers and the structure of the nanofiber network (Garg and Bowlin, 2011, Thompson et al., 2007). When the factors other than conductivity vary, the influence of CNCs on solution surface charge density which reduces fiber diameter and improves filtration performance remains unclear. Additionally, it will be difficult to estimate the fiber diameter once the beaded, bundled or ribbon-like fibers are formed. Therefore, it is no longer applicable to evaluate the filtration performance of the electrospun filters through fiber diameter. The effects of various properties of the electrospinning solution on $PM_{2.5}$ removal efficiency and pressure drop should be considered comprehensively and evaluated directly.

Previous studies have investigated the effect of electrospinning parameters through one-factor-at-a-time method (Ding et al., 2002, Garg and Bowlin, 2011, Supaphol and Chuangchote, 2008, Thompson et al., 2007). But previous methods were time consuming and did not examine interaction effects. Especially, when studying the effects of various properties of the electrospinning solution, different properties are normally varied simultaneously as the concentration or the composition of the solution changes. To overcome these limitations, response surface methodology (RSM) is often utilized (Bösiger et al., 2018, Meng et al., 2015, Sarlak et al., 2012). As an effective statistical modeling tool, RSM can be used for enhanced inference, studying interaction effects, and parameter optimization (Montgomery, 2017). It is a technique that maximizes inference while minimizing the number of experimental runs and costs of experimentation (Fu et al., 2016).

The objective of this study was to estimate the overall filtration performance of electrospun PVA/CNCs filters based on simultaneous effects of key factors, and to predict the optimum condition for fabricating PVA/CNCs filters using RSM. Two variables, ‘suspension concentration’ and ‘CNCs percentage’ were selected to represent the integral properties of PVA/CNCs suspension. The ‘removal efficiency’ for $PM_{2.5}$ and the ‘pressure drop’ of the electrospun filter were directly evaluated as responses. A face-centered central composite design (CCF) was applied for the RSM, and the coefficients of the constructed quadratic mathematical model were evaluated over the feasible operating space. The morphology of the electrospun filters fabricated under different conditions was also studied.

2. Experimental section

2.1. Materials

PVA (M_w 85000-124000) with degree of hydrolysis >99% was purchased from Sigma-Aldrich. CNCs (~12 wt%, produced by hydrolysis using sulfuric acid) with 150-200 nm length and 5-20 nm width were purchased from the University of Maine (Orono, ME). The commercial window screens used as collectors were purchased from Saint-Gobain ADFORS (Clear Advantage). The wire diameter and mesh size of the window screen were 0.25 mm and 1.2 mm × 1.2 mm, respectively. All the chemicals and materials were used as received.

2.2. Preparation of PVA/CNCs suspensions

PVA was fully dissolved in deionized water, and specified amounts of CNCs were added to obtain a CNCs percentage of PVA content ranging from 5% to 20% (wt/wt), while total concentration was kept from 6% to 8% (wt/wt). These feasible ranges of CNCs percentage and the suspension concentration were determined based on preliminary screening experiments. The prepared PVA/CNCs suspension was then mixed by ultrasonication (VCF-1500, Sonics) in an ice bath for 2 min under 600 W of power (Zhang et al., 2019).

2.3. Electrospinning of PVA/CNCs nanofibrous filters

The electrospinning setup is shown in Figure II-1. The prepared suspension was loaded into a 5 mL plastic syringe capped with 22-gauge metal needle and pumped out with a flow rate of 0.5 mL h^{-1}. A grounded metal rolling cylinder covered by window screen was placed at a working distance of 10 cm from the needle tip as a collector. The needle tip was applied with a high voltage of 22 kV by a voltage generator (Series EK, Glassman High Voltage). All the electrospinning processes were performed at room temperature and 50 ± 5% relative humidity.

2.4. Morphology characterizations

Scanning electron microscope (SEM) images of the electrospun filters were characterized using a Zeiss Auriga SEM/FIB crossbeam workstation. The SEM analysis was operated with an acceleration voltage of 5 kV. All samples were gold coated before

observation.

2.5. Filtration performance of electrospun PVA/CNCs filters for $PM_{2.5}$

The test of filtration performance followed the method described in our previous study (Zhang et al., 2019). Briefly, the fabricated filter was clamped between two flanges of two customized bottles (Figure II-2). An air compressor was connected to generate air flow and the flow rate was controlled at 0.2 m s^{-1} by a flow meter. Pressure drop across the filter was measured by a Testo 510 differential pressure gauge. PM particles were generated by burning incense, and a particle counter (DT-9851M, CEM) was used to measure the concentration of $PM_{2.5}$. The inflow $PM_{2.5}$ concentration was controlled at >500 μg m^{-3}. Removal efficiency (E) was calculated as:

$$E\ (\%) = (1 - C_t/C_0) \times 100 \quad (1)$$

where C_t and C_0 are the measured outflow $PM_{2.5}$ concentrations with and without filter, respectively.

2.6. Experimental design

Figure II-3 shows a graphic illustration of a two-factor orthogonal CCF. The factorial matrix consists of factorial points (blue points), axial points (red points) and center points. The estimation of response surface curvature in this design was augmented with the axial points, which are at the center of each face of the factorial space and representing intermediate values (high and low) for each factor. For fitting quadratic model, three levels of each factor ('CNCs percentage' and 'suspension concentration') were used (Table II-1). The levels were determined based on preliminary factorial experiments. The CCF provided a prediction over the entire feasible operating space.

The full factorial CCF experiments require a certain number of experimental runs, which could be calculated as:

$$N = 2^k + 2k + n_c \quad (2)$$

where k is the number of factors and n_c is the number of center points. 2^k represents the number of factorial points and $2k$ is the number of axial points. In this study, both k and n_c are 2. Therefore, with a replicate for each of the point, the total number of experimental runs of this design was n = 20, including 8 factorial points, 8 axial points and 4 center points. Experimental runs were randomized.

The quadratic mathematical model constructed for estimating the functional relationship between independent variables *x* and each response *y* can be described as:

$$y = b_0 + \sum_{i=1}^{k} b_i x_i + \sum_{i=1}^{k} b_{ii} x_i^2 + \sum_{i=1, j=i+1}^{k} b_{ij} x_i x_i + \varepsilon \quad (3)$$

where b_0 is a constant, b_i, b_{ii} and b_{ij} are the regression coefficients of the individual linear effect, quadratic effect and interaction effect between the variables, respectively; *k* is the number of factors and ε is the error component.

All statistical analyses were performed using JMP software (version 14, SAS Institute) which included an analysis of variance (ANOVA), regression coefficient estimation, quadratic model validation, and response surface plots.

3. Results and Discussion

3.1. Morphology characterization of electrospun filters

The filters were fabricated by electrospinning the suspensions of given concentrations and CNCs percentages (Table II-1). As shown in Figure II-4, the morphology of electrospun PVA/CNCs filters was strongly affected by the concentration of electrospinning suspension. A transition of the fibers from beaded to bead-free was observed as the concentration increased from 6% to 7% and 8%. The occurrence of beading is a common phenomenon in electrospinning, which could be resulted by various process parameters. When the concentration is low, due to the low viscosity, the initiating jet cannot be sufficiently elongated under the applied electrical field, and the low viscoelastic force is not enough to overcome the surface tension. The resulted capillary instability then caused the formation of beads (Ding et al., 2002, Fong et al., 1999, Thompson et al., 2007). As the CNCs percentage increased from 5% to 10% and 20%, the number of beads decreased and the beads were more elongated into a spindle-like shape (Figure II-4b and II-4c). This could be attributed to the increased charge density introduced by CNCs, which increased the electrostatic stretching force applied on the jet and suppressed the surface tension (Fong et al., 1999, Reneker and Yarin, 2008). Additionally, because the total concentration of 6% is relatively low, increased addition of CNCs may also play a role in the change of the suspension viscosity, which could increase the viscoelastic force and reduce the formation

of beads. As the suspension concentration was raised to 7%, regardless of the amount of added CNCs, the beads on the electrospun fibers were eliminated and the fibers formed smoothly and uniform. This could be explained by the improved stability of the Taylor cone. The increased viscoelastic force stabilized the initiating jet, allowed the jet being stretched evenly, and then produced uniform fibers (Figure II-4d) (Ding et al., 2002, Reneker and Yarin, 2008). Our previous study has demonstrated that adding CNCs up to 20% of PVA content in suspension with 7% total concentration, the viscosity was not changed due to the small amount of CNCs (Zhang et al., 2019). Therefore, the stability of the initiating jet was maintained as increasing the CNCs percentage. In addition, adding CNCs was expected to increase the surface charge density of the electrospinning suspension and thereby reducing the fiber diameter (Figure II-4e and II-4f) (Zhang et al., 2019). Similarly, bead-free fibers were also obtained as the suspension concentration was 8%. However, the prepared fibers appeared to be larger in diameter as the concentration increased, which is consistent with previous studies (Figure II-4g to II-4i) (Ding et al., 2002, Thompson et al., 2007). This may lower the filtration performance of the electrospun air filter.

3.2. Estimation of coefficients in mathematical polynomial function and model validation

The CCF design and the experimental results are presented in Table II-2. The pattern of experimental runs in this design was coded based on the independent variables. The symbols '+' and '-' represented the high and low level of the factorial points. The letters 'A' and 'a' represented the high and low extreme value of the axial points, and '0' was the center point. Within the operating space of the independent variables, the two responses, $PM_{2.5}$ removal efficiency and pressure drop, ranged from 82.8% to 96.6% and 54 Pa to 486 Pa, respectively. This indicated that both removal efficiency and pressure drop of the electrospun filter are affected by the suspension concentration and CNCs percentage. All the obtained experimental results were utilized as training data set for developing prediction quadratic model. The fitted model for describing the relationship between the response variable of removal efficiency and the factors is:

$$E = 91.98 + 2.39(S\text{-}7) + 0.12(C\text{-}12.5) + 0.18(S\text{-}7)(C\text{-}12.5) - 5.24(S\text{-}7)^2 + 0.01(C\text{-}12.5)^2 \quad (4)$$

where E is the removal efficiency, S is the suspension concentration and C is the CNCs percentage. The model for response variable of pressure drop and the factors is:

$$\Delta P = 47.91 - 97.76(S\text{-}7) - 5.88(C\text{-}12.5) + 4.49(S\text{-}7)(C\text{-}12.5) + 172.75(S\text{-}7)^2 + 0.58(C\text{-}12.5)^2 \quad (5)$$

where ΔP is the pressure drop, S is the suspension concentration and C is the CNCs percentage.

To estimate how well the models describe the experimental data, the goodness of fit test was applied. The actual versus predicted values plots were plotted in Figure II-5. According to the fitting results, there was a correlation between actual and predicted removal efficiencies, where the coefficient of determination R-squared (R^2) was 0.72 (Figure II-5a). The correlation between actual and predicted pressure drops was stronger, with a R^2 = 0.96 (Figure II-5b). The obtained R^2 indicated that both the suspension concentration model and the CNCs percentage model fit the experimental data well. The root mean square error (RMSE) for the two quadratic models were 2.44 and 29.01, respectively (Figure II-5).

The results of ANOVA for the two fitted models were summarized in Table II-3. The critical value for the F distribution, which is $F_{0.05, 5, 14} = 2.96$ (0.05 is the false rejection probability, 5 and 14 are the degrees of freedom of regression and residual, respectively), was used for both two models to determine whether reject the null hypothesis. As presented in Table II-3, the F-ratio for the removal efficiency model was 7.18, which is ~2.5 times greater than the critical value (2.96), indicating a statistical significance. However, a calculated F-ratio which is less than 3-5 times of the critical F value is considered as an indicator of relatively low significance (da Silva et al., 1999). For the pressure drop model, the F-ratio (72.38) was much higher, reaching ~25 times the critical value and suggesting a higher significance. Therefore, the model for pressure drop is considered more reliable than the model for removal efficiency. The significance of each coefficient in the models was evaluated based on p-value, and the coefficient with a p-value smaller than 0.05 is considered to be an important contributor to the model. In the removal efficiency model, the linear term suspension concentration, and the quadratic term suspension concentration^2 were significant, while the interaction term and CNCs percentage did not make significant contribution (Table II-3). Previous studies have demonstrated that the $PM_{2.5}$ removal

efficiency is associated with the specific surface area of the electrospun fibers and the porosity of the filter media (Kenawy et al., 2002, Podgórski et al., 2006), and adding CNCs could improve the removal efficiency by reducing the fiber diameter (Zhang et al., 2019). However, the results in this study indicated that, comparing with the effect of suspension concentration, the influence of CNCs on removal efficiency is relatively insignificant. This could be explained in that the changes in morphology of the electrospun fibers, which was caused by the variation of suspension concentration, had a greater impact on specific surface area of the fibers than the effect of CNCs on the reduction of fiber diameter. The estimated regression coefficients for term suspension concentration and term suspension concentration^2 were listed in Table II-4. In the model for pressure drop, the linear term suspension concentration and CNCs percentage, the quadratic term suspension concentration^2, and the interaction term were significant (Table II-3). The order of significance of the terms is: suspension concentration^2 ($p < 0.0001$), suspension concentration ($p < 0.0001$), CNCs percentage ($p = 0.0001$) and suspension concentration × CNCs percentage ($p = 0.0048$). As shown in Table II-4, CNCs percentage posed negative effect on pressure drop. These observations implied that, although CNCs percentage is not the main factor affecting removal efficiency when suspension concentration varies, increasing CNCs percentage within the operation space can significantly reduce the pressure drop across the filter.

To validate the fitted prediction models, additional experimental runs were conducted with randomly selected operating conditions. The ratio of training data to validation data was set as 0.7:0.3. Therefore, 8 additional data points were collected into the validation data set. The selected parameters for operation and the evaluated performance of the fabricated filters were listed in Table II-5. The figure of experimental responses from validation data set versus the predicted responses based on training data set were plotted in Figure II-6, and the fit of the regression was assessed using R^2 and RMSE. For the removal efficiency model, the calculated R^2 for validation was 0.64 (Figure II-6a), which was smaller than the one calculated based on training data ($R^2 = 0.72$) (Figure II-5a). The root mean square of prediction (RMSEP) for validation, which was calculated to be 1.66, was also smaller than the value from training data (RMSE = 2.44). Although smaller R^2 implied a lower correlation between the training and validation data, smaller RMSEP indicated a

better fit. These results indicated the constructed quadratic model can be used for predicting removal efficiency. As shown in Figure II-6b, the R^2 for validation of the pressure model (R^2 = 0.94) was similar to the value calculated from training data (R^2 = 0.96) (Figure II-5b); and the RMSEP = 20.19 was surprisingly smaller than the RMSE = 29.01 in the training data which sometimes occurs given that the validation n = 8 was smaller than n = 20 in training. Given these validation results, the fitted pressure drop model is considered adequate for prediction of pressure drop value and has better predictability for removal efficiency.

3.3. Optimization of $PM_{2.5}$ removal efficiency and pressure drop of electrospun PVA/CNCs nanofibrous filters

The response surface plots over the operation space of the two variables were utilized for examining the optimum condition of filter fabrication (Figure II-7a and II-7b). Two-dimensional contour plots were also used to help visualize the optimum along the response surfaces (Figure II-7c and II-7d). As shown in Figure II-7a, the response surface of removal efficiency showed a saddle-like shape. The maximum $PM_{2.5}$ removal efficiency was achieved (94.0%) at suspension concentration of 7.36% and CNCs percentage of 20%. In the contour plot of removal efficiency (Figure II-7c), it is clearly shown that only when the suspension concentration was over 6.5%, the effect of CNCs percentage on removal efficiency can be observed. According to the results of SEM tests (Figure II-4), it is believed that the electrospun fibers prepared with suspension concentration below 6.5% are mainly beaded. The addition of CNCs into PVA solution has limited effect on the fiber morphology. Therefore, the specific surface area of the fibers can hardly be influenced by CNCs. When the suspension concentration was higher than 6.5%, the removal efficiency was improved by increasing CNCs percentage (Figure II-7c). This could be attributed to the increased specific surface area, which was caused by the negative charge of CNCs. As the fibers became bead-free with increased suspension concentration, the negative charged CNCs elevated the surface charge density of the initial jet, and therefore promoted the formation of thinner fiber (Zhang et al., 2019).

The relationship between pressure drop and the two variables is shown in Figure II-7b. The minimum response was located at the center of the ellipses which were displayed in the contour plot (Figure II-7d). Combine the response surface and the contour plots, the

minimum pressure drop was observed as 24.5 Pa, where the corresponding suspension concentration was 7.2% and CNCs percentage was 16.6%. According to the result of estimation of regression coefficients, although CNCs percentage posed negative effect on pressure drop, the interaction between suspension concentration and CNCs percentage made opposite contribution to the response (Table II-4); hence, the minimum pressure drop was not achieved with a CNCs percentage of 20%.

To further determine the optimum processing condition with considering both responses, a prediction profiler analytical tool was utilized. Desirability in the profiler is a measure of how close the predicted value with optimal conditions to the desired value. The value of desirability ranges from 0 to 1, where 1 represents the ideal case. The desirability function is commonly used for parameters optimization in RSM, and the function is a smooth piecewise function that pass through three defining points. These points can be used to define the shape of desirability function to determine if the response should be maximized, minimized or close to some target value. The profile of prediction and the optimum condition for overall filtration performance is shown in Figure II-8. The desirability functions for removal efficiency and pressure drop were set as 'maximize' and 'minimize', respectively (Figure II-8, right column). The bottom row of the plot shows the trace of desirability for each factor. By adjusting the desirability, where the maximized geometric mean of desirability was obtained as 0.8674, the optimum condition for filter fabrication to achieve best overall filtration performance was revealed: suspension concentration of 7.34% and CNCs percentage of 20%. The estimated removal efficiency and pressure drop under the optimized processing conditions were 94% and 34.9 Pa, respectively.

It is worth mentioning that the RSM could also be used for optimizing parameters with some target response value. For example, if the $PM_{2.5}$ removal efficiency of the fabricated filter is required to be over 90%, the desirability function could be adjusted to be 0 when the removal efficiency is below 90%, and to be 'maximize' when the removal efficiency is over 90%. Additionally, the RSM also provided information about the scale of filtration performance of filters manufactured within the operating space. It is helpful to provide guidance on modifying parameters other than variables when there is a requirement need

to be meet, e.g., increasing electrospinning time to improve removal efficiency even though the pressure drop will be significantly elevated (Zhang et al., 2019).

4. Conclusions

In this study, the optimum operating parameters for fabricating PVA/CNCs nanofibrous air filter was investigated via RSM. The suspension concentration and CNCs percentage of the electrospinning suspension were selected as independent variables, and the removal efficiency for $PM_{2.5}$ and pressure drop across the filter were the two responses. A three-level-two factor CCF design was applied to study the integral effect of various properties of electrospinning suspension on the responses. Fitted quadratic prediction models estimated the responses effectively and were validated. The processing condition was successfully optimized, and the optimum filtration performance was achieved as removal efficiency was 94% and pressure drop was 34.9 Pa, with the suspension concentration of 7.34% and CNCs percentage of 20%. Adding CNCs improved the filtration performance of the filters by reducing the diameter of fibers when the electrospun fibers were bead-free. Comparing with conventional one-factor-at-a-time method, RSM gives more integrate and accurate results, while requiring less experimental runs and costs.

Appendix II

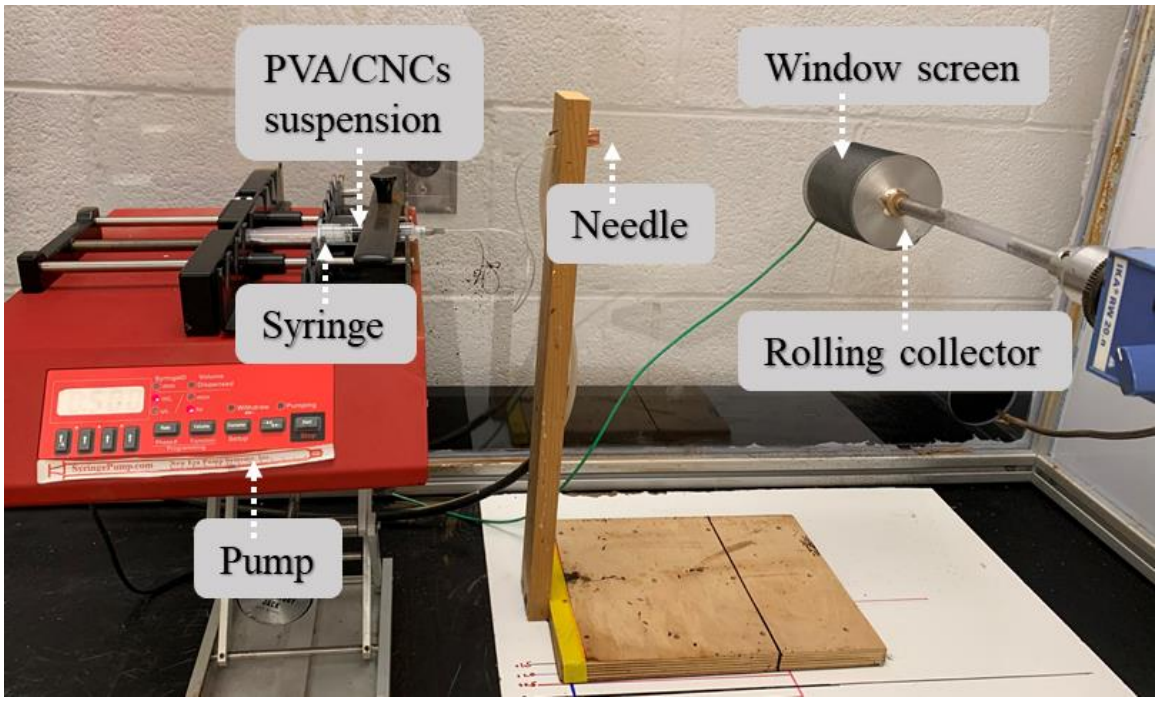

Figure II-1 Diagram of electrospinning experimental setup.

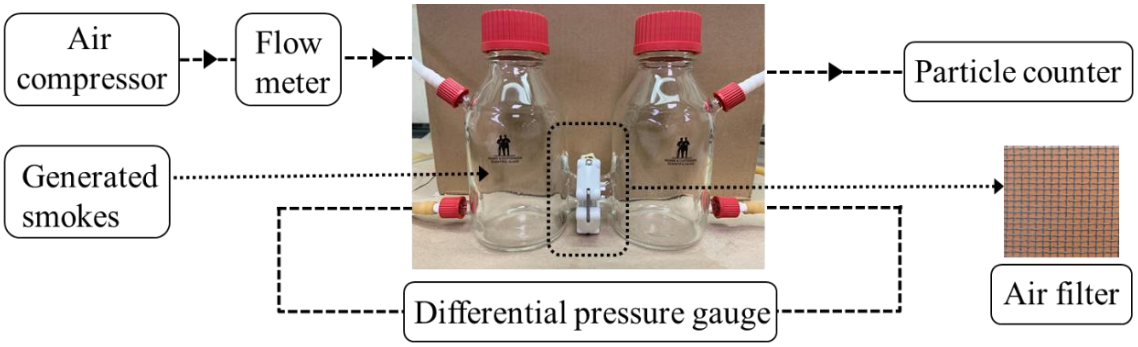

Figure II-2 Scheme of filtration system.

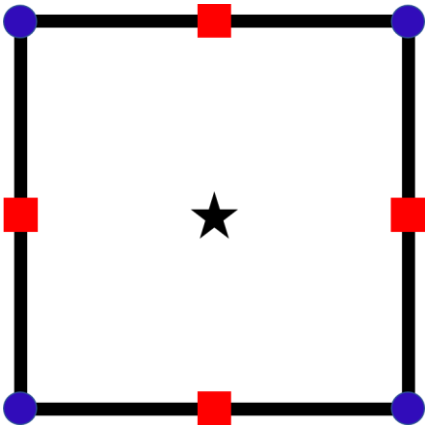

Figure II-3 Graphic illustration of two-factor CCF design.

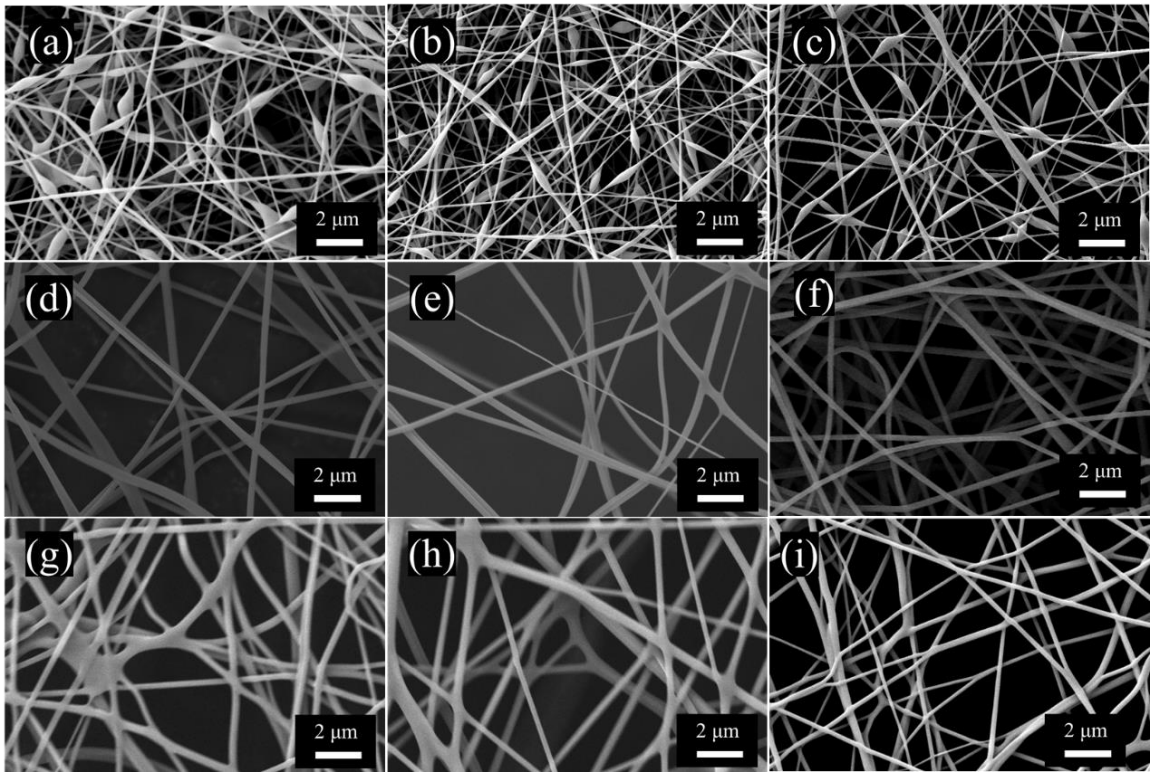

Figure II-4 SEM images of electrospun PVA/CNCs filters fabricated with suspension concentrations of (a-c) 6%, (d-f) 7% and (g-i) 8% and CNCs percentages of 5% (left), 10% (middle), and 20% (right).

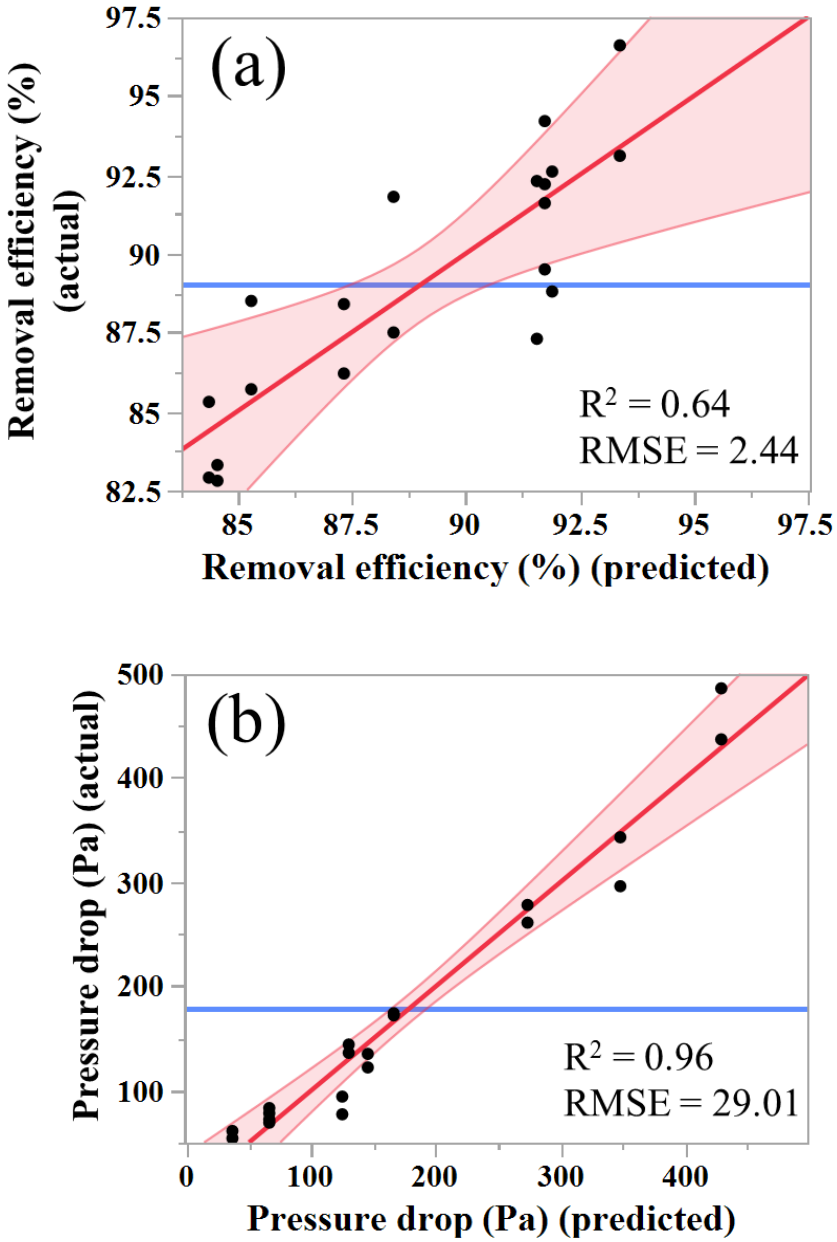

Figure II-5 Goodness of fit with training data between actual values and predicted values: (a) removal efficiency and (b) pressure drop.

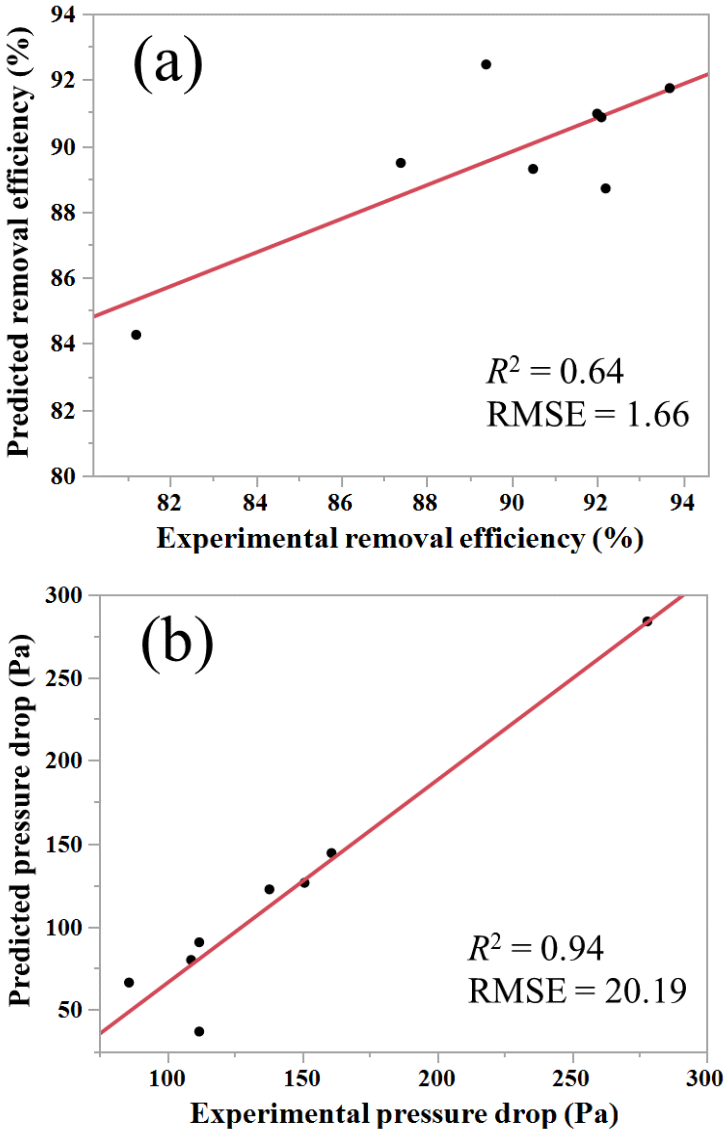

Figure II-6 Validation of developed prediction quadratic models: (a) removal efficiency and (b) pressure drop.

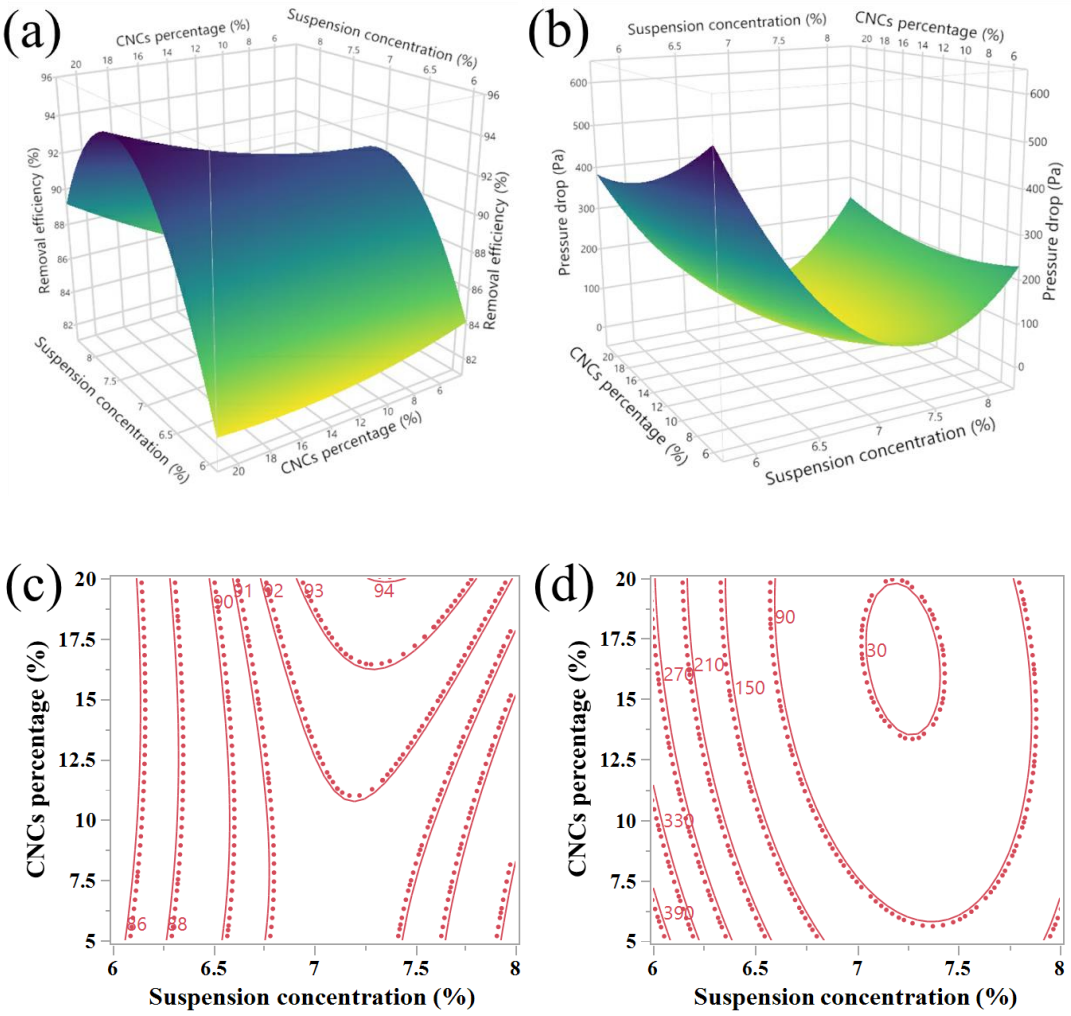

Figure II-7 Response surface plot of (a) removal efficiency and (b) pressure drop; and contour plot of (c) removal efficiency and (d) pressure drop.

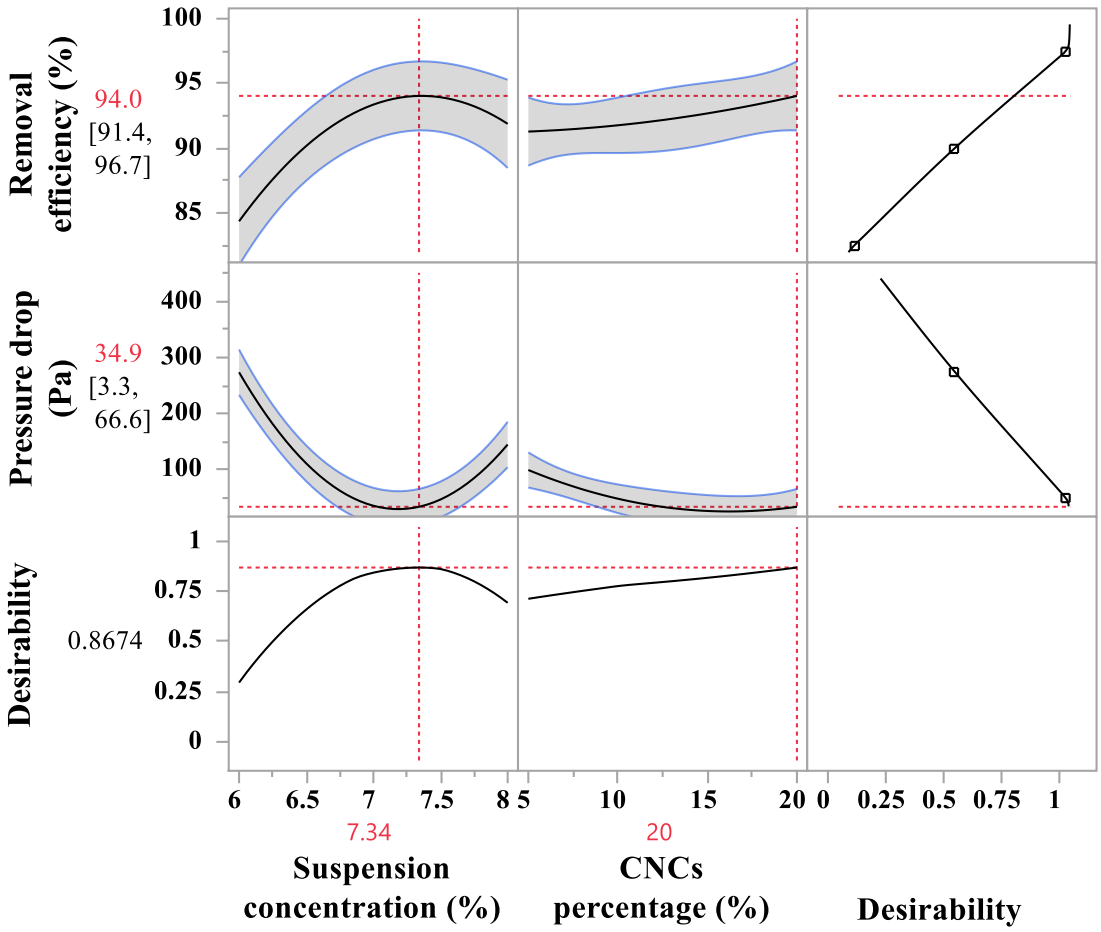

Figure II-8 Prediction profiler and desired conditions for optimum filtration performance.

Table II-1 The levels of each factor for CCF design.

Factor	Level		
	Low	Center	High
Suspension concentration (%)	6	7	8
CNCs percentage (%)	5	10	20

Table II-2 The CCF design and the experimental data for three-level-two factors response surface analysis.

Serial number	Pattern	Independent variable		Response variable	
		S (%)	*C* (%)	*E* (%)	Δ*P* (Pa)
1	++	8	20	92.6	135
2	++	8	20	88.8	122
3	A0	8	10	91.8	144
4	A0	8	10	87.5	136
5	+−	8	5	86.2	172
6	+−	8	5	88.4	174
7	0A	7	20	96.6	61
8	0A	7	20	93.1	54
9	00	7	10	92.2	78
10	00	7	10	94.2	83
11	00	7	10	89.5	69
12	00	7	10	91.6	72
13	0a	7	5	87.3	77
14	0a	7	5	92.3	94
15	−+	6	20	85.3	261
16	−+	6	20	82.9	278
17	a0	6	10	82.8	296
18	a0	6	10	83.3	343
19	−−	6	5	85.7	437
20	−−	6	5	88.5	486

S, suspension concentration; *C*, CNCs percentage; *E*, $PM_{2.5}$ removal efficiency; Δ*P*, pressure drop.

Table II-3 ANOVA for response surface quadratic models.

Source	Degree of freedom	Sum of squares	Mean squares	*F*-ratio	*p*-value
Removal efficiency (%)					
Model	5	213.55	42.71	7.18	0.0016*
S	1	67.10	67.10	11.27	0.0047*
C	1	9.90	9.90	1.67	0.2181
$S \times C$	1	15.60	15.60	2.62	0.1277
S^2	1	128.10	128.10	21.52	0.0004*
C^2	1	0.84	0.84	0.14	0.7130
Residual	14	83.33	5.95	-	-
Lack of fit	3	27.67	9.22	1.82	0.2013
Pure error	11	55.67	5.06	-	-
Total	19	296.88			
Pressure drop (Pa)					
Model	5	304613.44	60922.70	72.38	< 0.0001*
S	1	112669.74	112669.74	133.86	< 0.0001*
C	1	23320.08	23320.08	27.71	0.0001*
$S \times C$	1	9405.05	9405.05	11.17	0.0048*
S^2	1	139265.29	139265.29	165.46	< 0.0001*
C^2	1	3812.73	3812.73	4.53	0.0515
Residual	14	11783.36	841.7	-	-
Lack of fit	3	8929.363	2976.45	11.4720	0.0010*
Pure error	11	2854.000	259.45	-	-
Total	19	316396.80			

S, suspension concentration; *C*, CNCs percentage.

* Significant at $p \leq 0.05$

Table II-4 Estimated regression coefficients for removal efficiency and pressure drop.

Term	Estimate	Standard error	*t* Ratio	*p*-value	Lower 95%	Upper 95%
Removal efficiency (%)						
Intercept	91.98	1.145	80.30	<0.0001*	89.52	94.44
S	2.39	0.71	3.36	0.0047*	0.86	3.91
S^2	-5.24	1.13	-4.64	0.0004*	-7.67	-2.82
Pressure drop (Pa)						
Intercept	47.91	13.62	3.52	0.0034*	18.69	77.12
S	-97.76	8.45	-11.57	<0.0001*	-115.88	-79.64
C	-44.08	8.37	-5.26	0.0001*	-62.05	-26.12
$S \times C$	33.67	10.07	3.34	0.0048*	12.07	55.27
S^2	172.75	13.43	12.86	<0.0001*	143.95	201.55

S, suspension concentration; *C*, CNCs percentage.

* Significant at $p \leq 0.05$

Table II-5 Comparison of model predicted and experimental values of the two responses (validation data set).

Run order	*S* (%)	*C* (%)	*E* (%)		Δ*P* (Pa)	
			Experimental	Predicted	Experimental	Predicted
1	8	13	90.5	89.3	138	122
2	8	11	92.2	88.7	151	126
3	7.5	15	89.4	92.4	112	37
4	7.5	7	92.0	91.0	109	80
5	7.5	6	92.1	90.8	112	90
6	7	10	93.7	91.7	86	66
7	6.5	12	87.4	89.5	161	144
8	6	17	81.2	84.3	278	284

S, suspension concentration; *C*, CNCs percentage; *E*, $PM_{2.5}$ removal efficiency; Δ*P*, pressure drop.

CHAPTER III

PREPARATION OF ELECTROSPUN NANOFIBROUS POLY(VINYL ALCOHOL)/CELLULOSE NANOCRYSTALS AIR FILTER FOR EFFICIENT PARTICULATE MATTER REMOVAL WITH REPETITIVE USAGE CAPABILITY VIA FACILE HEAT TREATMENT

Zhang, Q.; Li, Q.; Zhang, L.; Wang, S.; Harper, D. P.; Wu, Q.; Young, T. M. Preparation of electrospun nanofibrous poly(vinyl alcohol)/cellulose nanocrystals air filter for efficient particulate matter removal with repetitive usage capability via facile heat treatment. *Chem. Eng. J.* **2020**, *399*, 125768.

Authors:

Qijun Zhang, Qian Li, Longfei Zhang, Siqun Wang, David P. Harper, Qiang Wu, Timothy M. Young

Center for Renewable Carbon, University of Tennessee, Knoxville, TN, United States

Qian Li, Qiang Wu
School of Engineering, Zhejiang A&F University, Hangzhou, China

Longfei Zhang
Research Institute of Wood Industry, Chinese Academy of Forestry, Beijing, China

Q. Zhang's primary contribution to this paper includes identifying the research objective, design and conduct of the experiments, process and interpretation of the data, drafting the paper.

Co-researchers' contributions are listed as follows:
Q. Li, provided research guideline, worked with Qijun to fabricate the nanofibrous air filters and analyze the experimental results.
L. Zhang worked with Qijun to analyze the experimental results.

S. Wang identified the research objective, provided research guideline and revised the paper.

D.P. Harper worked with Qijun to perform TGA and FTIR tests.

Q. Wu provided research guideline and worked with Qijun to analyze the experimental results

T.M. Young revised and language polished the paper.

Abstract

Air pollution has become a global concern, and numerous studies have focused on developing filters for particulate matter (PM) removal. However, the reusability of air filters, which could lower resources consumption and waste discharge, is also necessary to be investigated. In this study, a water washable electrospun poly (vinyl alcohol) (PVA)/cellulose nanocrystals (CNCs) nanofibrous air filter for PM removal was prepared. The water-soluble polymer composite was converted to be completely water-resistant via a facile heat treatment without adding any crosslinking agent. Our results indicate the increased crystallinity is the key factor to improve the aqueous stability of PVA/CNCs fibers. The CNCs provided additional nucleation sites for PVA crystallization during electrospinning and heating process. By loading 20% CNCs and heating at 140 ^{o}C for 5 min, the crystallinity degree and crystal size of PVA were increased from 54.7% and 3.3 nm to 85.4% and 6.3 nm, respectively. The reusability of fabricated filters was tested by water washing over 5 cycles. The results show the heavily fouled filters (pressure drop >1000 Pa) were regenerated effectively: the $PM_{2.5}$ removal efficiency was maintained at above 95%, meanwhile the pressure drop remained less than 100 Pa after repetitive usage ($PM_{2.5}$ mass concentration >500 μg m^{-3}). Considering the raw materials are nontoxic and biodegradable, the heating temperature is relatively low, and the process is short, it is a promising green method to manufacture long lifetime air filter.

1. Introduction

Air pollution is a significant environmental risk to public health given industrial growth, expansion of urban area populations, and the related increase in motor vehicle use (Landrigan et al., 2018). Over 90% of the world population was living in areas where ambient air quality levels exceed World Health Organization (WHO) limits (World Health Organization, 2016). One major air pollutant is particulate matter (PM), which is a mixture of small solid particles and liquid droplets. It contains both organic and inorganic compounds, and some components can be cytotoxic and carcinogenic (Harrison et al., 2016). Exposure to elevated levels of PM, especially $PM_{2.5}$ (particle aerodynamic diameter less than or equal to 2.5 μm), can cause respiratory and cardiovascular diseases, since finer PM can penetrate deeply into lungs and bronchi (Brook et al., 2010, Pope III et al., 2002). It was estimated that ~4.2 million premature deaths were attributed to $PM_{2.5}$ in 2015, globally (Cohen et al., 2017). Besides, $PM_{2.5}$ exhibit longer residence time in air than coarse particle, which enlarges its hazardous. Therefore, control and reduce PM level, especially $PM_{2.5}$ level, is a pressing task (Apte et al., 2015).

To protect individuals from $PM_{2.5}$ exposure, numerous studies have been conducted to develop air filters focusing on achieving higher filtration performance (Dai et al., 2018, Gopal et al., 2007, Khalid et al., 2017, Kim et al., 2018, Liu et al., 2015b, Vanangamudi et al., 2015, Xu et al., 2016, Zhang et al., 2016a, Zhang et al., 2016b, Zhang et al., 2016c). Among those studies, electrospinning is a technique commonly used to produce ultrafine nanofibrous filter (Doshi and Reneker, 1995, Huang et al., 2006). Smaller fiber diameter could provide large surface area to capture $PM_{2.5}$ (Kenawy et al., 2002, Podgórski et al., 2006), and also allows air molecules pass through due to slip-effect (Brown, 1993, Hung and Leung, 2011, Zhao et al., 2016). However, most filters have to be disposed once the filters are clogged, to avoid the high pressure drop resulted energy waste (Yun et al., 2007). Non-reusable air filters have higher costs given one-use which requires more cumulative raw materials and the related energy consumption during the manufacturing process. Additionally, inappropriate disposal of waste filters may cause environmental issues as well (Fan et al., 2018a, Fan et al., 2018b). Therefore, developing high-performance air filters with reusability has received increasing interests (Bai et al., 2018, Chen et al., 2017, Jeong et al., 2017, Lee et al., 2019, Li et al., 2017, Liu et al., 2015a, Zhao et al., 2017). But

most reusable air filters were prepared involving organic solvents. The flammable or toxic organic chemicals utilized during the manufacturing process could be harmful to both human health and environment (Jiang et al., 2016). Thus, it is necessary to further develop an environmentally friendly method to fabricate $PM_{2.5}$ filters which can meet the requirements of both high filtration-performance and reusability.

Our previous study successfully developed an electrospun poly(vinyl alcohol) (PVA)/cellulose nanocrystals (CNCs) air filter with high $PM_{2.5}$ removal efficiency and low air resistance (Zhang et al., 2019). Unlike other nanofibrous filters with ultrafine diameters, PVA/CNCs filters do not require additional mechanical support (Leung et al., 2010, Qin and Wang, 2008, Zhu et al., 2017) due to the strength enhanced by CNCs (Xu et al., 2018, Li et al., 2018). The presence of CNCs also promoted the formation of finer fibers because CNCs increased the surface charge density of electrospinning solution (Reneker and Yarin, 2008, Stranger et al., 2009, Zhang et al., 2019). The fabricating process is environmentally friendly because both PVA and CNCs are nontoxic, fully biodegradable and water-soluble. However, one common problem of air filters made from water-soluble polymers is that the filter is not stable in high-humidity environment and cannot be regenerated by water-washing after use. To improve the aqueous stability, maleic anhydride (Peresin et al., 2014, Qin and Wang, 2008), formaldehyde (Song et al., 2016) and 1,2,3,4-butanetetracarboxylic acid (Shalom et al., 2019) were used to crosslink PVA and CNCs. But the cross-linkers may create new environmental concerns (Liu et al., 2017, Zhu et al., 2018).

The aim of this study is to develop a simple and green method to improve the aqueous stability of PVA/CNCs air filter without adding any new additives. In this study, a facile heat treatment method was investigated to convert the water-soluble electrospun PVA/CNCs air filter into water-resistant. Despite many studies have shown that water stable PVA materials could be prepared after heat treatment due to the increased crystallinity (Hong, 2007, Wong et al., 2010), few researches have been conducted to investigate the effect of heat treatment on water resistance of electrospun PVA/CNCs fibers. Since CNCs may act as nucleating agent and promote crystallization of PVA (Popescu, 2017, Rescignano et al., 2014, Uddin et al., 2011), it is expected that a water-proof PVA/CNCs filter could be obtained under a milder heating condition comparing with reported studies (Hong, 2007, Wong et al., 2010). This study investigated the mechanism

systematically and demonstrated the feasibility of regenerating the used electrospun PVA/CNCs filter for $PM_{2.5}$ removal. It may provide a guidance on the cleaning and recycling strategies of CNCs-based electrospun filter for long-term usage.

2. Experimental section

2.1. Materials

PVA (M_w 85000-124000) was purchased from Sigma-Aldrich with degree of hydrolysis >99%. CNCs (~12 wt%, 5-20 nm in width, 150-200 nm in length, prepared by sulfuric acid hydrolysis) were obtained from the University of Maine (Orono, ME). Commercial window screens with 0.25 mm wire diameter and 1.2 mm × 1.2 mm mesh size were purchased from Saint-Gobain ADFORS (Clear Advantage). All chemicals and materials were used as received.

2.2. Electrospinning of PVA and PVA/CNCs nanofibrous filters

The suspensions of PVA and PVA/CNCs were electrospun to form nanofibrous filters as described in our previous work (Zhang et al., 2019). Briefly, PVA solution was prepared and specified amount of CNCs was added to obtain a CNCs percentage of PVA content is 20% (wt/wt), while total concentration was kept at 7 wt%. The amount of CNCs added into PVA was determined based on previous study to achieve best filtration performance (Zhang et al., 2019). PVA/CNCs suspension was mixed by a sonicator (VCF-1500, Sonics) in an ice bath for 2 min under 600 W of power. For comparison purposes, neat PVA solution was also prepared at 7 wt% and sonicated for 2 min. The obtained suspension was then loaded into a 5 mL plastic syringe with a 22-gauge needle. The flow rate of suspension was controlled at 0.5 mL h^{-1} by a syringe pump (NE-1800, New Era Pump System). Window screen was covered over a metal circular cylinder as a collector and placed at a working distance of 10 cm from the needle tip. The needle was connected to a voltage generator (Series EK, Glassman High Voltage) while the cylinder was grounded, and the operating voltage was set at 22 kV. The diagram of electrospinning set is shown in Figure III-1. Electrospinning was performed at room temperature and 50 ± 5% relative humidity. Electrospinning time of 6 min was applied to control the basis weight of the electrospun fibers to 60 mg m^{-2} (Zhang et al., 2019).

2.3. Heat treatment of electrospun PVA and PVA/CNCs filters

The heat treatment was conducted in an oven (Isotemp, Fisher Scientific). The prepared PVA and PVA/CNCs filters were heated at temperatures of 80, 100, 120 and 140 ^{o}C for 5 min, respectively. Then the samples were taken out to cool down at room temperature.

2.4. Morphology characterizations

The morphology of all the heated and unheated filters was studied using scanning electron microscope (SEM, Zeiss Auriga crossbeam workstation) with an acceleration voltage of 5 kV. All samples were gold coated by SPI sputter coating system before observation. Diameters were measured via SEM images and 50 fibers were evaluated for each filter.

2.5. Water resistance tests

The heat-treated filters were immersed in 20 ^{o}C deionized water for 8 h. Then the samples were transferred out and dried at room temperature. For comparison, the electrospun filters without heat treatment were also tested with the same procedure. All water immersed samples were then characterized by SEM.

2.6. X-ray diffraction (XRD) analysis

XRD analysis was carried out using a diffractometer (Empyrean, Panalytical) equipped with CuKα radiation (λ = 1.5418 Å), operating at 45 kV and 40 mA. The diffraction patterns were collected between 10 and 40^{o} with a 0.05^{o} step size. The degrees of crystallinity were calculated using the method of Hermans:

$$X_c = A_c/A_t \quad (1)$$

where X_c is the crystallinity degree, A_c is the sum of the signal areas of crystalline regions and A_t is the total area of the diffractogram (Popescu, 2017, Hermans and Weidinger, 1961). The crystal sizes (L) were estimated by Scherrer's equation:

$$L = K\lambda/B\cos\theta \quad (2)$$

where K = 0.94, λ is the X-ray wavelength (0.15418 nm), θ is the Bragg angle and B is the full width at half maximum intensity of the diffraction peak (Popescu, 2017).

2.7. Thermogravimetric analysis (TGA)

The thermal properties of prepared PVA and PVA/CNCs filters were analyzed by a Perkin Elmer Pyris 1 TGA. The samples were placed in an aluminum pan and heated from 30 to 600 ^{o}C with a 10 ^{o}C min^{-1} heating rate.

2.8. Fourier transfer infrared spectroscopy (FTIR) analysis

All the electrospun PVA and PVA/CNCs filters, before and after heat treatment, were analyzed by a FTIR spectrometer (Spectrum Two, Perkin Elmer) over a wavenumber range of 4000-500 cm^{-1}. All spectra were collected with a resolution of 4 cm^{-1} after 16 scans.

2.9. Filtration performance of heated electrospun PVA/CNCs filters for $PM_{2.5}$

The experiment setup for PM filtration is shown in Figure III-2. The filtration test followed the method described in our previous study (Zhang et al., 2019). Briefly, the fabricated filter was clamped between two Adams & Chittenden customized bottles with a sealing ring. PM particles were generated by burning incense, which are considered to be soft PM, due to its larger content of carbon and water than that of rigid inorganic PM (Liu et al., 2015b). The inflow concentration of $PM_{2.5}$ was controlled to >500 μg m^{-3} and the $PM_{2.5}$ concentration was measured by a particle counter (DT-9851M, CEM). Removal efficiencies (E) were calculated as:

$$E\ (\%) = (1 - C_t/C_0) \times 100 \quad (3)$$

where C_t and C_0 are the measured outflow $PM_{2.5}$ concentrations with and without filter, respectively. The air flow was generated by an air compressor and the flow rate was controlled at 0.2 m s^{-1} via flow meter. Pressure drops across the filters were measured by a Testo 510 differential pressure gauge. All tests were conducted in triplicate. To evaluate the overall performances of electrospun filters in terms of both removal efficiency and pressure drop, a quality factor, Q_f, was used as an indicator. Q_f is defined as:

$$Q_f = -\ln(1-E)/\Delta P \quad (4)$$

where E is PM removal efficiency and ΔP is pressure drop across the filter.

2.10. Regeneration of clogged filters

After recording the removal efficiency and pressure drop of the first filtration test, the inflow concentration of $PM_{2.5}$ was elevated ~400 times of 500 μg m^{-3}. Therefore, the filters

were clogged quickly and the reusability of the heated electrospun PVA/CNCs filters could be evaluated efficiently. The heavily fouled filters were then cleaned by immersed into 20 ^{o}C water and waggled mildly for 30 s. After drying at room temperature, the filters were applied for second filtration performance evaluation. This filtration-wash-dry cycle was repeated 5 times. All tests were conducted in triplicate.

2.11. Statistical analysis

The significance tests for the effect of heat treatment and water immersion on fiber diameter, effect of heat treatment on fiber crystallinity, and the effect of regeneration times on filter pressure drop, were evaluated by *t*-test using JMP software (version 14, SAS Institute). The differences between group means with a *p*-value ≤ 0.05 were considered statistically significant.

3. Results and Discussion

3.1. Effect of heat treatment on water resistance of electrospun filter

The morphologies of the electrospun PVA and PVA/CNCs fibers are shown in Figure III-3a and III-3b. The average diameters of PVA and PVA/CNCs fibers are 207.6 and 130.7 nm, respectively (Table III-1), indicating the addition of CNCs favored the formation of smaller-diameter fibers, which is consistent with our previous study (Zhang et al., 2019). After 140 ^{o}C heat treatment, the morphological features of both PVA and PVA/CNCs fibers remained unchanged (Figure III-3c and III-3d). In addition, PVA and PVA/CNCs fibers treated at all the heating temperatures (80, 100, 120 and 140 ^{o}C) showed no significant diameter changes (Table III-1). Therefore, the morphology and size of the electrospun fiber were not significantly changed by the heat treatment. All the prepared filters were then immersed in water for 8 h to evaluate their aqueous stability. Both the as-spun PVA and PVA/CNCs fibers were completely dissolved due to the hydrophilicity (Figure III-4). As shown in Figure III-5, the PVA fibers became more water-resistant as heating temperature increased from 80 to 140 ^{o}C. Similar trend has also been observed for PVA/CNCs fibers. This could be attributed to that the heat treatment facilitated the mobility of polymer chains, and then the amorphous region of chains can align and fold to form crystallites (Wong et al., 2010). With the increased crystallinity, the accessibility of infusion water to polymer

structure is reduced and the water resistance of polymers is expected to be improved (Kenney and Willcockson, 1966). Although neither PVA nor PVA/CNCs fibers were completely dissolved after they were treated at 80 °C, their water stability is very limited and most of the air filter-morphological features were lost (Figure III-5a and III-5e). Similarly, the 100 °C treated samples did not exhibit good water resistance either. The fibers were fused into membranes and bundles, though the PVA/CNCs fibers appeared to retain part of the characteristics of electrospun fibers (Figure III-5b and III-5f). For the filters heated at 120 and 140 °C, the cylindrical feature of fibers was observed and the average diameter were measured to quantify the aqueous stability (Table III-1 to III-3). The average diameters of PVA fibers treated at 120 and 140 °C are 771.1 and 393.2 nm, respectively, after immersed in water. This swelling is due to absorption of water. However, with the addition of CNCs, the fibers were less swelled after water immersion, and the average diameters of PVA/CNCs fibers heated at 120 and 140 °C are 258.1 and 127.5 nm, respectively. From the *t*-tests, there is no significant diameter change between PVA/CNCs fibers before and after water immersion, as heated at 140 °C. As shown in Figure III-5h, the morphology of the PVA/CNCs fibers was completely conserved. Therefore, the water resistance of water-soluble electrospun filter is considerably enhanced by adding CNCs and heating at 140 °C for 5 min.

3.2. Characterizations of electrospun PVA and PVA/CNCs filters

The XRD patterns of PVA and PVA/CNCs fibers heated at different temperatures are shown in Figure III-6. The peak at $2\theta = 19.5^{o}$ is corresponding to the (101) plane of PVA (Figure III-6a). For the PVA/CNCs fibers, the new shoulder peak appeared at $2\theta = 22.2^{o}$ is due to the (200) plane of CNCs (Figure III-6b) (Voronova et al., 2015). The small signals at 14.8^{o} and 16.8^{o} also indicate the presence of CNCs, which are attributed to the (101) and $(10\bar{1})$ planes, respectively (Figure III-6b) (Popescu, 2017). Since CNCs are primarily consist of crystalline domain and have restricted chain mobility, their crystallinity degrees and crystal sizes are considered relatively unchanged at each heat treatment level. The average crystallinity degree of the unheated PVA and PVA/CNCs fibers were 54.7% and 59.6%, respectively. By applying heat treatment and increasing the heating temperature from 80 to 140 °C, the crystallinity degree of PVA and PVA/CNCs fibers both increased gradually and achieved the highest value of 73.7% and 85.4%, respectively (Table III-4).

This is consistent with previous results of water resistance test. Higher heating temperature provided more polymer chains mobility and facilitated the formation of crystallinities (Table III-5 to III-6). The crystal sizes calculated in Table III-4 were based on the peaks of PVA (101) plane. As shown in Table III-4, the crystal size of PVA in PVA fibers was increased from 3.3 ± 0.1 nm to 4.9 ± 0.1 nm after a 140 ^{o}C heat treatment. This additionally proved that heat treatment effectively promoted the crystallization of PVA (Table III-7). Similarly, the heat treatment also significantly promoted the growth of PVA crystals in PVA/CNCs fibers (Table III-8). By adding CNCs into the PVA, the crystallinity degree of as-spun fibers increased ~5%. As the heating temperature increased from 80 to 140 ^{o}C, the differences of crystallinity degrees between PVA/CNCs and PVA fibers at each heat treatment level are 4.8 ± 1.6%, 7.6 ± 1.8%, 10.8 ± 2.1% and 11.7 ± 0.9%, respectively. This rising tendency of the difference of crystallinity degrees implied a combined effect of heating and CNCs, indicating CNCs promoted the crystallization of polymer matrix (Table III-9). Comparing the crystal size between PVA and PVA/CNCs fibers (Table III-4), it also shows that the presence of CNCs significantly promoted the growth of PVA crystals under same heating condition (Table III-10). This could be explained by the nucleating effect. The CNCs could act as nucleating agents and provide additional nucleation sites for PVA crystallization (Popescu, 2017, Rescignano et al., 2014, Uddin et al., 2011). It is noticed that several previous researches stated that adding CNCs into PVA could cause decrease of crystallinity degree (Desmaisons et al., 2018, Peresin et al., 2010, Roohani et al., 2008). Two mechanisms were proposed: (1) randomly distributed CNCs may decrease the PVA nucleation and disorder the polymer chains; (2) CNCs may connect to each other and form a percolating network, which prevents the growth of polymer spherulites. These researches may provide evidence that CNCs in this study are not aggregated and are well dispersed in the PVA matrix. Since electrospinning process could facilitate the orientation of CNCs along the PVA/CNCs fiber axis and increase the alignment of both PVA and CNCs (Lee et al., 2016, Zhang et al., 2019), it is feasible that well aligned CNCs could effectively promote the crystallization of PVA.

To further investigate the effect of heat treatment on electrospun PVA and PVA/CNCs fibers, thermogravimetric tests were conducted. As shown in Figure III-7, PVA/CNCs fibers started losing weight at 150 ^{o}C, which is lower than 190 ^{o}C of PVA. This initial mass

loss (~5 wt%) could be attributed to the degradation of hydroxy groups and sulfate groups of CNCs (Nan et al., 2017). The onset temperature of first decomposition region of PVA fibers is 210 ^{o}C and the peak temperature is 255 ^{o}C (Figure III-7b). This stage of decomposition is mainly corresponding to elimination reactions; and the second stage of degradation occurred above 400 ^{o}C involving carbonaceous matter decomposition caused by chain-scission reactions (Voronova et al., 2015). By adding CNCs, the onset and peak temperatures of decomposition of PVA/CNCs fibers both shifted to higher temperatures (225 ^{o}C and 330 ^{o}C, respectively), indicated that CNCs enhance thermal stability of the composite material. According to previous studies, the enhanced thermal stability of the composite was resulted by the hydrogen bond formed between PVA and CNCs (Miri et al., 2015, Park et al., 2019, Voronova et al., 2015), which is consistent with the results of XRD analysis. The PVA/CNCs fibers lost more weight than PVA fibers under 400 ^{o}C could be attributed to the decomposition of CNCs (Huan et al., 2016, Park et al., 2019). For both PVA and PVA/CNCs fibers, no obvious weight loss was observed before 140 ^{o}C. This indicated that bound water is less contained after electrospinning, and the increased degree of crystallinity was not caused by eliminating the water molecules within the amorphous region of polymers.

The FTIR spectra collected for PVA and PVA/CNCs filters with different heat treatment are shown in Figure III-8. In the spectra of PVA filters, the strong absorption peak at 1094 cm^{-1} is due to C-O stretching and O-H bending; the peaks at 2942 and 2910 cm^{-1} are the typical C-H stretching from alkyl groups; and the broad band from 3200 to 3550 cm^{-1} is corresponding to the stretching of O-H from intermolecular and intramolecular hydrogen bonds (Figure III-8a) (Huan et al., 2016, Hui et al., 2014). For PVA/CNCs filters, the additional peak observed at 1059 cm^{-1} is assigned to the C-OH stretching of cellulose (Figure III-8b) (Qua et al., 2009). By adding CNCs, there is no shift in the PVA peaks. It was noticed a change in shape of band from 3200 to 3550 cm^{-1} was caused by the presence of CNCs. This could be attributed to the formed hydrogen bond between PVA and CNCs (Peresin et al., 2010). As heating temperature increased from 80 to 140 ^{o}C, the intensity of peak at 1143 cm^{-1} in the spectra of PVA filters increased gradually (Figure III-8a). This peak is assigned to the stretching of the C–O associated with the crystalline parts of the polymeric chain (Mansur et al., 2008, Peppas, 1977). The increased peak intensity

indicated an increase in crystallinity degree, which is consistent with the previous XRD results. Similar results have also been observed for PVA/CNCs filters. For all the FTIR spectra, no newly formed C-O-C or C=C bonds were observed (Peresin et al., 2014). The FTIR analysis results indicated there is no intermolecular or intramolecular etherification occurring with heat treatment under 140 ^{o}C (Lyons and Olson, 1972). Thus, it is reasonable to assume that the enhanced water resistance of heat-treated filters is achieved solely due to the increased crystallinity.

The inference based on FTIR results can be further proved by immersing the heated filters in hot water. The 140 ^{o}C heated PVA/CNCs filter was dissolved completely after immersion in 80 ^{o}C water for 8 hours, demonstrating there is no strong chemical bond (e.g. C-O-C, C=C) formed between PVA and CNCs. The elevated temperature promoted the infusion of water and facilitated the accessibility of water molecules to polymers structure. It is worth mentioning that the 140 ^{o}C heated PVA/CNCs filter could be dissolved after placed in 60 ^{o}C for 10 min with vigorous stirring. This feature might be an advantage for recycling the window screen substrate since the procedure is simple.

3.3. Regeneration of clogged electrospun PVA/CNCs filters

To evaluate the capability of repetitive usage of heated PVA/CNCs filter, the 140 ^{o}C treated PVA/CNCs filter was used for the test of PM removal. For the first filtration test, the removal efficiency for $PM_{2.5}$ was ~96%, and the pressure drop was ~60 Pa. As our previous study demonstrated, the addition of CNCs dramatically improved the overall filtration performance of PVA/CNCs filter. The fiber diameter was reduced as CNCs increased the surface charge density of electrospinning solution. Therefore, the thinner fibers increased the specific surface area to volume ratio of the filter and improved the PM removal efficiency. In addition, filters with smaller fiber diameter possess higher filter medium porosity, which allows air molecules to pass through more easily. After a filtration of ultra-high concentration of PM (~400 times of 500 μg m^{-3}), the filter was clogged by 'oily substance' (Figure III-9a). Since burning incense produces PM, volatile organic compounds and gaseous pollutants (Mannix et al., 1996, Lin et al., 2008), the generated PM contains large amount of carbon and water. This type of PM is considered as soft PM, which is more difficult to be captured than rigid inorganic PM (Liu et al., 2015b). The PM deformed and wrapped around the nanofibers after contact, and then formed bead-shaped

particles on the fibers (Zhang et al., 2019). Besides, the PM particles can also directly attach to the PM already captured on the fiber and merge together. As the captured PM became bigger and filled the pores, it formed a membrane-like structure and clogged the air filter (Figure III-9a). Regeneration of the PVA/CNCs filter was then managed by a water washing for 30 s. As shown in Figure III-9b, most of the attached particles were washed off and the morphological features of the filter was clear and well maintained. As shown in Figure III-9c, small amount of particles remained on the fibers after water washing. These residuals could be explained by the affinity between the carbon content of PM and fiber surface. Considering the captured organic PM is more difficult to be cleaned than inorganic PM (Lee et al., 2019), our electrospun filters is promising for removal of PM generated from different sources.

The pressure drop of the PVA/CNCs filter was significantly increased to ~1000 Pa from 60 Pa, when the filter was clogged with massive PM (Figure III-9a). After first cleaning, the pressure drop was recovered to 77 Pa (Figure III-9b). As shown in Figure III-10a, the removal efficiency for $PM_{2.5}$ was maintained consistently (>95%) after 5 filtration cycles, indicating the filtration efficiency was not affected by regeneration. However, the pressure drop was significantly increased to 94 Pa (Table III-11). This could be attributed to the accumulated residual PM on the fibers. Since the PM concentration was elevated ~400 times for quick filter blocking in this regeneration evaluation, the lifetime of this PVA/CNCs filter is expected to be considerably long. The quality factor (Q_f) was also employed to evaluate the overall performance of fabricated air filter after each filtration cycle. Although the pressure drop was increased by 156.7% after 5 cycles, it was still less than 100 Pa. The Q_f of regenerated filter after 5 cycles remained above 0.035 Pa^{-1}, which is comparably superior (Zhang et al., 2019).

4. Conclusions

In this study, a reusable PVA/CNCs filter with outstanding $PM_{2.5}$ filtration performance was developed via electrospinning and facile heat treatment. Without adding any crosslinking agent, the environmentally friendly water-soluble filter was converted to be completely waterproof in room temperature water by heating at 140 ^oC for 5 min. The CNCs and heat treatment synergistically improved the crystallinity of PVA polymers.

Given that the amount of added CNCs is small, the heating temperature is low, and the heating time is short, the results imply a cost-effective manufacturing process for the production of electrospun PVA/CNCs nanofibrous filters. A thirty second immersion in water at room temperature also effectively recovers its filtration capability, which is an easy and low-cost solution for household use. This PVA/CNCs filter is promising for PM removal with its low cost and superior reusability. Furthermore, the filter can be strategically dissolved with 60 ^{o}C water, which means the filter substrate can be easily recycled. With proper treatment, the dissolved PVA and CNCs might be reutilized as well.

APPENDIX III

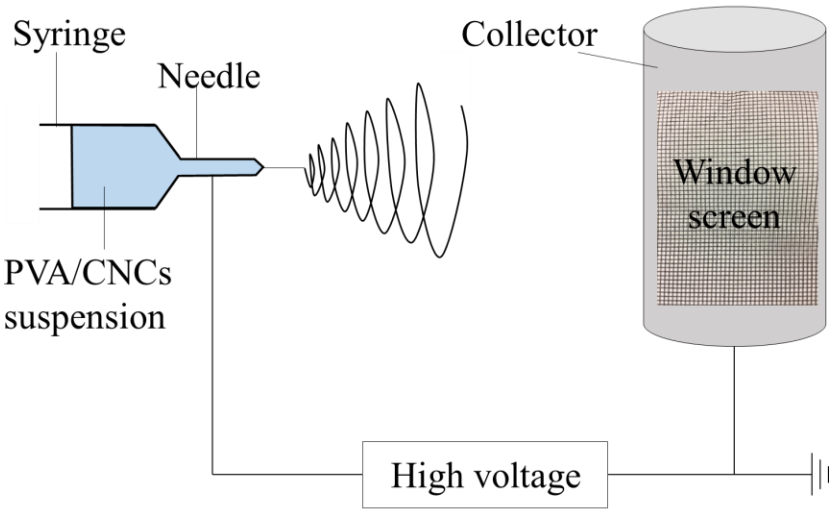

Figure III-1 Diagram of electrospinning set.

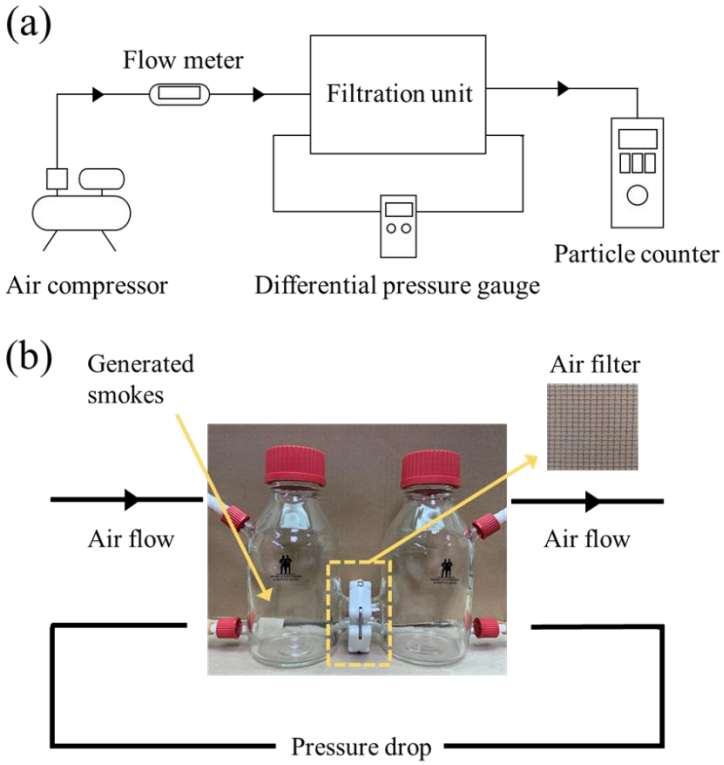

Figure III-2 (a) Scheme of filtration system and (b) photo of filtration unit.

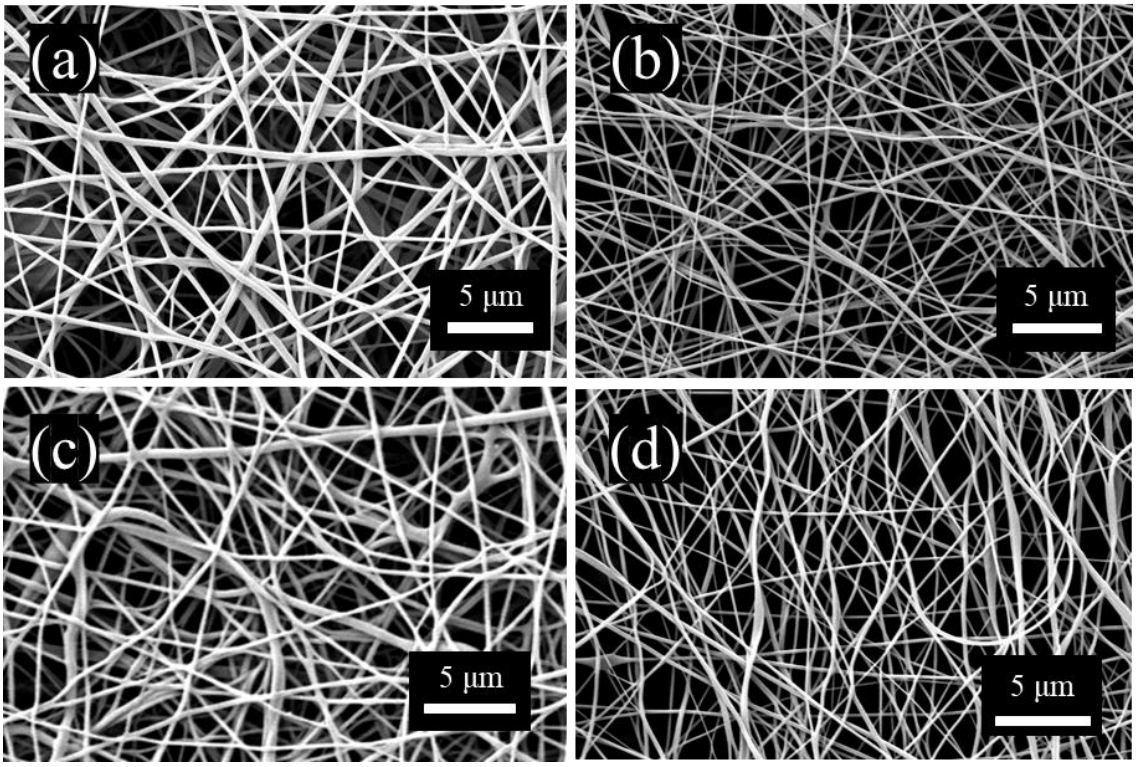

Figure III-3 SEM images of electrospun fibers: (a) PVA, (b) PVA/CNCs, (c) PVA heated at 140 ºC and (d) PVA/CNCs heated at 140 ºC.

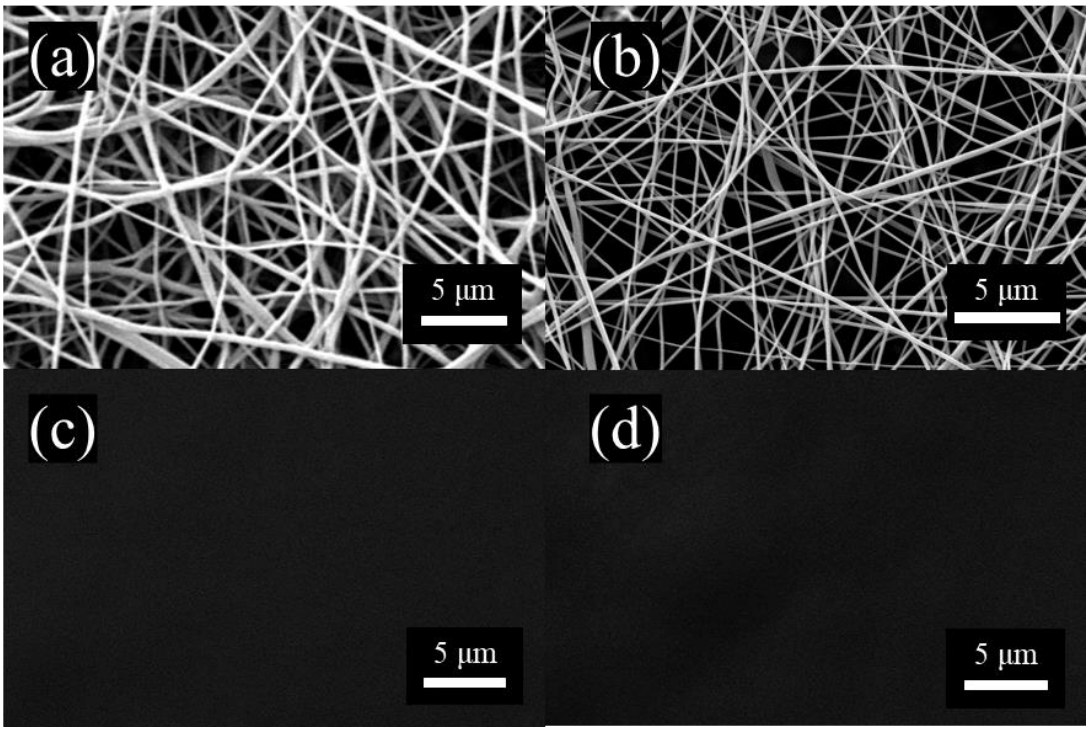

Figure III-4 SEM images of electrospun (a) PVA and (b) PVA/CNCs fibers. Both completely dissolved in 20 ^{o}C water after 8 h immersion: (c) and (d).

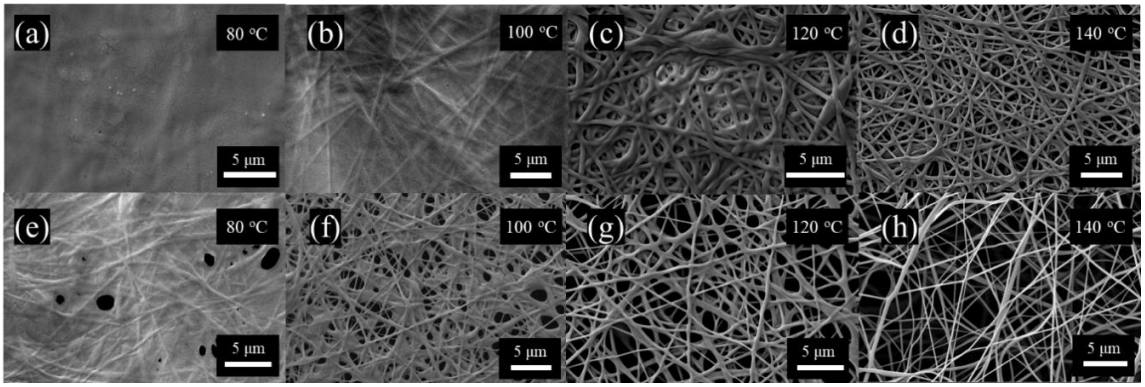

Figure III-5 SEM images of electrospun (a-d) PVA and (e-h) PVA/CNCs heated at different temperatures after immersed in water for 8 h.

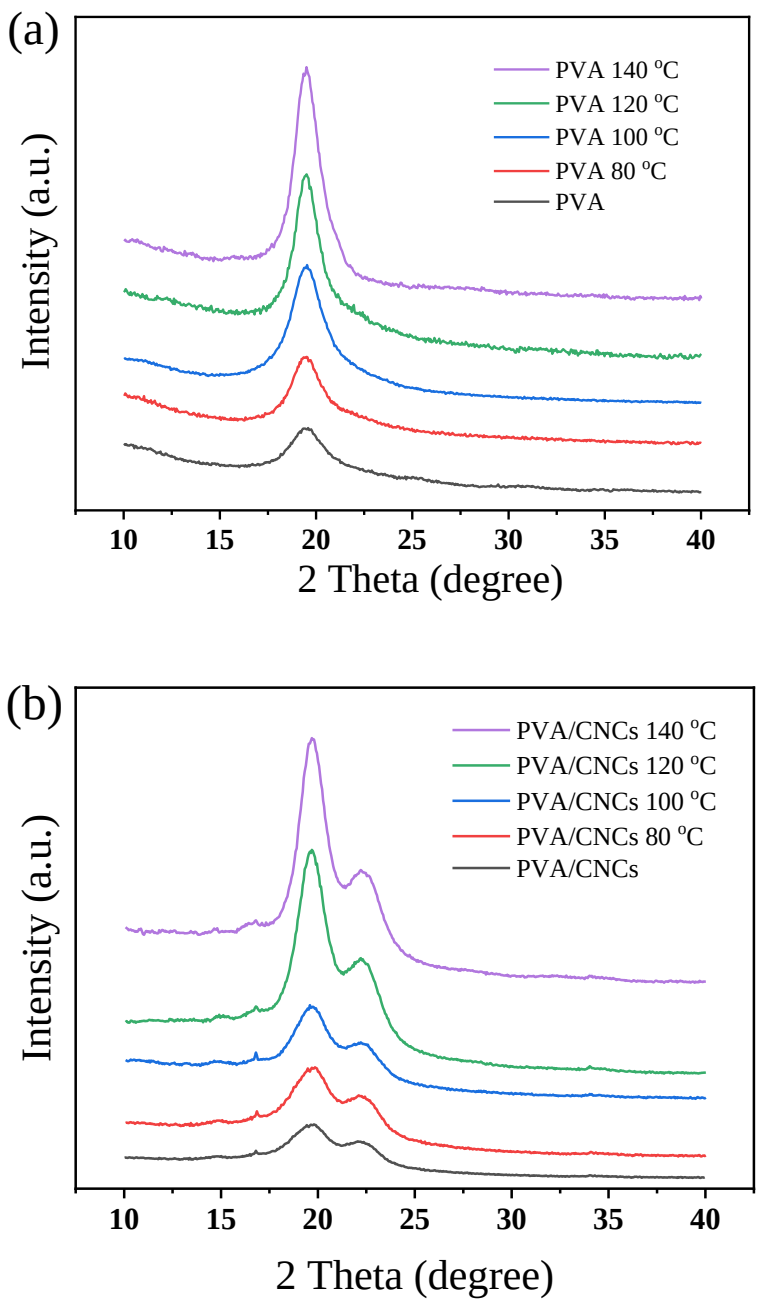

Figure III-6 XRD patterns of (a) PVA and (b) PVA/CNCs electrospun fibers heated at different temperature.

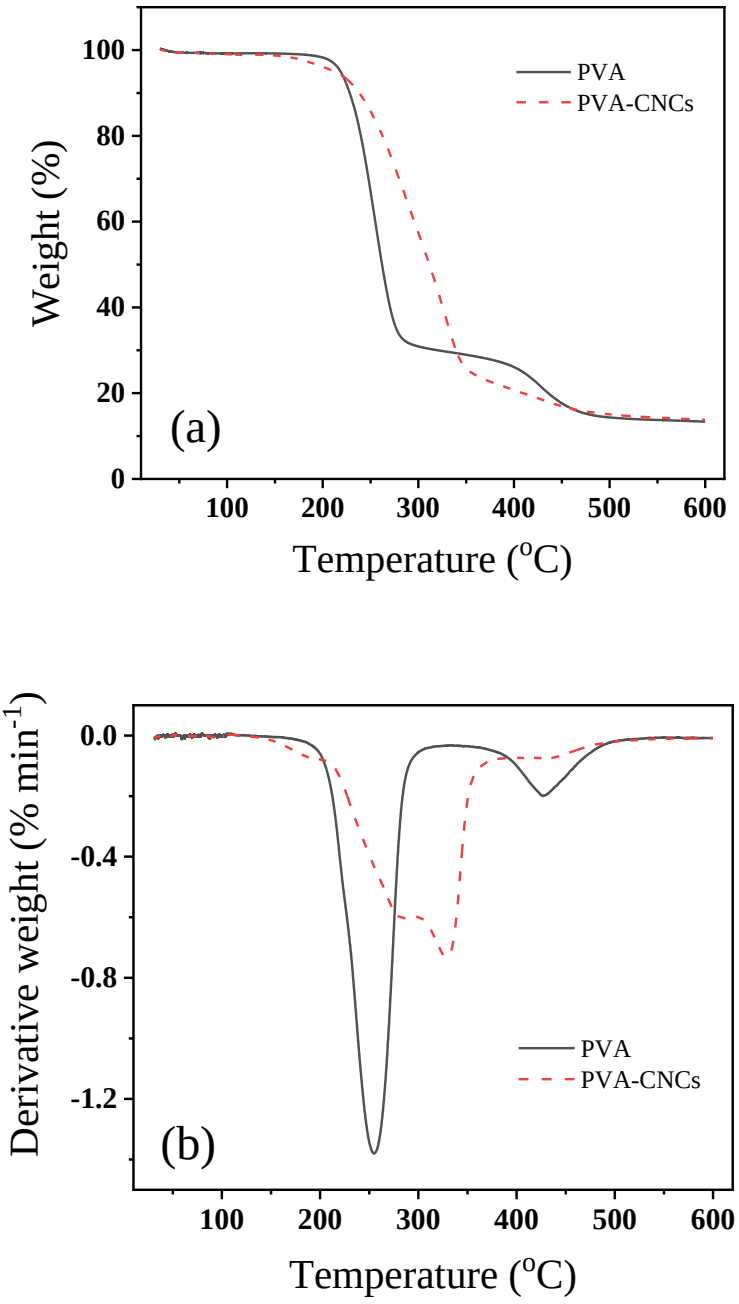

Figure III-7 (a) Thermogravimetric and (b) derivative thermogravimetric analysis curves of electrospun PVA and PVA/CNCs fibers.

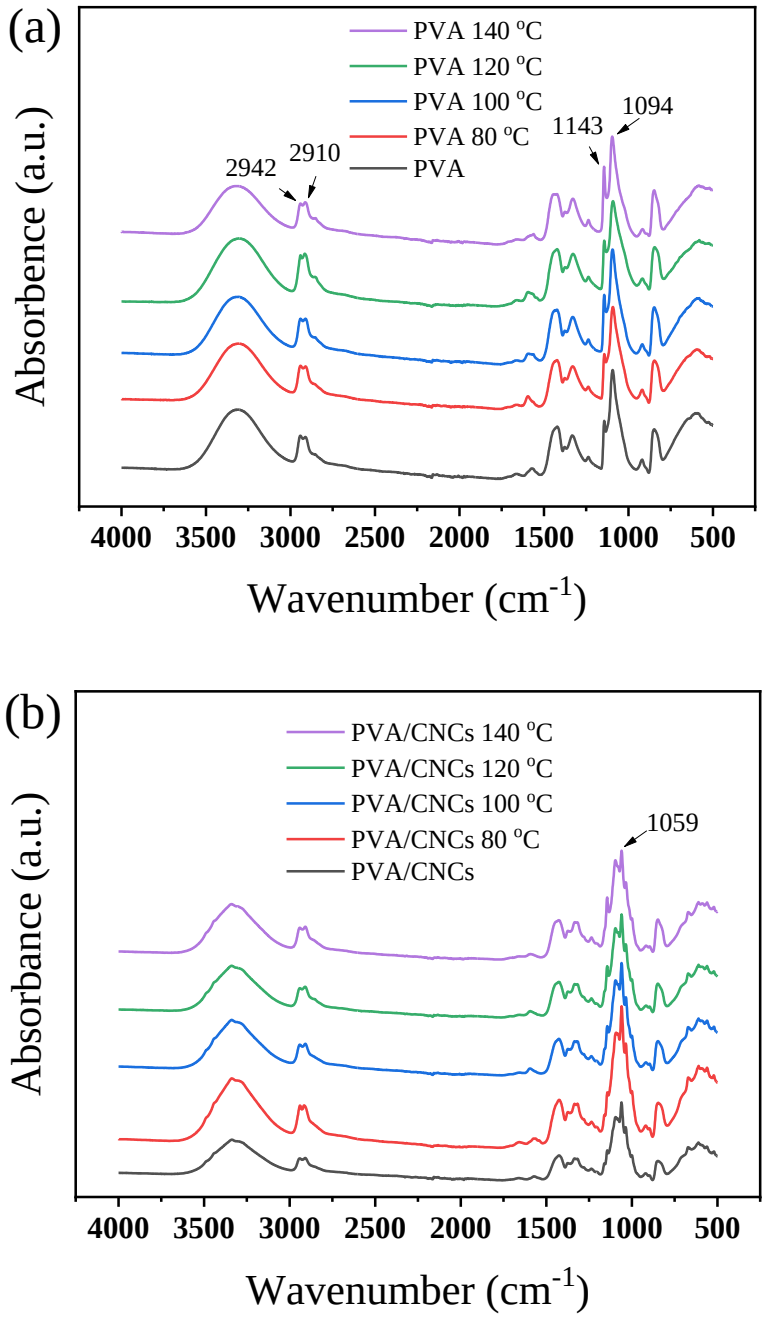

Figure III-8 FTIR spectra of (a) PVA and (b) PVA/CNCs fibers treated at different temperature.

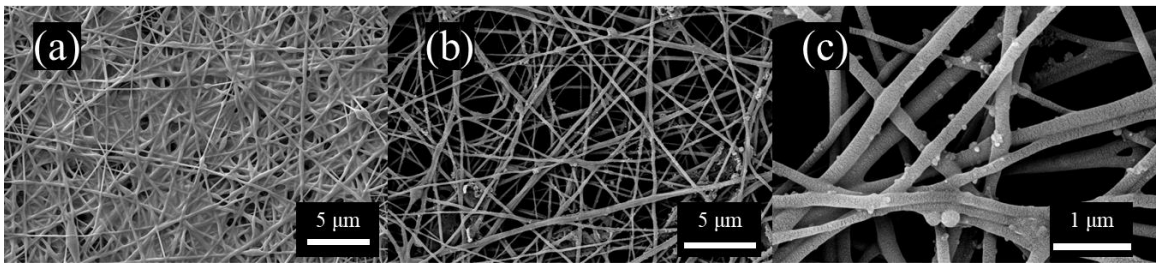

Figure III-9 SEM images of fouled PVA/CNCs filters (a) before and (b, c) after water washing.

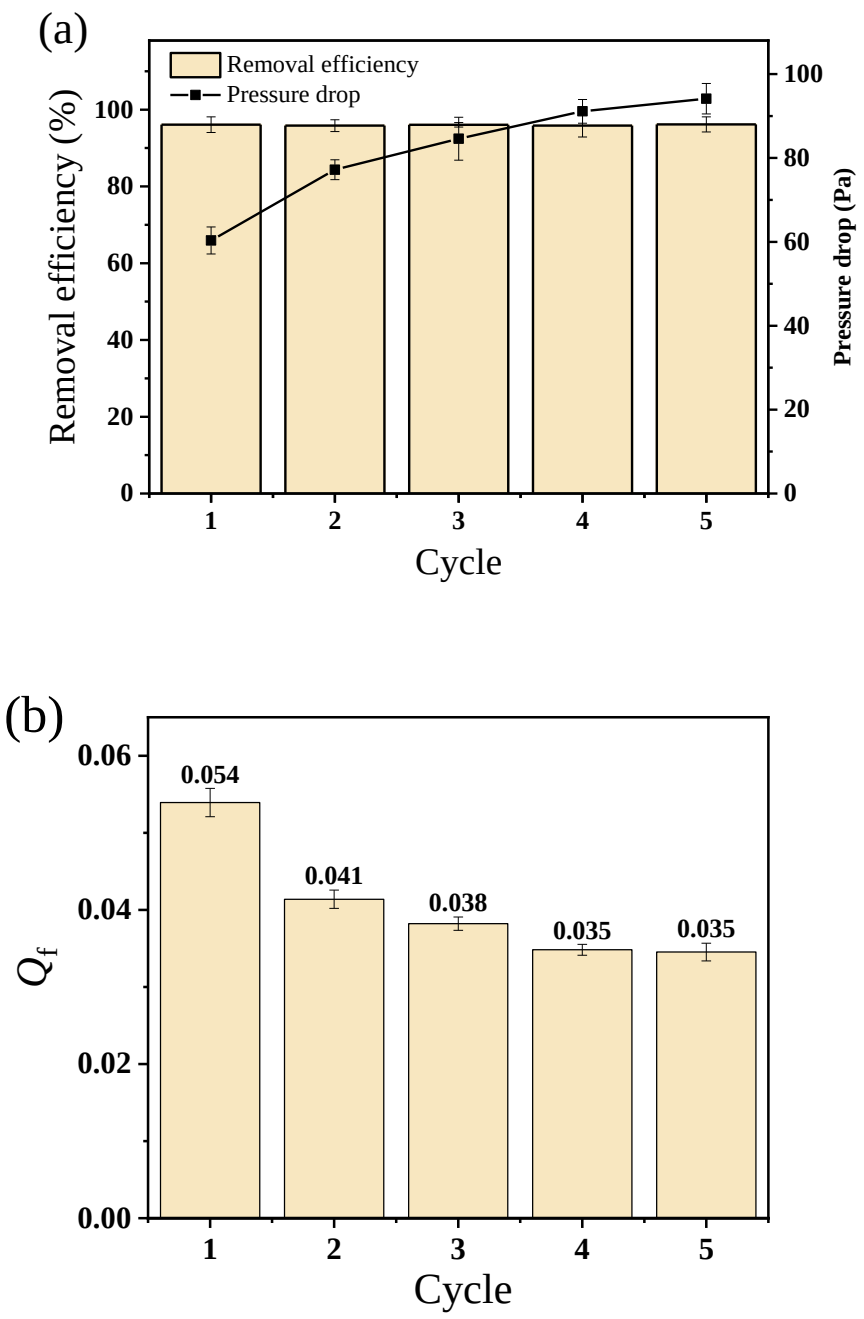

Figure III-10 Reusability of heated electrospun PVA/CNCs filter.

Table III-1 Diameters of electrospun air filters before and after water immersion with different heat treatment.

samples	*T* (°C)	*D* (nm)	
		Before water immersion	After water immersion
PVA	-	207.6 ± 49.7	-
	80	209.2 ±51.0	-
	100	211.3 ± 54.5	-
	120	204.8 ± 47.4	771.1 ± 103.5
	140	205.5 ± 28.8	393.2 ± 63.9
PVA/CNCs	-	130.7 ± 31.3	-
	80	125.1 ± 28.2	-
	100	131.3 ± 38.4	-
	120	128.8 ± 26.6	258.1 ± 52.3
	140	128.3 ± 23.8	127.5 ± 33.9

T, temperature of heat treatment; *D*, diameter of fiber.

Table III-2 *t*-test of diameters between groups of PVA fibers with different heat treatment after immersed in water for 8 h.

Level, *T* (°C)	- Level, *T* (°C)	Difference	Standard error of deviation	*p*-value
120	Not heated	565.6163	16.13578	<0.0001*
120	140	377.9214	16.13578	<0.0001*
140	Not heated	187.6950	16.13578	<0.0001*

T, temperature of heat treatment.

Table III-3 *t*-test of diameters between groups of PVA/CNCs fibers with different heat treatment after immersed in water for 8 h.

Level, *T* (°C)	- Level, *T* (°C)	Difference	Standard error of deviation	*p*-value
120	Not heated	129.7598	8.613786	<0.0001*
120	140	130.5432	8.613786	<0.0001*
140	Not heated	0.7835	8.613786	0.9277

T, temperature of heat treatment.

Table III-4 Effect of heat treatment on the crystallinity of electrospun fibers.

samples	T (°C)	X_c (%)	L (nm)
PVA	-	54.7 ± 1.6	3.3 ± 0.1
	80	61.9 ± 1.2	3.7 ± 0.1
	100	65.0 ± 1.6	4.1 ± 0.2
	120	68.2 ± 1.8	4.5 ± 0.2
	140	73.7 ± 0.5	4.9 ± 0.1
PVA/CNCs	-	59.6 ± 1.0	3.5 ± 0.1
	80	66.7 ± 1.0	4.3 ± 0.1
	100	72.6 ± 0.9	4.7 ± 0.1
	120	79.0 ± 1.0	5.2 ± 0.1
	140	85.4 ± 0.7	6.3 ± 0.1

T, temperature of heat treatment; X_c, degree of crystallinity; L, crystal size

Table III-5 *t*-test of crystallinity degree of PVA fibers with different heat treatment.

Level, *T* (°C)	- Level, *T* (°C)	Difference	Standard error of deviation	*p*-value
140	Not heated	19.00000	1.147558	<0.0001*
120	Not heated	13.50000	1.147558	<0.0001*
140	80	11.83333	1.147558	<0.0001*
100	Not heated	10.26667	1.147558	<0.0001*
140	100	8.73333	1.147558	<0.0001*
80	Not heated	7.16667	1.147558	<0.0001*
120	80	6.33333	1.147558	0.0003*
140	120	5.50000	1.147558	0.0007*
120	100	3.23333	1.147558	0.0182*
100	80	3.10000	1.147558	0.0223*

T, temperature of heat treatment.

Table III-6 *t*-test of crystallinity degree of PVA/CNCs fibers with different heat treatment.

Level, *T* (°C)	- Level, *T* (°C)	Difference	Standard error of deviation	*p*-value
140	Not heated	25.85333	0.7664753	<0.0001*
120	Not heated	19.38667	0.7664753	<0.0001*
140	80	18.75000	0.7664753	<0.0001*
100	Not heated	12.98667	0.7664753	<0.0001*
140	100	12.86667	0.7664753	<0.0001*
120	80	12.28333	0.7664753	<0.0001*
80	Not heated	7.10333	0.7664753	<0.0001*
140	120	6.46667	0.7664753	<0.0001*
120	100	6.40000	0.7664753	<0.0001*
100	80	5.88333	0.7664753	<0.0001*

T, temperature of heat treatment.

Table III-7 *t*-test of crystal size of PVA in PVA fibers with different heat treatment.

Level, *T* (°C)	- Level, *T* (°C)	Difference	Standard error of deviation	*p*-value
140	Not heated	1.643333	0.1027186	<0.0001*
120	Not heated	1.260000	0.1027186	<0.0001*
140	80	1.223333	0.1027186	<0.0001*
120	80	0.840000	0.1027186	<0.0001*
140	100	0.823333	0.1027186	<0.0001*
100	Not heated	0.820000	0.1027186	<0.0001*
120	100	0.440000	0.1027186	0.0016*
80	Not heated	0.420000	0.1027186	0.0022*
100	80	0.400000	0.1027186	0.0030*
140	120	0.383333	0.1027186	0.0039*

T, temperature of heat treatment.

Table III-8 *t*-test of crystal size of PVA in PVA/CNCs fibers with different heat treatment.

Level, *T* (°C)	- Level, *T* (°C)	Difference	Standard error of deviation	*p*-value
140	Not heated	2.770000	0.0748331	<0.0001*
140	80	1.956667	0.0748331	<0.0001*
120	Not heated	1.756667	0.0748331	<0.0001*
140	100	1.593333	0.0748331	<0.0001*
100	Not heated	1.176667	0.0748331	<0.0001*
140	120	1.013333	0.0748331	<0.0001*
120	80	0.943333	0.0748331	<0.0001*
80	Not heated	0.813333	0.0748331	<0.0001*
120	100	0.580000	0.0748331	<0.0001*
100	80	0.363333	0.0748331	0.0007*

T, temperature of heat treatment.

Table III-9 *t*-test of crystallinity degrees between PVA and PVA/CNCs fibers at different heating temperature.

T (°C)	Level	- Level	Difference	Standard error of deviation	*p*-value
-	PVA	PVA/CNCs	4.880000	1.085004	0.0108*
80	PVA	PVA/CNCs	4.816667	0.9088026	0.0061*
100	PVA	PVA/CNCs	7.600000	1.049868	0.0019*
120	PVA	PVA/CNCs	10.76667	1.199074	0.0009*
140	PVA	PVA/CNCs	11.73333	0.4666667	<0.0001*

T, temperature of heat treatment.

Table III-10 *t*-test of crystal sizes between PVA and PVA/CNCs fibers at different heating temperature.

T (°C)	Level	- Level	Difference	Standard error of deviation	*p*-value
-	PVA	PVA/CNCs	0.2300000	0.0867948	0.0570
80	PVA	PVA/CNCs	0.6233333	0.0735603	0.0011*
100	PVA	PVA/CNCs	0.5866667	0.1097472	0.0059*
120	PVA	PVA/CNCs	0.7266667	0.1047749	0.0023*
140	PVA	PVA/CNCs	1.356667	0.0664162	<0.0001*

T, temperature of heat treatment.

Table III-11 *t*-test of pressure drops between groups with different filtration cycles.

Level	- Level	Difference	Standard error of deviation	*p*-value
5	1	35.62400	1.677370	<0.0001*
4	1	31.23333	1.677370	<0.0001*
3	1	24.56667	1.677370	<0.0001*
5	2	18.82400	1.677370	<0.0001*
2	1	16.80000	1.677370	<0.0001*
4	2	14.43333	1.677370	<0.0001*
5	3	11.05733	1.677370	<0.0001*
3	2	7.76667	1.677370	0.0009*
4	3	6.66667	1.677370	0.0026*
5	4	4.39067	1.677370	0.0257*

CONCLUSIONS

To solve globally environmental issues caused by PM pollution, and to improve existing air filter technologies, a novel method for fabricating electrospun PVA/CNCs air filters was proposed in this dissertation. The nanofibrous air filter prepared via this method was highly efficient for PM removal, environmentally friendly, cost-effective and reusable. The three chapters in this dissertation describe the completed studies of the feasibility of fabricating electrospun PVA/CNCs filter, the optimization of the fabricating conditions, and the development of the reusability of the air filter, respectively. The technique for fabricating electrospun PVA/CNCs air filters was successfully developed and systematically improved in the researches supporting this dissertation.

The PVA/CNCs composite filter with low air resistance and high PM removal efficiency was fabricated via electrospinning for the first time. The addition of slight amount of CNCs (2 to 16 mg m^{-2}) resulted in a dramatic improvement in the overall filtration performance. CNCs effectively reduced the electrospun fiber diameter due to their negative charge. The highest removal efficiency for $PM_{2.5}$ was achieved as 99.1% when the electrospinning time was 8 min, while the filters prepared with electrospinning time of 6 min possesses the best compromise between removal efficiency and pressure drop, where Q_f value went as high as 0.054 Pa^{-1}. The entire process for fabricating the electrospun filter was environmentally friendly. No organic or toxic solvents were involved, and both PVA and CNCs are environmentally benign materials. In addition, the basis weight of the filter was very low, which made the filters potentially cost-effective.

To achieve the best overall filtration performance, the optimum operating conditions for fabricating PVA/CNCs filter was investigated via RSM within the operating space, where suspension concentration ranges from 6% to 8%, and CNCs percentage ranges from 5% to 20%. A three-level-two factor CCF design was applied to study the integral effect of various properties of electrospinning suspension on the responses. Fitted quadratic prediction models estimated the responses effectively and were validated. The processing condition was successfully optimized, and the optimum filtration performance was achieved as removal efficiency was 94% and pressure drop was 34.9 Pa, with the suspension concentration of 7.34% and CNCs percentage of 20% (electrospinning time was 6 min). CNCs could improve the filtration performance by reducing the diameter of

fibers only when the electrospun fibers were bead-free. Comparing with conventional one-factor-at-a-time method, RSM gives more integrate and accurate results, while requires less experimental runs. RSM is reliable to be utilized for evaluating the true structure of the processing condition and provide guidance on adjusting manufacturing parameters.

Without adding any crosslinking agent, the environmentally friendly water-soluble PVA/CNCs filter was converted to be completely waterproof in room temperature water by heating at 140 ^{o}C for 5 min. The CNCs and heat treatment synergistically improved the crystallinity of PVA polymers. The study provided a cost-effective manufacturing process to produce electrospun PVA/CNCs nanofibrous filter with aqueous stability. A thirty second immersion in water at room temperature effectively recovers the filtration capability of the filter, which is an easy and low-cost solution for household use. This PVA/CNCs filter is promising for PM removal with its low cost and superior reusability. In addition, the filter can be strategically dissolved with 60 ^{o}C water, which means the filter substrate can be easily recycled. With proper treatment, the dissolved PVA and CNCs might be reutilized as well. This electrospun PVA/CNCs filters are highly promising for indoor air purification applications.

FUTURE WORK

The work performed in this dissertation covers the preparation and characterization of electrospun PVA/CNCs filter, and optimization of the electrospinning conditions. It is focused on developing an environmentally friendly and cost-effectively method to produce air filters with superior filtration performance for PM and reusability. PM was the pollutant targeted to remove. Based on the existed results, future work could focus on broadening the application of this novel air filter by:

(1) Investigating the removal efficiency for microorganisms, such as bacteria and viruses.

(2) Incorporating metal nanoparticles to improve the antibacterial properties of the filter. Therefore, the potential risk caused by microorganisms enriched on the filter during filtration could be avoided.

(3) Incorporating catalyst on the fibers to remove volatile organic compounds in the air (such as formaldehyde) through catalytic degradation.

REFERENCES

Ahn, Y. C.; Park, S. K.; Kim, G. T.; Hwang, Y. J.; Lee, C. G.; Shin, H. S.; Lee, J. K. Development of high efficiency nanofilters made of nanofibers. *Curr. Appl. Phys.* **2006**, *6*, 1030-1035.

Anandjiwala, R. D.; Boguslavsky, L. Development of needle-punched nonwoven fabrics from flax fibers for air filtration applications. *Text. Res. J.* **2008**, *78*, 614-624.

Apte, J. S.; Marshall, J. D.; Cohen, A. J.; Brauer, M. Addressing global mortality from ambient $PM_{2.5}$. *Environ. Sci. Technol.* **2015**, *49*, 8057-8066.

Bai, Y.; Han, C. B.; He, C.; Gu, G. Q.; Nie, J. H.; Shao, J. J.; Xiao, T. X.; Deng, C. R.; Wang, Z. L. Washable multilayer triboelectric air filter for efficient particulate matter $PM_{2.5}$ removal. *Adv. Funct. Mater.* **2018**, *28*, 1706680.

Barhate, R. S.; Ramakrishna, S. Nanofibrous filtering media: filtration problems and solutions from tiny materials. *J. Membr. Sci.* **2007**, *296*, 1-8.

Bian, Y.; Wang, R.; Ting, S. H.; Chen, C.; Zhang, L. Electrospun SF/PVA nanofiber filters for highly-efficient $PM_{2.5}$ capture. *IEEE Trans. Nanotechnol.* **2018a,** *17*, 934-939.

Bian, Y.; Wang, R.; Wang, S.; Yao, C.; Ren, W.; Chen, C.; Zhang, L. Metal-organic framework-based nanofiber filters for effective indoor air quality control. *J. Mater. Chem. A* **2018b,** *6*, 15807-15814.

Bian, Y.; Zhang, L.; Chen, C. Experimental and modeling study of pressure drop across electrospun nanofiber air filters. *Build. Environ.* **2018c,** *142*, 244-251.

Booth, B.; Bellouin, N. Climate change: black carbon and atmospheric feedbacks. *Nature* **2015**, *519*, 167-168.

Bösiger, P.; Richard, I. M. T.; Le Gat, L.; Michen, B.; Schubert, M.; Rossi, R. M.; Fortunato, G. Application of response surface methodology to tailor the surface chemistry of electrospun chitosan-poly(ethylene oxide) fibers. *Carbohyd. Polym.* **2018**, *186*, 122-131.

Brook, R. D.; Rajagopalan, S.; Pope, C. A.; Brook, J. R.; Bhatnagar, A.; Diez-Roux, A. V.; Holguin, F.; Hong, Y.; Luepker, R. V.; Mittleman, M. A. Particulate matter air pollution and cardiovascular disease: an update to the scientific statement from the American Heart Association. *Circulation* **2010**, *121*, 2331-2378.

Brown, R. C. *Air filtration: an integrated approach to the theory and applications of fibrous filters*; Pergamon Press: Oxford, U.K., 1993.

Chen, Y.; Zhang, S.; Cao, S.; Li, S.; Chen, F.; Yuan, S.; Xu, C.; Zhou, J.; Feng, X.; Ma, X.; Wang, B. Roll-to-roll production of metal-organic framework coatings for particulate matter removal. *Adv. Mater.* **2017**, *29*, 1606221.

Cohen, A. J.; Brauer, M.; Burnett, R.; Anderson, H. R.; Frostad, J.; Estep, K.; Balakrishnan, K.; Brunekreef, B.; Dandona, L.; Dandona, R.; Feigin, V.; Freedman, G.; Hubbell, B.; Jobling, A.; Kan, H.; Knibbs, L.; Liu, Y.; Martin, R.; Morawska, L.; Pope, C. A.; Shin, H.; Straif, K.; Shaddick, G.; Thomas, M.; van Dingenen, R.; van Donkelaar, A.; Vos, T.; Murray, C. J. L.; Forouzanfar, M. H. Estimates and 25-year trends of the global burden of disease attributable to ambient air pollution: an analysis of data from the Global Burden of Diseases Study 2015. *Lancet* **2017**, *389*, 1907-1918.

da Silva, F. L. H.; Rodrigues, M. I.; Maugeri, F. Dynamic modelling, simulation and optimization of an extractive continuous alcoholic fermentation process. *J. Chem. Technol. Biot.* **1999***, 74*, 176-182.

Dai, X.; Li, X.; Wang, X. Morphology controlled porous poly(lactic acid)/zeolitic imidazolate framework-8 fibrous membranes with superior PM2.5 capture capacity. *Chem. Eng. J.* **2018**, *338*, 82-91.

Desmaisons, J.; Rueff, M.; Bras, J.; Dufresne, A. Dufresne, Impregnation of paper with cellulose nanocrystal reinforced polyvinyl alcohol: synergistic effect of infrared drying and CNC content on crystallinity. *Soft Matter* **2018**, *14*, 9425-9435.

Ding, B.; Kim, H. Y.; Lee, S. C.; Lee, D. R.; Choi, K. J. Preparation and characterization of nanoscaled poly(vinyl alcohol) fibers via electrospinning. *Fiber. Polym.* **2002**, *3*, 73-79.

Ding, B.; Kimura, E.; Sato, T.; Fujita, S.; Shiratori, S. Fabrication of blend biodegradable nanofibrous nonwoven mats via multi-jet electrospinning. *Polymer* **2004**, *45*, 1895-1902.

Dong, H.; Strawhecker, K. E.; Snyder, J. F.; Orlicki, J. A.; Reiner, R. S.; Rudie, A. W. Cellulose nanocrystals as a reinforcing material for electrospun poly(methyl methacrylate) fibers: formation, properties and nanomechanical characterization. *Carbohyd. Polym.* **2012**, *87*, 2488-2495.

Dong, X. M.; Revol, J.-F.; Gray, D. G. Effect of microcrystallite preparation conditions on

the formation of colloid crystals of cellulose. *Cellulose* **1998**, *5*, 19-32.

Doshi, J.; Reneker, D. H. Electrospinning process and applications of electrospun fibers. *J. Electrost.* **1995**, *35*, 151-160.

Fan, X.; Wang, Y.; Kong, L.; Fu, X.; Zheng, M.; Liu, T.; Zhong, W. H.; Pan, S. A nanoprotein-functionalized hierarchical composite air filter. *ACS Sustain. Chem. Eng.* **2018a,** *6* (9), 11606-11613.

Fan, X.; Wang, Y.; Zheng, M.; Dunne, F.; Liu, T.; Fu, X.; Kong, L.; Pan, S.; Zhong, W. H. Morphology engineering of protein fabrics for advanced and sustainable filtration. *J. Mater. Chem. A* **2018b,** *6* (43), 21585-21595.

Feng, X.; Yang, Z.; Chmely, S.; Wang, Q.; Wang, S.; Xie, Y. Lignin-coated cellulose nanocrystal filled methacrylate composites prepared via 3D stereolithography printing: Mechanical reinforcement and thermal stabilization. *Carbohyd. Polym.* **2017**, *169*, 272-281.

Finch, C. A. *Polyvinyl alcohol: properties and applications*; Wiley: New York, 1973.

Fong, H.; Chun, I.; Reneker, D. H. Beaded nanofibers formed during electrospinning. *Polymer* **1999**, *40*, 4585-4592.

Fu, J.; He, C.; Huang, J.; Chen, Z.; Wang, S. Cellulose nanofibril reinforced silica aerogels: optimization of the preparation process evaluated by a response surface methodology. *RSC Adv.* **2016**, *6*, 100326-100333.

Garg, K.; Bowlin, G. L. Electrospinning jets and nanofibrous structures. *Biomicrofluidics* **2011**, *5*, 13403-13403.

Gopal, R.; Kaur, S.; Feng, C. Y.; Chan, C.; Ramakrishna, S.; Tabe, S.; Matsuura, T. Electrospun nanofibrous polysulfone membranes as pre-filters: particulate removal. *J. of Memb. Sci.* **2007**, *289* (1), 210-219.

Habibi, Y.; Lucia, L. A.; Rojas, O. J. Cellulose nanocrystals: chemistry, self-assembly, and applications. *Chem. Rev.* **2010**, *110*, 3479-3500.

Harrison, R. M., Hester, R. E., Querol, X., Eds. Airborne Particulate Matter: Sources, Atmospheric Processes and Health, 1st ed.; Royal Society of Chemistry: Cambridge, U.K., 2016.

Heal, M. R.; Kumar, P.; Harrison, R. M. Particles, air quality, policy and health. *Chem. Soc. Rev.* **2012**, *41*, 6606-6630.

Hermans, P. H.; Weidinger, A. On the determination of the crystalline fraction of polyethylenes from X-ray diffraction, Makromol. *Chem*. **1961**, *44*, 24-36.

Hong, K.H. Preparation and properties of electrospun poly(vinyl alcohol)/silver fiber web as wound dressings. *Polym. Eng. Sci.* **2007**, *47*, 43-49.

Huan, S.; Bai, L.; Cheng, W.; Han, G. Manufacture of electrospun all-aqueous poly(vinyl alcohol)/cellulose nanocrystal composite nanofibrous mats with enhanced properties through controlling fibers arrangement and microstructure. *Polymer* **2016**, *92*, 25-35.

Huang, C.; Chen, S.; Lai, C.; Reneker, Darrell H.; Qiu, H.; Ye, Y.; Hou, H. Electrospun polymer nanofibres with small diameters. *Nanotechnology* **2006**, *17*, 1558-1563.

Huang, J.; Lyu, S.; Fu, F.; Wu, Y.; Wang, S. Green preparation of a cellulose nanocrystals/polyvinyl alcohol composite superhydrophobic coating. *RSC Adv.* **2017**, *7*, 20152-20159.

Huang, J.; Wang, S.; Lyu, S.; Fu, F. Preparation of a robust cellulose nanocrystal superhydrophobic coating for self-cleaning and oil-water separation only by spraying. *Ind. Crop. Prod.* **2018**, *122*, 438-447.

Hui, B.; Zhang, Y.; Ye, L. Preparation of PVA hydrogel beads and adsorption mechanism for advanced phosphate removal. *Chem. Eng. J.* **2014**, *235*, 207-214.

Hung, C. H.; Leung, W. W. F. Filtration of nano-aerosol using nanofiber filter under low Peclet number and transitional flow regime. *Sep. Purif. Technol.* **2011**, *79* (1), 34-42.

Hutten, I. M. *Handbook of nonwoven filter media*; Elsevier: Oxford, U.K., 2007.

Jeong, S.; Cho, H.; Han, S.; Won, P.; Lee, H.; Hong, S.; Yeo, J.; Kwon, J.; Ko, S. H. High efficiency, transparent, reusable, and active PM2.5 filters by hierarchical Ag nanowire percolation network. *Nano Lett.* **2017**, *17*, 4339-4346.

Jeun, J. P.; Jeon, Y. K.; Nho, Y. C.; Kang, P. H. Effects of gamma irradiation on the thermal and mechanical properties of chitosan/PVA nanofibrous mats. *J. Ind. Eng. Chem.* **2009**, *15*, 430-433.

Jiang, S.; Hou, H.; Agarwal, S.; Greiner, A. Polyimide nanofibers by “green” electrospinning via aqueous solution for filtration applications. *ACS Sustain. Chem. Eng.* **2016**, *4* (9), 4797-4804.

Kenawy, E. R.; Bowlin, G. L.; Mansfield, K.; Layman, J.; Simpson, D. G.; Sanders, E. H.; Wnek, G. E. Release of tetracycline hydrochloride from electrospun poly(ethylene-co-

vinylacetate), poly(lactic acid), and a blend. *J. Control. Release* **2002**, *81* (1), 57-64.

Kenney, J. F.; Willcockson, G. W. Structure-Property relationships of poly(vinyl alcohol). III. Relationships between stereo-regularity, crystallinity, and water resistance in poly(vinyl alcohol). *J. Polym. Sci. A-1 Polym. Chem.* **1966**, *4*, 679-698.

Khalid, B.; Bai, X.; Wei, H.; Huang, Y.; Wu, H.; Cui, Y. Direct blow-spinning of nanofibers on a window screen for highly efficient $PM_{2.5}$ removal. *Nano Lett.* **2017**, *17*, 1140-1148.

Kim, H.-J.; Park, S. J.; Park, C. S.; Le, T.-H.; Hun Lee, S.; Ha, T. H.; Kim, H.-i.; Kim, J.; Lee, C.-S.; Yoon, H.; Kwon, O. S. Surface-modified polymer nanofiber membrane for high-efficiency microdust capturing. *Chem. Eng. J.* **2018**, *339*, 204-213.

Koplitz, S. N.; Jacob, D. J.; Sulprizio, M. P.; Myllyvirta, L.; Reid, C. Burden of disease from rising coal-fired power plant emissions in Southeast Asia. *Environ. Sci. Technol.* **2017**, *51*, 1467-1476.

Landrigan, P. J.; Fuller, R.; Acosta, N. J. R.; Adeyi, O.; Arnold, R.; Basu, N.; Baldé, A. B.; Bertollini, R.; Bose-O'Reilly, S.; Boufford, J. I.; Breysse, P. N.; Chiles, T.; Mahidol, C.; Coll-Seck, A. M.; Cropper, M. L.; Fobil, J.; Fuster, V.; Greenstone, M.; Haines, A.; Hanrahan, D.; Hunter, D.; Khare, M.; Krupnick, A.; Lanphear, B.; Lohani, B.; Martin, K.; Mathiasen, K. V.; McTeer, M. A.; Murray, C. J. L.; Ndahimananjara, J. D.; Perera, F.; Potočnik, J.; Preker, A. S.; Ramesh, J.; Rockström, J.; Salinas, C.; Samson, L. D.; Sandilya, K.; Sly, P. D.; Smith, K. R.; Steiner, A.; Stewart, R. B.; Suk, W. A.; van Schayck, O. C. P.; Yadama, G. N.; Yumkella, K.; Zhong, M. The Lancet Commission on pollution and health. *Lancet* **2018**, *391*, 462-512.

Lang, G.; Jokisch, S.; Scheibel, T. Air filter devices including nonwoven meshes of electrospun recombinant spider silk proteins. *J. Vis. Exp.* **2013,** e50492.

Lee, S.; Cho, A. R.; Park, D.; Kim, J. K.; Han, K. S.; Yoon, I.-J.; Lee, M. H.; Nah, J. Reusable polybenzimidazole nanofiber membrane filter for highly breathable $PM_{2.5}$ dust proof mask. *ACS Appl. Mater. Inter.* **2019**, *11*, 2750-2757.

Lee, W. J.; Clancy, A. J.; Kontturi, E.; Bismarck, A.; Shaffer, M. S. P. Strong and stiff: high-performance cellulose nanocrystal/poly(vinyl alcohol) composite fibers. *ACS Appl. Mater. Inter.* **2016**, *8*, 31500-31504.

Lee, Y.; Wadsworth, L. C. Structure and filtration properties of melt blown polypropylene webs. *Polym. Eng. Sci.* **1990**, *30*, 1413-1419.

Lepeule, J.; Laden, F.; Dockery, D.; Schwartz, J. Chronic exposure to fine particles and mortality: an extended follow-up of the Harvard Six Cities study from 1974 to 2009. *Environ. health persp.* **2012**, *120*, 965-970.

Leung, W. W.-F.; Hung, C.-H.; Yuen, P.-T. Effect of face velocity, nanofiber packing density and thickness on filtration performance of filters with nanofibers coated on a substrate. *Sep. Purif. Technol.* **2010**, *71*, 30-37.

Li, M.; Feng, Y.; Wang, K.; Yong, W. F.; Yu, L.; Chung, T.-S. Novel hollow fiber air filters for the removal of ultrafine particles in $PM_{2.5}$ with repetitive usage capability. *Environ. Sci. Technol.* **2017**, *51*, 10041-10049.

Li, X.; Wu, Q.; Zheng, M.; Li, Q.; Wang, S.; Zhang, C. Mechanical, thermal properties and curing kinetics of liquid silicone rubber filled with cellulose nanocrystal. *Cellulose* **2018**, *25*, 473-483.

Lin, T. C.; Krishnaswamy, G.; Chi, D. S. Incense smoke: clinical, structural and molecular effects on airway disease. *Clin. Mol. Allergy* **2008**, *6*, 3.

Liu, B.; Zhang, S.; Wang, X.; Yu, J.; Ding, B. Efficient and reusable polyamide-56 nanofiber/nets membrane with bimodal structures for air filtration. *J. Colloid Interf. Sci.* **2015a**, *457*, 203-211.

Liu, C.; Hsu, P. C.; Lee, H. W.; Ye, M.; Zheng, G.; Liu, N.; Li, W.; Cui, Y. Transparent air filter for high-efficiency $PM_{2.5}$ capture. *Nat. Commun.* **2015b**, *6*, 6205.

Liu, J. Study on healthy risk assessment and simulation on residential indoor environmental based on stochastic theory. Ph.D. Dissertation, Hunan University, Changsha, China, 2007.

Liu, K.; Liu, C.; Hsu, P. C.; Xu, J.; Kong, B.; Wu, T.; Zhang, R.; Zhou, G.; Huang, W.; Sun, J.; Cui, Y. Core-shell nanofibrous materials with high particulate matter removal efficiencies and thermally triggered flame retardant properties. *ACS Cent. Sci.* **2018**, *4*, 894-898.

Liu, X.; Souzandeh, H.; Zheng, Y.; Xie, Y.; Zhong, W. H.; Wang, C. Soy protein isolate/bacterial cellulose composite membranes for high efficiency particulate air filtration. *Compos. Sci. Technol.* **2017**, *138*, 124-133.

Long, J.; Tang, M.; Liang, Y.; Hu, J. Preparation of fibrillated cellulose nanofiber from lyocell fiber and its application in air filtration. *Materials* **2018,** *11*, 1313.

Lu, Z.; Su, Z.; Song, S.; Zhao, Y.; Ma, S.; Zhang, M. Toward high-performance fibrillated cellulose-based air filter via constructing spider-web-like structure with the aid of TBA during freeze-drying process. *Cellulose* **2018,** *25*, 619-629.

Lyons, D. W.; Olson, E. S. Effect of drying and heat-setting temperatures on the removal characteristics of polyvinyl alcohol size. *Text. Res. J.* **1972**, *42*, 199-202.

Ma, L.; Zhang, Y.; Wang, S. Preparation and characterization of acrylonitrile-butadiene-styrene nanocomposites reinforced with cellulose nanocrystal via solution casting method. *Polym. Composite.* **2017**, *38*, E167-E173.

Mannix, R. C.; Nguyen, K. P.; Tan, E. W.; Ho, E. E.; Phalen, R. F. Physical characterization of incense aerosols. *Sci. Total Environ.* **1996**, *193*, 149-158.

Mansur, H. S.; Sadahira, C. M.; Souza, A. N.; Mansur, A. A. P. FTIR spectroscopy characterization of poly (vinyl alcohol) hydrogel with different hydrolysis degree and chemically crosslinked with glutaraldehyde. *Mater. Sci. Eng. C* **2008**, *28*, 539-548.

Matulevicius, J.; Kliucininkas, L.; Prasauskas, T.; Buivydiene, D.; Martuzevicius, D. The comparative study of aerosol filtration by electrospun polyamide, polyvinyl acetate, polyacrylonitrile and cellulose acetate nanofiber media. *J. Aerosol Sci.* **2016**, *92*, 27-37.

Meng, Y.; Wang, X.; Wu, Z.; Wang, S.; Young, T. M. Optimization of cellulose nanofibrils carbon aerogel fabrication using response surface methodology. *Eur. Polym. J.* **2015**, *73*, 137-148.

Miri, N. E.; Abdelouahdi, K.; Zahouily, M.; Fihri, A.; Barakat, A.; Solhy, A.; Achaby, M. E. Bio-nanocomposite films based on cellulose nanocrystals filled polyvinyl alcohol/chitosan polymer blend. *J. Appl. Polym. Sci.* **2015**, *132*, 42004.

Mohod, A. V.; Gogate, P. R. Ultrasonic degradation of polymers: effect of operating parameters and intensification using additives for carboxymethyl cellulose (CMC) and polyvinyl alcohol (PVA). *Ultrason. Sonochem.* **2011**, *18*, 727-734.

Montgomery, D. C. *Design and analysis of experiments*; John wiley & sons: New York, U.S., 2017.

Moon, R. J.; Martini, A.; Nairn, J.; Simonsen, J.; Youngblood, J. Cellulose nanomaterials review: structure, properties and nanocomposites. *Chem. Soc. Rev.* **2011**, *40*, 3941-3994.

Nan, F.; Nagarajan, S.; Chen, Y.; Liu, P.; Duan, Y.; Men, Y.; Zhang, J. Enhanced toughness and thermal stability of cellulose nanocrystal iridescent films by alkali treatment. *ACS*

Sustain. Chem. Eng. **2017**, *5*, 8951-8958.

Park, Y.; You, M.; Shin, J.; Ha, S.; Kim, D.; Heo, M. H.; Nah, J.; Kim, Y. A.; Seol, J. H. Thermal conductivity enhancement in electrospun poly(vinyl alcohol) and poly(vinyl alcohol)/cellulose nanocrystal composite nanofibers. *Sci. Rep.* **2019**, *9*, 3026.

Peppas, N.A. Infrared spectroscopy of semicrystalline poly(vinyl alcohol) networks, Die *Makromolekulare Chemie* **1977**, *178*, 595-601.

Peresin, M. S.; Habibi, Y.; Zoppe, J. O.; Pawlak, J. J.; Rojas, O. J. Nanofiber composites of polyvinyl alcohol and cellulose nanocrystals: manufacture and characterization. *Biomacromolecules* **2010**, *11*, 674-681.

Peresin, M. S.; Vesterinen, A. H.; Habibi, Y.; Johansson, L. S.; Pawlak, J. J.; Nevzorov, A. A.; Rojas, O. J. Crosslinked PVA nanofibers reinforced with cellulose nanocrystals: water interactions and thermomechanical properties. *J. Appl. Polym. Sci.* **2014**, *131*, 40334.

Podgórski, A.; Bałazy, A.; Gradoń, L. Application of nanofibers to improve the filtration efficiency of the most penetrating aerosol particles in fibrous filters. *Chem. Eng. Sci.* **2006**, *61*, 6804-6815.

Pope III, C. A.; Burnett, R. T.; Thun, M. J.; Calle, E. E.; Krewski, D.; Ito, K.; Thurston, G. D. Lung cancer, cardiopulmonary mortality, and long-term exposure to fine particulate air pollution. *Jama* **2002**, *287*, 1132-1141.

Popescu, M.-C. Structure and sorption properties of CNC reinforced PVA films. *Int. J. Biol. Macromol.* **2017,** *101*, 783-790.

Qin, X. H.; Wang, S. Y. Electrospun nanofibers from crosslinked poly(vinyl alcohol) and its filtration efficiency. *J. Appl. Polym. Sci.* **2008,** *109*, 951-956.

Qua, E. H.; Hornsby, P. R.; Sharma, H. S. S.; Lyons, G.; McCall, R. D. Preparation and characterization of poly(vinyl alcohol) nanocomposites made from cellulose nanofibers. *J. Appl. Polym. Sci.* **2009,** *113*, 2238-2247.

Raaschou-Nielsen, O.; Andersen, Z. J.; Beelen, R.; Samoli, E.; Stafoggia, M.; Weinmayr, G.; Hoffmann, B.; Fischer, P.; Nieuwenhuijsen, M. J.; Brunekreef, B. Air pollution and lung cancer incidence in 17 European cohorts: prospective analyses from the European Study of Cohorts for Air Pollution Effects (ESCAPE). *Lancet Oncol.* **2013**, *14*, 813-822.

Reneker, D. H.; Yarin, A. L. Electrospinning jets and polymer nanofibers. *Polymer* **2008**, *49*, 2387-2425.

Rescignano, N.; Fortunati, E.; Montesano, S.; Emiliani, C.; Kenny, J. M.; Martino, S.; Armentano, I. PVA bio-nanocomposites: a new take-off using cellulose nanocrystals and PLGA nanoparticles. *Carbohydr. Polym.* **2014,** *99*, 47-58.

Roohani, M.; Habibi, Y.; Belgacem, N. M.; Ebrahim, G.; Karimi, A. N.; Dufresne, A. Cellulose whiskers reinforced polyvinyl alcohol copolymers nanocomposites. *Eur. Polym. J.* **2008,** *44*, 2489-2498.

Sarlak, N.; Nejad, M. A. F.; Shakhesi, S.; Shabani, K. Effects of electrospinning parameters on titanium dioxide nanofibers diameter and morphology: an investigation by Box-Wilson central composite design (CCD). *Chem. Eng. J.* **2012**, *210*, 410-416.

Scholten, E.; Bromberg, L.; Rutledge, G. C.; Hatton, T. A. Electrospun polyurethane fibers for absorption of volatile organic compounds from air. *ACS Appl. Mater. Inter.* **2011**, *3*, 3902-3909.

Shafiei-Sabet, S.; Hamad, W. Y.; Hatzikiriakos, S. G. Rheology of nanocrystalline cellulose aqueous suspensions. *Langmuir* **2012**, *28*, 17124-17133.

Shalom, T. B.; Nevo, Y.; Leibler, D.; Shtein, Z.; Azerraf, C.; Lapidot, S.; Shoseyov, O. Cellulose nanocrystals (CNCs) induced crystallization of polyvinyl alcohol (PVA) super performing nanocomposite films. *Macromol. Biosci.* **2019,** *19*, 1800347.

Song, T.; Tanpichai, S.; Oksman, K. Cross-linked polyvinyl alcohol (PVA) foams reinforced with cellulose nanocrystals (CNCs). *Cellulose* **2016,** *23*, 1925-1938.

Stranger, J.; Staiger, M. P.; Tucker, N.; Kirwan, K. Effect of charge density on the taylor cone in electrospinning. *Solid State Phenom.* **2009**, *151*, 54-59.

Su, Z.; Zhang, M.; Lu, Z.; Song, S.; Zhao, Y.; Hao, Y. Functionalization of cellulose fiber by in situ growth of zeolitic imidazolate framework-8 (ZIF-8) nanocrystals for preparing a cellulose-based air filter with gas adsorption ability. *Cellulose* **2018,** *25*, 1997-2008.

Supaphol, P.; Chuangchote, S. On the electrospinning of poly (vinyl alcohol) nanofiber mats: a revisit. *J. Appl. Polym. Sci.* **2008**, *108*, 969-978.

Thomas, D.; Penicot, P.; Contal, P.; Leclerc, D.; Vendel, J. Clogging of fibrous filters by solid aerosol particles experimental and modelling study. *Chem. Eng. Sci.* **2001**, *56*,

3549-3561.

Thompson, C. J.; Chase, G. G.; Yarin, A. L.; Reneker, D. H. Effects of parameters on nanofiber diameter determined from electrospinning model. *Polymer* **2007**, *48*, 6913-6922.

Tian, H.; Fu, X.; Zheng, M.; Wang, Y.; Li, Y.; Xiang, A.; Zhong, W.-H. Natural polypeptides treat pollution complex: moisture-resistant multi-functional protein nanofabrics for sustainable air filtration. *Nano Res.* **2018,** *11*, 4265-4277.

Uddin, A. J.; Araki, J.; Gotoh, Y. Extremely oriented tunicin whiskers in poly(vinyl alcohol) nanocomposites. *Polym. Int.* **2011,** *60*, 1230-1239.

Vanangamudi, A.; Hamzah, S.; Singh, G. Synthesis of hybrid hydrophobic composite air filtration membranes for antibacterial activity and chemical detoxification with high particulate filtration efficiency (PFE). *Chem. Eng. J.* **2015,** *260*, 801-808.

Voronova, M. I.; Surov, O. V.; Guseinov, S. S.; Barannikov, V. P.; Zakharov, A. G. Thermal stability of polyvinyl alcohol/nanocrystalline cellulose composites. *Carbohydr. Polym.* **2015,** *130*, 440-447.

Wanasekara, N. D.; Santos, R. P. O.; Douch, C.; Frollini, E.; Eichhorn, S. J. Orientation of cellulose nanocrystals in electrospun polymer fibres, *J. Mater. Sci.* **2015**, *51*, 218-227.

Wang, Z.; Zhao, C.; Pan, Z. Porous bead-on-string poly(lactic acid) fibrous membranes for air filtration. *J. Colloid Interf. Sci.* **2015**, *441*, 121-129.

Watson, J. G. Visibility: science and regulation. *J. Air Waste Manage. Assoc.* **2002**, *52*, 628-713.

Wong, K. K. H.; Zinke-Allmang, M.; Hutter, J. L.; Hrapovic, S.; Luong, J. H. T.; Wan, W. The effect of carbon nanotube aspect ratio and loading on the elastic modulus of electrospun poly(vinyl alcohol)-carbon nanotube hybrid fibers. *Carbon* **2009**, *47*, 2571-2578.

Wong, K. K. H.; Zinke-Allmang, M.; Wan, W. Effect of annealing on aqueous stability and elastic modulus of electrospun poly(vinyl alcohol) fibers. *J. Mater. Sci.* **2010,** *45*, 2456-2465.

World Health Organization, Ambient air pollution: a global assessment of exposure and burden of disease, **2016**.

Xu, C.; Wang, Q.; Li, N.; Chang, J.; Lin, X.; Xu, D. Investigation of indoor fine particles

in public places and influencing factors. *J. Environ. Health* **2014**, *11*, 993-996.

Xu, J.; Liu, C.; Hsu, P.-C.; Liu, K.; Zhang, R.; Liu, Y.; Cui, Y. Roll-to-roll transfer of electrospun nanofiber film for high-efficiency transparent air filter. *Nano Lett.* **2016,** *16*, 1270-1275.

Xu, K.; Liu, C.; Kang, K.; Zheng, Z.; Wang, S.; Tang, Z.; Yang, W. Isolation of nanocrystalline cellulose from rice straw and preparation of its biocomposites with chitosan: physicochemical characterization and evaluation of interfacial compatibility. *Compos. Sci. Technol.* **2018,** *154*, 8-17.

Yun, K. M.; Hogan, C. J.; Matsubayashi, Y.; Kawabe, M.; Iskandar, F.; Okuyama, K. Nanoparticle filtration by electrospun polymer fibers. *Chem. Eng. Sci.* **2007**, *62*, 4751-4759.

Zhang, D.; Bhat, G.; Malkan, S.; Wadsworth, L. Structure and properties of polypropylene filaments in a spunbonding process. *J. Therm. Anal. Calorim.* **1997**, *49*, 161-167.

Zhang, Q.; Li, Q.; Zhang, L.; Wang, S.; Harper, D. P.; Wu, Q.; Young, T. M. Preparation of electrospun nanofibrous poly(vinyl alcohol)/cellulose nanocrystals air filter for efficient particulate matter removal with repetitive usage capability via facile heat treatment. *Chem. Eng. J.* **2020**, *399*, 125768.

Zhang, Q.; Li, Q.; Young, T. M.; Harper, D. P.; Wang, S. A novel method for fabricating an electrospun poly(vinyl alcohol)/cellulose nanocrystals composite nanofibrous filter with low air resistance for high-efficiency filtration of particulate matter. *ACS Sustain. Chem. Eng.* **2019,** *7*, 8706-8714.

Zhang, R.; Liu, C.; Hsu, P. C.; Zhang, C.; Liu, N.; Zhang, J.; Lee, H. R.; Lu, Y.; Qiu, Y.; Chu, S.; Cui, Y. Nanofiber air filters with high-temperature stability for efficient $PM_{2.5}$ removal from the pollution sources. *Nano Lett.* **2016a**, *16*, 3642-3649.

Zhang, S.; Liu, H.; Yin, X.; Yu, J.; Ding, B. Anti-deformed polyacrylonitrile/polysulfone composite membrane with binary structures for effective air filtration. *ACS Appl. Mater. Inter.* **2016b,** *8*, 8086-8095.

Zhang, Y.; Yuan, S.; Feng, X.; Li, H.; Zhou, J.; Wang, B. Preparation of nanofibrous metal-organic framework filters for efficient air pollution control. *J. Am. Chem. Soc.* **2016c,** *138*, 5785-5788.

Zhao, X.; Li, Y.; Hua, T.; Jiang, P.; Yin, X.; Yu, J.; Ding, B. Cleanable air filter transferring

moisture and effectively capturing $PM_{2.5}$. *Small* **2017,** *13*, 1603306.

Zhao, X.; Wang, S.; Yin, X.; Yu, J.; Ding, B. Slip-effect functional air filter for efficient purification of $PM_{2.5}$. *Sci. Rep.* **2016**, *6*, 35472.

Zhu, M.; Han, J.; Wang, F.; Shao, W.; Xiong, R.; Zhang, Q.; Pan, H.; Yang, Y.; Samal, S. K.; Zhang, F. Electrospun nanofibers membranes for effective air filtration. *Macromol. Mater.* Eng. **2017**, *302*, 1600353.

Zhu, M.; Hua, D.; Pan, H.; Wang, F.; Manshian, B.; Soenen, S. J.; Xiong, R.; Huang, C. Green electrospun and crosslinked poly(vinyl alcohol)/poly(acrylic acid) composite membranes for antibacterial effective air filtration. *J. Colloid Interf. Sci.* **2018**, *511*, 411-423.

VITA

Qijun Zhang was born in Guiyang, Guizhou province, China. He received his B.S. degree in Environmental Science from Wuhan University of Technology, Wuhan, China, in 2012. He then entered Nanjing University, Nanjing, China, for his M.S. degree in Environmental Science, and received it in 2015. By participating in the China-US EcoPartnership Scholars Program, Qijun started his study for doctoral degree in Natural Resources at the University of Tennessee, Knoxville in 2015. He worked under Dr. Siqun Wang and Dr. Timothy M. Young as graduate research assistant in the Center for Renewable Carbon, Department of Forestry, Wildlife and Fisheries.